TURBULENCE MEASUREMENTS OF HEATED SUPERSONIC SLOT INJECTION INTO A SUPERSONIC STREAM

by

Camillus Randolph Hyde, Jr.

Thesis submitted to the Faculty of the

Virginia Polytechnic Institute and State University

in partial fulfillment of the requirements for the degree of

MASTER OF SCIENCE

in

AEROSPACE ENGINEERING

APPROVED:

Dana A. Walker, Chairman

Joseph A. Schetz

Wing F. Ng

February, 1989

Blacksburg, Virginia

TURBULENCE MEASUREMENTS OF HEATED SUPERSONIC SLOT INJECTION INTO A SUPERSONIC STREAM

by

Camillus Randolph Hyde, Jr.

Dana A. Walker, Chairman

AEROSPACE ENGINEERING

(ABSTRACT)

Experimental results of hot-wire measurements of turbulence in a supersonic shear layer are presented. A multiple-overheat single-wire method based on high-speed, computer-controlled sampling was used in order to obtain large sample sets in short time intervals. The Mach 3 main stream had a total pressure of 95 psia and a Re/cm of 2×10^6. The Mach 1.7 secondary stream was injected parallel to the main flow at 10.7 psia, resulting in a slightly overexpanded flow. The injection slot had a height of 1.2 cm. The flow was monitored at four streamwise stations (x/H = .25, 4, 10, 20). The total temperature of the injected stream was varied from 300 K (equal to that of the main stream) to 420 K. The effects on the flow of these changes in density, velocity and temperature was investigated. Measured quantities included the mean and rms levels of the mass flux and total temperature. Nanosecond Shadowgraphs and spark Schlieren photographs were taken. The Favre-averaged velocity fluctuation, $\overline{u''}$, was also calculated. Small increases in absolute turbulence levels were seen in the heated flow, and the location of the maximum turbulence shifted significantly. Heating

greatly enhanced the mixing in the shear layer and in the injected flow by the last station. An investigation of shock interaction with the shear layer generally resulted in elevated turbulence, but had little effect on $\overline{u''}$. The measurement technique and reduction method proved accurate in the unheated flow, but greater uncertainty was found for the heated injection case.

Acknowledgements

Without the aid of others, this work could not have been completed. First, I need to thank my parents and the rest of my family for their love and support throughout the past 6 years of school.

I would like to thank Dr. Dana A. Walker for his confidence in me and his willingness to discuss this research at almost any time. His patience in answering my many questions is greatly appreciated.

I need to thank Dr. Joseph A. Schetz and Dr. Wing F. Ng for their helpful advice. Next, I must mention , who shared this project with me and worked diligently the entire time. and Dr. Russ Thomas worked on a similar project before Ben and me. Their many useful suggestions saved us a lot of time.

Among the many others who helped my efforts were

This work was supported by the Applied Physics Laboratory of Johns Hopkins University. The technical monitor was Dr. Harold E. Gilreath.

Table of Contents

List of Illustrations

List of Symbols

a,b .....hot wire calibration constants

c .....hot wire constant

d_w.....hot wire diameter

E .....voltage

e.....instantaneous voltage with zero mean

i_w.....hot wire current

k_t.....thermal conductivity of air at stagnation conditions

l_w .....length of hot wire

l/d.....length to diameter ratio of wire

m .....mass flux, ρu

M .....Mach number

Nu .....Nusselt number at stagnation conditions

p_t.....local stagnation pressure

Pr .....Prandtl number

q_w.....heat transfer from hot wire

R_w .....resistance of hot wire

R_1, R_2, R_3.....other bridge resistances

Re.....Reynolds number at stagnation conditions

T.....local temperature

x,y,z,f,g.....constituents of matrix coefficients

x, y .....Cartesian coodinate system

Greek symbols

δ .....boundary layer thickness

ρ .....local density

τ .....temperature loading of hot wire, $\frac{T_w - T_e}{T_t}$

μ_t .....viscosity of air at stagnation conditions

Subscripts

20 .....reference temperature in degrees (C)

α .....temperature coefficient of resistance of hot wire

e.....equilibrium

i.....specific overheat

j.....reference to injectant or jet

leads.....denotes wire prongs and leads from wire to circuit

metrabyte .....denotes value recorded at A/D inputs of the computer

ref.....reference condition, 20 C

t.....total condition

∞ .....free-stream condition

w.....denotes hot wire

Superscripts

$( )'$ .....rms turbulent quantity

$\overline{( )''}$.....Favre-averaged quantity

$\overline{( )}$ .....arithmetic mean value

List of Tables

Chapter 1

INTRODUCTION

Recent interest in supersonic and hypersonic atmospheric vehicles has revealed a need for increased research of high-speed flows. The goal of a practical hypersonic intercontinental/orbital transport as defined by the National Aerospace Plane project illuminates the difficulties in studying such phenomena.

Computer computations of supersonic flow, increasingly commonplace, have been hindered by limited understanding of the physics of compressible turbulent flows. Existing numerical algorithms rely on turbulence models derived largely from mean flow measurements. Since computational results can depend heavily on the models used, improved turbulence models are greatly desired [1,2].

Extending turbulence models based on contant density flows often results in poor prediction of variable-density, high-speed flows. Turbulence measurements can improve the modelling and the understanding of the physics of such flows. Much experimental hypersonic research is aimed at thorough

studies of simple benchmark test configurations to produce a data base for computer modelling and testing of models useful in specific applications.

The study of slot injection of a secondary stream into a parallel primary flow is useful in both respects. This is of possible interest in fuel injection, surface cooling, and either skin friction reduction or energy addition to the boundary layer to prevent separation [1,3]. Injection from a rearward-facing step also enhances transition to turbulence which could be a problem at high altitude [3]. In the case of tangential fuel injection, thrust is derived from the fuel, the surface is cooled, and skin friction is reduced.

Research of this type has been performed in the past in both subsonic and supersonic flows. Many studies have concerned supersonic shear layers where the mixing layer is distant from any wall, but studies in which both mean and turbulence measurements have been made are rare [4-10]. The reason is that direct and accurate measurement of supersonic turbulence is difficult and fundamentally different than measuring mean quantities such as skin friction. Laser doppler velocimetry (LDV) and hot-wire anemometry can measure turbulence [11]. LDV in supersonic flows was pioneered by Pike, Yanta and others [12,13]. Hot wires have been used in supersonic flow since their systematic investigation by Kovásznay and Morkovin in the 1950's [14-16].

Hot wires respond to changes in flow density, velocity, and total temperature. For high Reynolds number flows with Mach numbers from 1.2 to 5, hot wire sensitivities to ρ and u are equal and independent of M so that the wire response can be resolved into ρu and T_t fluctuations [14,17]. By varying the

temperature loading, τ, the wire's sensitivity to each can be adjusted. In low intensity turbulence Kovásznay showed that turbulence could be separated into three modes (each composed of different ρu and T_t dependence), but in cases of large turbulent fluctuations and high relative Mach number, the modes are coupled [16]. Without other information or simplifying assumptions, ρ and u cannot be separated.

Two unknowns require multiple measurements. One method uses two very closely spaced wires operating simultaneously at different overheats (wire temperatures). The method used here has one wire operating at many temperatures cycled quickly. Redundancy of overheats allows a least squares analysis. Both well-known methods have advantages and disadvantages as explained in Walker, Ng, and Walker [18].

Problems associated with hot-wire anemometry include limited frequency response. The cutoff frequency of the wire is about 90 Hz in still air [19] and on the order of 1000 Hz in this case [20]. Constant-temperature feedback in the circuit raises the cutoff frequency to about 100 kHz. Increasing this while maintaining a large gain and low noise level is a major problem. A constant current anemometer circuit can achieve high frequencies if it is compensated for its frequency roll-off rate. The rate and position of this roll-off change with the wire and the flow conditions, however, so that any given compensation setting is applicable to only one restricted case. The constant-current method also requires a wire with known response characteristics. A constant temperature anemometer, on the other hand, maintains the wire at a fixed operating point, so its nonlinear

thermal response characteristic is irrelevant, and it is capable of high frequencies without knowledge of the roll-off.

The wire/shock system itself is small compared to the energy-containing disturbances in the flow, and the signal can be sampled digitally in the MHz range. However, only about 90% of the turbulent energy is in the range from 0 to 100 kHz, so the circuit frequency response is the limiting factor in turbulence spatial resolution by this method [21]. Other difficulties include wire breakage, contamination, strain gaging, and end effects.

The current study models, in a basic research sense, a scramjet combustor. It consists of a Mach 1.7 air stream injected parallel to a Mach 3 air free steam, separated by a shear layer. The free-stream Mach number is a typical internal-flow value for flight Mach numbers near Mach 8 [22]. Free-stream total pressure and temperature are 655 kPa (95 psia) and 300 K (80°F), respectively. The well-developed incoming boundary layer is consistent with an aircraft whose forebody is used for early flow compression. The slot height was of the order of the boundary thickness.

Injected into the primary flow from the slot, the secondary flow temperature was varied from 300 K to 420 K (80°F to 300°F) to test effects of density and velocity changes, to test using temperature as a flow marker, and to confirm the experiment performed by Campbell [22].

In this and a parallel study by Smith [23], both mean and turbulent quantities were measured using Pitot, cone-static, diffuser thermocouple and hot-wire probes. Computer-controlled instrumentation greatly improved the

amount and quality of the data taken. It reduces the effect of unsteadiness in a blow down tunnel by regulating total pressure and by sampling fast enough to allow completion of a station before the flow can change significantly in the mean. It is essential for the use of a multiple-overheat single-wire method of determining flow variables from hot-wire voltage data.

To obtain a complete picture of the flow, measurements were made at multiple vertical positions at each of four streamwise stations. In addition, spark Schlieren photographs and nanosecond Shadowgraphs were taken to aid interpretation of results and allow measurement of prominent flow features. Measurements were also taken to determine the effect of weak shock impingement on the shear layer between the two downstream stations.

Chapter 2

EXPERIMENTAL FACILITY

2.1 The Wind Tunnel

These measurements were conducted in the Virginia Tech Supersonic Wind Tunnel. It has a 23 by 23 cm (9 by 9 inch) test section and two-dimensional nozzles capable of Mach numbers 2.4, 3, and 4. A blow down facility, its sixteen storage tanks with a volume of 79 cubic meters are filled by air from four Ingersoll Rand Model 90 reciprocating compressors. The system is water cooled, and the air is passed through driers and oil absorbers to clean the flow. The settling chamber is equipped with a perforated transition cone, four screens, and total temperature and pressure probes. A computer-controlled feedback circuit maintains constant total pressure during each run. In the test configuration, pressure was maintained at an absolute pressure of 655 ± 7 kPa

(95 ± 1 psi) for approximately 8 seconds. Total temperature dropped by about 13% during each run because of adiabatic expansion in the storage tanks.

2.2 The Model

The stainless steel injector model was placed in the lower half of the Mach 3 nozzle and test section. Shown in Figure 1 on page 135, it consisted of a rearward-facing open step injecting the secondary stream and an upper surface splitter plate separating the injected from the primary stream. The slot height was 1.2 cm (0.47 in.) - on the order of the incoming boundary layer. The splitter plate was as thin as practically possible, 0.052 cm (0.0205 in.), to minimize its wake. The splitter plate was part of a continuous surface on the tunnel centerline from the nozzle throat to the test section. It preserved the nozzle area ratio and served as the tunnel floor. The cross-sectional area of the flow upstream of the injector was 11.4 by 23 cm (4.5 by 9 in.).

The test section floor plate was carefully aligned with the bottom of the slot to prevent shocks or expansions at the joint. The floor plate (made of polished 304 stainless steel) had eight holes, 0.635 cm (0.25 in.) in diameter, for insertion of the probe holders. These holes were located 7.78 cm (3.06 in.) downstream of each measurement station and 2.54 cm (1.0 in.) on either side of the tunnel centerline to allow a check on the two-dimensionality the flow. Free-stream Re/cm were on the order of 2×10^6. The free stream Mach number,

M_∞, was 3.0, and the slot or jet flow had a Mach number, M_j, of 1.7 and a total pressure of 73.8 kPa (10.7 psia) (Figure 2 on page 136). This mild overexpansion was chosen to minimize adjustment shocks at the slot lip. It also turned the main flow slightly toward the floor, which increased the merging of the shear layer and the lower wall boundary layer evident by the last station. To study shock/boundary layer interaction, a 10 degree wedge was used to generate a 27.5 degree oblique shock which intersected the viscous region before the last station. This was compared with the no-shock case.

2.3 The Injector

The injected flow was bled from the main flow upstream of the settling chamber. It passed through an on/off valve into a 2.8 cm (1.1 in.) inner diameter Inconel pipe to a gate valve which regulated the injector pressure. This last valve, once manually adjusted for a 73.8 kPa (10.7 psia) injection pressure, did not deviate more than 0.2 percent. From the control valve, the flow passed through first and second stage manifolds which distributed the flow across the width of the slot. The first manifold split the flow into two streams, and the second distributed the flow through 130, 0.318 cm (.125 in.) diameter holes. A flow straightener honeycomb, capped on both ends with screens and made of 440 - 5 cm (1.97 in.) lengths of 0.476 cm (3/16 in.) diameter steel tubing, followed. From there, the flow passed through a curved plenum chamber and a

converging-diverging nozzle where the air stream was turned 90 degrees to parallel the main flow and accelerated (Figure 3 on page 137). This small nozzle had an area ratio of 1.34. A Pitot probe in the plenum chamber was used to adjust the slot total pressure. The pressure was measured by a Pressure Systems, Inc. Digital Pressure Measurement System, model 780B/T. It had a Data Acquisition and Control Unit, a Pressure Calibration Unit, and a 32-port remote transducer array. The system automatically calibrates its transducers immediately before acquiring data. The plenum total pressure was monitored during tunnel operation as it was adjusted.

In the ambient temperature injection case the total temperatures of both streams were virtually the same, nominally 300 K. In the case of heated injection, eleven band heaters made by Chromalox, catalog no. HBA-32050, drawing 500 watts each and 4 linear heating elements drawing 300 watts each heated the pipe (Figure 4 on page 138). Its temperature varied between 644 and 811 K (700 and 1000°F).

Monitored with a chromel-alumel thermocouple and a Microcomputer Thermometer Model HH-71K2 made by Omega, the total temperature of the injected flow near the slot was maintained between 413 to 433 K (283 to 320°F) through trial and error. T_{t_j} was measured with an Omega chromel-alumel 0.005 inch thermocouple. Its output was displayed on a Moseley Model 7100B Strip Chart Recorder using a Model 17501A amplifier. Other factors which affected slot-temperature adjustment included the outside temperature and the number and frequency of previous runs.

2.4 The Optical System

The facility is equipped to take both nanosecond Shadowgraphs and spark Schlierens. The light source for the Schlierens was a General Radio Company Type 1531-AB Strobotac with a 1.2 μs flash. The source for the nanosecond Shadowgraphs was a Xenon Corporation Novatron 289B Nanopulse Lamp powered by a Model-437A Nanopulser which had a 20 nanosecond flash. The light from the sources was reflected by a collimating mirror into the test section to illuminate it with a parallel beam of light. The photographic plate was placed 30 cm (11.8 in.) from the window for the Shadowgraph. For the Schlieren photographs the light beam was focused on a horizontal knife-edge (to emphasize vertical gradients) before entering the camera. The film was Polaroid Type 57 (ASA 3000), and the windows are of Schlieren quality.

Chapter 3

INSTRUMENTATION

3.1 Computer

An IBM-PC controlled tunnel operation and data acquisition using the FORTRAN program, Hwstep.FOR, listed in Appendix C. Installed in the PC was a Metrabyte model Dash-16F multifunction, high-speed, A/D I/O expansion board with a maximum sampling rate of 100 kHz. The board sent tunnel control messages and digitally sampled analog signals from the various probes. A schematic of the instrumentation is shown in Figure 5 on page 139. Signals in the 0-10V range were converted to digital values from 0 to 4095. The PC has 512k RAM, with 64k configured as a virtual disk, and a clock speed of 4.7 MHz.

The computer opened a pneumatically-actuated butterfly valve to start the run. The program then sent a signal setting the operation pressure to a feedback

circuit that controlled the tunnel stagnation pressure by the action of a hydraulically-actuated valve. The computer also controlled the stepper motor that moved the probe, changed the wire overheat ratio, recorded input signals, and closed the butterfly valve to end the run.

3.2 Input Signals

3.2.1 Settling Chamber Probes

The total temperature in the settling chamber, T_{t_∞} , was measured by a precision, fine wire, butt-welded Chromel-Alumel thermocouple made by Omega Engineering Incorporated. The 0.0127 cm (0.005 in.) diameter probe had a time constant on the order of 0.1 second [24]. The signal was amplified by a Thermocouple D. C. Millivolt Amplifier model Omni IIB, type K, (Omega, Inc.) with a built-in ice point junction and gain set at 100.

The total pressure in the settling chamber was measured by a Pitot probe with a 0-100 psia Setra Systems 50 mv/psia pressure transducer. In addition to being recorded, the signal was used in the controller feedback circuit which regulated the tunnel pressure.

3.2.2 Hot-Wire Probe and Traverse System

The hot wire used was a Dantec miniature wire probe, model 55P11, shown in Figure 6 on page 140. It is a straight probe with the sensor perpendicular to the probe axis and has a length of 1.25 mm and diameter of 5μm, giving an l/d ratio of 250. It has a listed maximum operating temperature of 300 C, maximum ambient flow temperature of 150 C, and maximum flow velocity of 500 m/s. The temperature coefficient of resistance of the platinum-coated tungsten wire was 0.0036/C at 20 C, and the resistance was nominally 3.5 ohms.

The probe support shown in Figure 6 was a model 55H20 from Dantec. It was bonded with epoxy to the inside of a cantilevered probe holder made of stainless steel tubing and connected to a stepper motor (Computer Devices Corporation, model 34D-9209A). Following the computer's instructions, the traverse motor moved the probe assembly through one of the eight access holes in the test section floor plate. Originally constructed of 0.476 cm (3/16 in.) tubing, the probe holder was strengthened by a 0.635 cm (1/4 in.) stainless steel sleeve on its straight portion to prevent flexing under aerodynamic load. Movement of the probe displaced a Trans-Tek Series 240 linear voltage displacement transducer (LVDT) which produces a voltage linearly corresponding to each height.

3.2.3 Hot-Wire Anemometer Circuit

The constant temperature hot-wire circuit was designed by Walker [18] to step the hot wire through 8 wire temperatures in quick succession, each temperature lasting 10 milliseconds (Figure 7 on page 141). A final 10 msec delay after the last temperature allowed the wire to reach thermal equilibrium at the lowest overheat at the next vertical position. Ten msec is on the order of 1000 integral times, so taking less than 1000 samples assures that each sample is independent of the previous one.

A simplified diagram of the hot-wire bridge, Figure 8 on page 142, shows R_1 and R_2 , which were equal to 7.54Ω, and R_3, equal to the resistance of the hot-wire leg and its leads to the circuit. Therefore, the wire temperature was varied by changing R_3. A sample sequence of stepped wire voltages is shown in Figure 9 on page 143. Depicted are digitized voltages at two vertical positions as the wire temperature was cycled. An overheat level is defined as $\frac{R_w - R_{w_{ref}}}{R_{w_{ref}}}$, a ratio involving the operating and reference resistances. Since changes in the wire resistance are proportional to changes in the wire temperature, setting an overheat is equivalent to setting a wire temperature. The Metrabyte board stepped the hot wire by switching a series of mercury relays that are part of R_3. In addition, the whole series of overheats can be uniformly offset by a set of switches on the printed circuit board to compensate for different hot-wire reference resistances (referenced at 20 C) to obtain appropriate wire operating temperatures. At the chosen setting, R_3 had a minimum value of 4.74 ohms and

a maximum of 7.28 ohms. The highest wire temperatures produce the best sensitivity, largest signal to noise ratio, and largest voltage signal [19]. On the other hand, they have less total-temperature sensitivity, and operating at temperatures near 300 C can cause oxidation which changes the wire cold resistance.

3.2.4 Signal Protection and Filtering

Large amounts of noise initially contaminating the input signals were reduced by several methods. Buffers were placed at the outputs of the pressure and temperature probe circuits to prevent loading of their amplifiers. Ringing in the hot-wire and total pressure coaxial transmission cables was eliminated by resistors at their outputs. Load resistors were connected across all of the Metrabyte board's inputs for the same reason. Right before input to the Metrabyte A/D ports, the LVDT and total temperature signals were filtered by four pole Bessel filters with buffered inputs and 400 Hz cutoff frequencies; see Figure 10 on page 144 [22]. Bessel filters were chosen for their uniform time delay (0.011 seconds) independent of frequency. Elimination of power supply 60 Hz noise required placement of ceramic and electrolytic capacitors between power leads and ground in all amplifiers, buffers and filters.

Chapter 4

PROCEDURES AND SIGNAL PROCESSING

4.1 Measurement Stations

Four streamwise measurement stations were chosen. Representing the slot height as H, the stations were x/H = 0.25, 4, 10, and 20. For the purpose of defining streamwise stations, the nominal value of H was used, 1.27 cm (0.5 in.). The actual slot height, 1.21 cm (0.475 in.), was used to specify dimensionless height, y/H. Station 1 was located as near as possible to the x = 0 plane to document the initial conditions, but was complicated by waves from the slot and the flow adjustment at the splitter-plate lip. Station 2 was a more practical initial point for computational simulations. Station 3, an intermediate region, was placed where the shear layer and the lower boundary layer were still separated. By Station 4 the potential core had virtually disappeared.

4.2 Mean Flow Measurements

In addition to the hot-wire measurements, complete measurements of mean flow conditions were taken of the same model at the same time. This is the topic of the paper by Smith [23]. Static pressure was measured by a cone probe with a 10° half-angle. It had four ports drilled perpendicular to its surface to reduce its sensitivity to misalignment. The time constant of this probe, measured at 0.08 seconds [1], was significant because data were taken in short intervals: a profile was measured in eight seconds. A Pitot probe measured total pressures. Total temperatures were measured by a diffuser thermocouple probe. It had a ceramic tip to reduce errors caused by radiation and conduction in the probe and had a recovery factor of about 0.98 [22]. It was made with a 0.0127 cm (.005 in.) chromel-alumel thermocouple from Omega with an expected time constant of 0.1 second [24]. The probes had sampling areas of about 1 mm^2 (0.0016 $in.^2$). Traverses were up to 3.5 slot heights from the floor.

All of the probe holders were of the same form as that for the hot-wire - a 3/16 inch o.d. cantilever stainless steel tube with an additional 1/4 inch o.d. stainless steel tube to strengthen the vertical portion. The settling chamber total temperature and total pressure and the probe height were described earlier.

Measured quantities were free-stream total temperature and total pressure, total pressure and total temperature at each station, and cone-static pressure. Major computed outputs were mean profiles of Mach number, static pressure, density, velocity, and total temperature coefficient.

Profiles of $\overline{\rho u}$ were used to calibrate the hot-wire probe. They were also used along with the hot-wire data to calculate $\overline{u''}$.

4.3 Data Reduction

4.3.1 Auxiliary Variables

At each of the four streamwise stations, measurements were taken at 105 vertical positions above the lower wall. During each run, turbulence was measured at 35 positions, 1/3 of an entire profile. There was a small vertical overlap of 0.6 mm (0.024 in.) between runs. The probe, which started at the floor, was lowered back to the floor at the end for protection from the unstarting shock. The probe was traversed to its maximum height, y/H = 3.5, in one 35-position hot-wire calibration run. T_{t_∞} , p_{t_∞}, and the LVDT were sampled simultaneously at 2 kHz with 16 samples of each taken at each location. To avoid the slow process of writing to a file during a run, the computer held the mean values in an array during each run and wrote them to a file on a diskette after the traverse was completed. Because the Metrabyte board's DAS16FOR FORTRAN library limits array sizes to 16,350 two-byte samples and 44,000 hot wire samples were taken during a traverse, the hot-wire data array was transferred to a RAM disk after each height. It, too, was written to a floppy disk

after the run. It was written in binary form because of its high transfer rate and to conserve space on the 5 1/4 inch diskette.

The auxiliary equipment needed to be calibrated. First, all equipment was hooked up exactly as it was to be used during tests, and voltages were measured at the computer's A/D inputs along with the environmental conditions causing them. Accurate pressures were applied to the pressure transducer by a Mansfield and Green pneumatic dead-weight pressure tester, type K, model MK 100, accurate to 0.05 percent. The thermocouple was placed in a water bath whose temperature was varied from 0 to 100 C. The temperature was measured with a thermometer accurate to 0.5 C. For each probe a series of at least 8 points was fitted with a straight line calibration curve.

Heights were measured by a PTI cathetometer, catalog number 2210, which can be read to 0.001 cm (0.0004 in.), but our results were repeatable only to 0.02 cm (0.0079 in.). To find the initial probe position, the height of the probe and its reflection on the floor were measured and the difference divided by two; this divided any errors. This was done for each probe at each station. For each station, the slope was found using multiple voltage/height pairs. Voltages in all cases were multiplied by 409.5 since the metrabyte measures 0-10 volts in the digital sequence 0 to 4095.

To avoid transient or slew-rate problems which may have occurred, the beginning and ending points of all three channels were dropped, leaving 14 samples per location per channel for analysis. An intermittent problem never

resolved, the switching of recorded input channels by the Metrabyte board, could only be corrected manually after the data were partially reduced.

4.3.2 Hot Wire

The derivation shown below follows Walker,Ng, and Walker [18].

At each height, data were taken at as many as eight distinct overheats. In all of our cases, the seventh and eighth overheats were the same. In the heated injection cases overheats 1 and 2 were sometimes the same. In the cold injection cases 156 samples per overheat were taken. In the hot injection cases 159 samples per overheat were taken. During analysis, the first and last samples were dropped as above. In addition, the largest and smallest samples were removed to eliminate possible spurious data caused by oil impact on the wire. Averages, mean square values, and variances were calculated using the remaining points, as shown in Figure 11 on page 145 and Figure 12 on page 146. Figure 11 is a plot of the average digitized voltages at Station 3 in the unheated case; one curve represents each overheat. Figure 12 is a similar plot of the rms voltage where the peaks correspond to increased turbulence.

A considerable amount of compressor oil contaminated the flow during several of the heated injection measurements. Impacts occuring during the third and sixth overheats are shown in Figure 13 on page 147, a plot of digitized voltage versus sample number. In an attempt to remove the affected data, values outside of 2.9 standard deviations from the mean were removed as specified by

Chauvenet's criterion [25]. This scheme was ineffective, however, because the most important oil strikes were those that changed the values of a large percentage of the 159 samples, distorting the mean and standard deviation. As a result, this method had virtually no effect on the oil problem and was removed from the reduction process to increase its speed. Consequently, it was necessary to discard all data from a small percentage of probe locations. Program Ave.FOR (listed in Appendix C) handles the above tasks: removing points; forming rms, mean square, and average values of the hot-wire data; and using appropriate calibration curves to calculate temperature, pressure, and height. The partially reduced files, greatly diminished in size, were easily manipulated.

In the highly turbulent, compressible flow encountered in this study, the heat loss of a cylinder normal to the flow depends on mass flux and total temperature. From Kovásznay we get Nu = Nu(l/d, M, Re, Pr, τ). The wire length-to-diameter ratio is l/d. The local Mach number and the Prandtl number are M and Pr, respectively. The temperature loading factor, τ, is $\frac{T_w - T_e}{T_t}$. T_e is the equilibrium temperature the unheated wire would reach if placed in the flow. This is typically greater than 97% of T_t. The other dimensionless numbers are defined here as

$$\text{(4.1)} \qquad \mathrm{Nu} = \frac{q_w}{\pi l_w (T_w - T_e) k_t} \quad \text{and} \quad \mathrm{Re} = \frac{\rho u d_w}{\mu_t}$$

The Reynolds number is based on the wire diameter. Note that the total temperature and a viscosity and a thermal conductivity based on the total temperature are used to calculate Nu and Re. This is plausible since much of the

heat transfer takes place in the stagnation region. The heat transfer rate, $q_w = i_w^2 R_w$, was substituted for the wire resistance heating [14].

If the Prandtl number is assumed constant and the wire length is large compared to the diameter (250 times larger in this case), Nu = Nu(Re, M, τ), which reduces to King's formula for $M \simeq 0$. The data for a variety of supersonic Mach and Reynolds numbers collapse onto a line of equation, $\mathrm{Nu} = (a\sqrt{\mathrm{Re}} + b)(1 - C\tau)$, which holds for Reynolds numbers much larger than 1. The constant, C, for a given wire, is less than 1. For a given overheat, i, with its fixed value of τ, this relationship can be reduced to

$$\mathrm{Nu}_i = a_i\sqrt{\mathrm{Re}} + b_i \tag{4.2}$$

Removal of τ and substitution of T_t for T_e result in no error, if this is consistently done in both calibration and later reduction.

Calculation of the Nusselt number proceeds as follows. R_{leads} and R_3 are known. $R_w = R_3 - R_{leads}$ and $i_w = \dfrac{E_T}{R_2 + R_3}$. E_T, the voltage drop across the hot-wire bridge, is given by $E_T = E_{metrabyte} \times 1.0656$, found by a simple circuit analysis. The wire temperature in Kelvin is

$$\mathrm{T}_w = 20 + \frac{R_w - R_{w_{ref}}}{R_{w_{ref}}\,\alpha_{20}} + 273.15 \tag{4.3}$$

The reference wire temperature is 20 C. The temperature coefficient of resistance, α_{20}, is 0.0036/C, assumed constant. In cases of unheated injection, T_{t_∞} was used for the total temperature since it was measured during the hot wire runs.

Although not rigorously applicable in the slot flow, T_{t_∞} was accurate to within 2% even in the slot. During heated injection, however, the total temperature measured in the slot during corresponding mean flow runs by Smith was used [23]. Because the flow total temperature varied from run to run with the outside temperature, cooling water temperature, and compressor temperature, values of T_{t_∞} were used in the the free stream. Since these temperatures only have a role in calculating μ, k , and $(T_w - T_t)$, any slight inaccuracies introduced were not critical.

Calibration requires the calculation of the wire Nusselt number as well as an independently measured Reynolds number. Mean flow measurements by Smith yielded a profile of $\overline{\rho u}$ [23]. In regions of low turbulence away from mixing zones and boundary layers, this is used to approximate $\overline{\rho u}$. This, in turn, is part of $\sqrt{\overline{Re}}$ which approximates $\overline{\sqrt{Re}}$, the quantity in eq. (4.2) when its mean is taken. The viscosity of air was calculated using the Sutherland formula, and thermal conductivity was calculated using a curve fit of a table in Reference 38.

Using the mass fluxes of the free-stream and the potential core regions at Station 2 provided a spread of $\sqrt{\overline{Re}}$ values from 5 to 11 with which to calculate a least squares curve fit for eq. (4.2). The result, a set of calibration constants a_i and b_i for a given wire, is valid in supersonic flow as long as the wire properties do not change (for example $R_{w_{ref}}$) because of oil strikes or oxidation. Program Calib.FOR calibrates each wire given $R_{w_{ref}}$ and data pairs of average Nusselt and Reynolds numbers. For example, wire B was calibrated as in Figure 14 on page 148, where the lines represent eq. (4.2) for each overheat. Its match to a mean

flow result is in Figure 15 on page 149. Figure 15, a pair of mean mass flux profiles, shows the $\overline{\rho u}$ profile from a hot-wire calibration run and illustrates how it was forced to match, in the slot and in the free stream, the $\overline{\rho u}$ profile found by the mean flow probes. Appendix F contains calibrations of other wires.

With the wire calibrated, all that is needed to resolve $\overline{\rho u}$ (and $\overline{T}_t$ as a check) is an independent total temperature measurement. Equation (4.2) was solved for T_t, $\sqrt{Re}$, and $T_t\sqrt{Re}$, and the mean was taken. The result is

$$z_i = \overline{\sqrt{Re}} - \overline{T}_t y_i - \overline{T_t\sqrt{Re}}\, x_i \tag{4.4}$$

where

$$z_i = \frac{\overline{(E_i^2)}}{a_i R_{w_i} \pi l_w k_t T_{w_i}} - \frac{b_i}{a_i}, \quad y_i = \frac{b_i}{T_{w_i} a_i} \quad \text{and} \quad x_i = \frac{1}{T_{w_i}}$$

The variables z, x, and y are known at each of the N wire temperatures. The correlation was treated as an independent unknown. Because its value should be the product of the other two unknowns, it served as a consistency check. Solving three equations and unknowns yields unsatisfactory results because the matrix is nearly singular. Instead of forming a simple 3x3 matrix, a least squares analysis was performed [26]:

$$Error_i = z_i - \overline{\sqrt{Re}} + \overline{T}_t y_i + \overline{T_t\sqrt{Re}}\, x_i \tag{4.5}$$

Each overheat's error was squared, and the sum of all of these squared errors was found. Setting the derivatives with respect to each unknown of the sum of errors

equal to zero formed a new matrix. Its value is fixed for each wire. N is the number of overheats. The matrix is

$$(4.6)\qquad \begin{bmatrix} -N & \sum_{i=1}^{N} y_i & \sum_{i=1}^{N} x_i \\ -\sum_{i=1}^{N} y_i & \sum_{i=1}^{N} y_i y_i & \sum_{i=1}^{N} x_i y_i \\ -\sum_{i=1}^{N} x_i & \sum_{i=1}^{N} x_i y_i & \sum_{i=1}^{N} x_i x_i \end{bmatrix} \begin{bmatrix} \overline{\sqrt{Re}} \\ \overline{T}_t \\ \overline{T_t \sqrt{Re}} \end{bmatrix} = \begin{bmatrix} -\sum_{i=1}^{N} z_i \\ -\sum_{i=1}^{N} y_i z_i \\ -\sum_{i=1}^{N} x_i z_i \end{bmatrix}$$

The use of redundant overheats minimizes errors, which can have a large effect on an ill-conditioned matrix. In such a case, small changes in the matrix coefficients can cause large changes in the answers. This least squares analysis makes the coefficients as accurate as possible; but, in practice, the determinant is still near double-precision machine zero in relation to N. To improve the condition, the temperature unit was converted to 1000's of degrees Kelvin, which makes the components and determinant of the matrix of order one. Program Mean.FOR builds this matrix and performs matrix operations in double precision. The data was smoothed by a binomial three-point spatial filter.

Turbulence quantities, $(\rho u)'$ and T_t' , were also resolved using equation (4.2). First, it was rewritten as $i_w^2 R_w = \pi\, l_w\, k_t (T_w - T_e)\,(a\sqrt{Re} + b)$. Substitution of $E_w^2 = i_w^2 R_w^2$ puts the equation in terms of the wire voltage,

$$\frac{E_w^2}{R_w} = \pi\, l_w\, k_t (T_w - T_e)\,(a\sqrt{Re} + b) \tag{4.7}$$

Taking the logarithmic derivative with respect to time of both sides results in

$$\left(\frac{e}{\overline{E}}\right)_i = -f_i\left(\frac{m}{\overline{m}}\right) + g_i\left(\frac{T_t}{\overline{T}_t}\right) \tag{4.8}$$

where

$$f_i = \frac{1}{4\left(1 + \dfrac{b_i}{a_i\sqrt{Re}}\right)} \quad \text{and} \quad g_i = -\frac{\overline{T}_t}{2(T_{w_i} - \overline{T}_t)}$$

and e, m, and T are zero-mean instantaneous values. Equation (4.8) relates wire voltage fluctuations to the flow changes which cause them. Squaring this equation and taking the mean produces a 3x3 matrix. Again, since this matrix is ill-conditioned, its errors were minimized by forming its coefficients with the least squared error. The resulting matrix, also using multiple overheats, is

$$(4.9)\qquad \begin{bmatrix} \sum_{i=1}^{N} f_i^4 & \sum_{i=1}^{N} f_i^2 g_i^2 & 2\sum_{i=1}^{N} f_i^3 g_i \\ \sum_{i=1}^{N} f_i^2 g_i^2 & \sum_{i=1}^{N} g_i^4 & 2\sum_{i=1}^{N} g_i^3 f_i \\ 2\sum_{i=1}^{N} f_i^3 g_i & 2\sum_{i=1}^{N} g_i^3 f_i & 4\sum_{i=1}^{N} f_i^2 g_i^2 \end{bmatrix} \begin{bmatrix} \left(\frac{m'}{\overline{m}}\right)^2 \\ \left(\frac{T_t'}{\overline{T}_t}\right)^2 \\ \left(\frac{m'T_t'}{\overline{m}\overline{T}_t}\right) \end{bmatrix} = \begin{bmatrix} \sum_{i=1}^{N} f_i^2 \overline{\left(\frac{e'}{\overline{E}}\right)^2} \\ \sum_{i=1}^{N} g_i^2 \overline{\left(\frac{e'}{\overline{E}}\right)^2} \\ \sum_{i=1}^{N} f_i g_i \overline{\left(\frac{e'}{\overline{E}}\right)^2} \end{bmatrix}$$

Unlike the previous case, mean-flow conditions enter into the matrix coefficients. Since they are subject to change, measurements must be completed before the mean conditions can change, hence the value of high-speed sampling. Taking the derivative of eq. (4.8) is an inherent approximation of a linear relation between wire voltage and the local mass flux. This is discussed in Appendix B and in Conclusions. Program Rms.FOR fills this matrix (this must be done at each height) and inverts it in double precision. A simplification it uses is

$$(4.10)\qquad \left(\frac{e'^2}{\overline{E}^2}\right)_w = \left(\frac{e'^2}{\overline{E}^2}\right)_{metrabyte}$$

There is no need to convert to the wire voltage in this case.

Scatter in the turbulence data resulted in some negative values, especially in T_t', which were removed before the data were smoothed by a five-point

binomial spatial filter. Also removed before filtering (to end the overlapping of runs) were the two lowest samples in each traverse. The computations encoded as FORTRAN programs Ave.FOR, Calib.FOR, Mean.FOR, and Rms.FOR are listed in Appendix C.

In the calculation of the Favre-averaged velocity, a term often neglected is $\frac{\overline{u''}}{\overline{u}}$. A formula derived from its definition is $\frac{\overline{u''}}{\overline{u}} = 1 - \frac{\overline{(\rho u)}}{\overline{\rho}\,\overline{u}}$. The hot wire supplies $\overline{\rho u}$, and the mean probe measurements of Smith provide $\overline{\rho}$ and $\overline{u}$ [23].

Chapter 5

RESULTS

5.1 Slot Injection

5.1.1 Spark Schlierens and Nanosecond Shadowgraphs

Figure 16 on page 150 and Figure 17 on page 151 are spark Schlieren photographs of the entire flow field. Together with the flow diagram of Figure 2, they reveal the major features of the flow. With the settings used here, Schlierens respond to the first derivative of density, making rarefactions appear as light regions and compressions appear dark.

Clearly seen are the low-energy acoustics in the free stream, probably a significant part of the $(\rho u)'$ observed there. The expansion fan and shock

emanating from the lip of the splitter plate adjust the main stream to the compression of the overexpanded slot flow. Small waves present in the injected stream originate at the joint of the slot and the splitter plate. The shock running from the splitter plate to the floor adjusts the injectant static pressure to that of the main stream, and the reflection of this shock merges with the lip shock in the free stream. The pictures also show the evolution of the incoming boundary layer into a shear layer. After initially angling slightly downward, the boundary/shear layer becomes roughly parallel to the floor by Station 3. From there, the layer appears to grow - primarily downward.

Some differences in the pictures exist. The wave caused by a small surface step upstream of the splitter plate in the case of heated injection slightly changed the free-stream conditions. Smith found that M_∞ at Station 1 dropped by 3.5 percent in the heated case [23]. The complete disappearance of the central core of the unheated injectant near Station 3 is an artifact of the lighting only. The boundary layer in the unheated slot flow does appear to grow the fastest, however, despite its higher Reynolds number. Due to the density gradients in the heated cases, the other difference caused by changing the injectant temperature is a lighter white streak leaving the splitter plate beneath the boundary layer. The initial main-stream boundary layer thickness measured from the Schlieren photographs was about 7 percent larger in the heated case. This small change in the initial conditions resulted in a slightly thicker shear layer downstream. This obscured any subsequent change in thickness of the shear layer that may have been caused by heating the injectant. Inconsistencies in lighting prevent

resolution of more differences in the flows, but these are apparent in the figures discussed below.

Nanosecond Shadowgraphs, responding to the second derivative of the density distribution, reveal the strongest gradients more clearly than do Schlierens. The complexity of the shock structure and the small scale turbulence is clearer in Figure 18 on page 152. The scale of the largest visible turbulent structures in the shear layer of the heated case was on the order of 1/3 of its thickness. It appears about twice as large as and is better defined than that in the nanosecond Shadowgraphs taken by Campbell for the unheated case [22]. The increased structure size is an indication of the entrainment of large pockets of low-density gas into the lower-temperature shear layer. Lighting differences were less of a factor in this case. The large-scale structure angle in both cases appears about 50 degrees.

5.1.2 Mean Mass Flux and Temperature Profiles

Figures 19 through 21 show the mean measurements derived from the averaged hot wire signals. The mean mass flux intensities of Figure 19 on page 153 have been normalized by their respective free streams values, $[\rho(t)u(t)]_\infty$, listed in Table 1. This was done for two reasons. Initial flow conditions were slightly different between heated and unheated cases (such as the upstream wave) because they were measured at different times. It was difficult to precisely duplicate them for each session in the tunnel. Also, because of the interaction of

the primary flow with the shear layer, the local free-stream mass fluxes were different at each station. For example, the free stream of Station 2 is directly below the lip shock. Free-stream values are functions of time because T_{t_∞} is. Note that the mean variables present in the profile figures are not indicated by an over-bar as they are in the text. Appendices A, D, and E contain corresonding dimensional profiles and tables of the plotted values.

The profiles of Station 1 in Figure 19 correspond well and show the major initial flow change caused by the heating : a roughly 33 percent drop in the mass flux issuing from the slot. The momentum deficit in the heated slot flow is seen to remain essentially unchanged through Station 3. The lower shear-layer mass flux values in the heated injection cases of Stations 2 and 3 (y/H = 0.8 to 1.7) are due partially to the diffusion of heated gas upward from the slot flow. Additionally, the heated injectant warmed the splitter plate in this case so that the conditions upstream of the slot are slightly different. The differences between the shear-layer values of the Station 2 and Station 3 profiles may be slightly exaggerated, because the temperature profiles discussed below show only a slightly elevated temperature in this region. Possibly, the profiles are shifted vertically with respect to each other because the data were taken during different sessions in the tunnel. By Station 4, where the relative position of the shear layer mass fluxes has reversed, the profiles have nearly merged; but the heated-case injectant seems to have picked up more momentum from the free stream. Profiles of the slot flow no longer show a vertical segment at Station 4, indicating that the potential core has deteriorated. As seen in the photographs, the top of the shear

layer stays near y/H = 1.6 at all of the stations, but the bottom of the layer moves toward the wall.

The mean total temperature of the heated flow profiles was normalized to remove slight variations of jet temperatures, T_{t_j}, from run to run and to compensate for the adiabatic expansion-induced drop in the main stream total temperature, T_{t_∞}. Table 1 lists the jet total temperatures of each run. Figure 20 on page 154 shows the evolution of the distribution of the total temperature variable, $\theta = \frac{\overline{T}_t - T_{t_\infty}}{T_{t_j} - T_{t_\infty}}$. This parameter, chosen to have a maximum value of 1.0, reached this value only at Station 1. The maximum value of θ at Stations 2, 3, and 4 is 0.8. An explanation for the uniform decrease in θ between the first two stations has not been found. One possibility is an error in the measurement of the jet temperature. At Stations 2 and 3, the heated gas had diffused into the shear layer, as noted earlier. By Station 4 the hot slot flow was limited to half its former vertical distribution but reciprocal heating of the cooler gas of the shear layer was somewhat limited. An especially clear demarcation at Station 1 is in contrast to the exponential decay present in the θ profile measured by Smith [23].

The mean total temperature profiles in the case of ambient injection, $\overline{T}_t(y)$, reveal an accuracy in the measurement of the initial free-stream temperature of better than 3 percent (Figure 21 on page 155). Because of the lack of a temperature gradient, the oscillations in the shear layer are more clearly seen in this simple profile than in the θ profile. In general, the temperature measurements had more scatter than the mass flux measurements, and the scatter increased with increased fluctuations in the flow.

5.1.3 Turbulent Mass Flux and Temperature Measurements

Figure 22 on page 156 and Figure 23 on page 157 are plots of turbulence intensity expressed as percentages of the local mean values. The initial injected flow was very uniform in both the heated and unheated cases, and the low turbulence levels only slightly increased by Station 3. The free-stream turbulence levels were slightly elevated in the heated case, especially at Stations 2, 3, and 4. This may be the result of an unsteadiness downstream. Campbell had problems with an unsteadiness in the diffusor propagating upstream [22], which may have reappeared in our measurements. This elevated fluctuation level decreased when the tunnel was operated at higher total pressures.

Scatter in the data resulted in some negative turbulence values in the slot flow, especially at Station 1 where the waves interfered with measurements. The rms total temperature in the heated region had the most such errors. These were removed from the plots before they were smoothed. Listings in Appendices D and E have zeroes substituted for these values.

Comparing heated and unheated turbulence levels in Figure 22, it appears that heating the flow had contradictory effects on the relative magnitudes of the mass flux turbulence. It increased this turbulence at Stations 2 and 3 and slightly decreased it at Stations 1 and 4. Heating the injectant increased the rms mass flux on average, but its effects in this respect may be within experimental accuracy. There is an important effect, however. The peak turbulence in the heated profiles occured lower in the shear layer than that in the unheated cases,

highly correlated with the position of the temperature gradient in the plots of θ in Figure 20. In contrast, in the unheated profiles the maximum mass flux turbulence stayed in the upper middle of the shear layer between y/H = 1.25 and 1.5. Note that this effect is limited at Station 1, where the turbulence peak is close to that of the unheated case. The turbulence distributions in both cases are similar to that of the incoming main-stream boundary layer because the temperature, density, and velocity gradients did not affect the flow appreciably by x/H = 0.25. At Station 4 the turbulence peak had moved to within the injected region, eliminating the remnants of the potential core.

Smits, *et al.*, under similar total pressure and Reynolds number conditions, made hot-wire measurements in a Mach 2.9 boundary layer. When normalized by the free-stream mass flux (not the case in Figure 22), Smits found a maximum mass flux turbulence intensity of 0.12 which occurred at 0.65 δ, the boundary layer thickness [27]. These measurements are in good agreement with conditions at Station 1 in the unheated case. In this case the maximum turbulence intensity (normalized by the free-stream mass flux) was 0.15, and it was located 70 percent of the distance from the bottom of the main-stream boundary layer to its upper edge.

Figure 23 on page 157 shows total temperature fluctuations, which have trends similar to those of the mass flux. In the case of unheated injection, the turbulence intensity, much lower at almost all points than that in the heated injection flow, is nearly zero in the free stream and in the injectant. This is expected because the temperature is essentially uniform over the entire flow.

Slight elevations in the shear layer are largely due to increased scatter resulting from larger flow fluctuations. This was seen earlier in the $\overline{T}_t$ profiles. In the heated flow the turbulence near the wall was low as well, and it reached a peak at Stations 2 and 3 during initial mixing of hot and cold pockets of gas. The turbulence is seen to drop somewhat while spreading across the layer at Station 4, as seen earlier in the rms mass flux profiles.

The calculation of Favre averaged velocity usually neglects the $\overline{u''}$ term shown in Figure 24 on page 158. Comparisons of mass flux profiles found by the hot wire and the mean probes are shown in Figure 25 on page 159 and Figure 26 on page 160. The profiles, which are used to find $\overline{u''}$, compare well in the unheated case except for an apparent vertical shift at Station 1. Since they should match in the low turbulence regions where the two mean mass flux quantities ($\overline{\rho u}$ and $\overline{\rho}\,\overline{u}$) are the same, this is expected. They match less well in the heated case.

The effects of the differences are visible in the $\overline{u''}$ profiles. Still, heating the injectant raised values of this quantity at Stations 2 and 3. At Station 4 the spread of the turbulence toward the wall is seen again.

5.2 Shock Boundary Layer Interaction

5.2.1 Spark Schlieren and Nanoshadowgraph

Figure 27 on page 161 and Figure 28 on page 162 are a spark Schlieren photograph and a nanosecond Shadowgraph of the shock impingement upstream of the last station caused by the 10° wedge inserted into the tunnel. The oblique shock interacts with and penetrates through most of the shear layer and reflects as a shock. Campbell measured a pressure rise on the wall for ambient injection of 1.8 occuring over three boundary layer thicknesses [22]. At Station 4, Smith, in the study coordinated with this one, found a static pressure increase of a factor of 2 between the shocked and shockless cases for heated injection [23]. An approximately ten percent increase in shear layer thickness is clearly seen, although in neither injection case did the boundary layer separate.

5.2.2 Mean Mass Flux and Temperature Measurements

Figure 29 on page 163 compares mean profiles at Station 4 for cases with and without shock interaction in both the heated and unheated injection cases. These profiles are nondimensionalized in the way used in section 5.1.2 to remove run variations. The mass flux in the shock interaction cases was normalized by

the free-stream values of their corresponding shockless cases to reveal the rise in $\overline{\rho u}$ outside of the mixing layer.

The mean temperature in the unheated injection case is unaffected by the shock except for a small increase in the shear layer. Even this may actually be cross-talk from the increased mass flux intensity. All of the regions exhibited the increased scatter typical of this station as seen in Figure 21 on page 155. In the case of heated injection, however, the hotter gas moved farther out into the flow under the influence of the shock, which stopped the progression of the higher temperatures toward the wall that was seen in Figure 20 on page 154. The mass flux profiles showed an increase in $\overline{\rho u}$ above the mixing region but almost no change below. Apparently, the limited shock penetration isolated the secondary flow from some of the shock's effects.

5.2.3 Turbulence Intensity Measurements

Figure 30 on page 164 shows the effect of shock impingement on nondimensional temperature and mass flux turbulence. As before, in section 5.1.3, these values are normalized by local mean quantities.

In unheated injection, as expected, $\frac{T_t'}{\overline{T}_t}$ is unaffected by the shock. In heated injection, however, the large increase in T_t' indicates a large amount of mixing of the warm and cool air streams. This agrees with the large amount of movement of hot air away from the wall seen in the mean profiles of Figure 29.

In the ambient injection case the shock increased $\frac{(\rho u)'}{\overline{\rho u}}$ uniformly up to y/H = 1.5. Free-stream increases also occurred in the expansion fan downstream of the reflected shock. In the heated injectant the turbulent mass flux rose in the lower shear layer under the influence of the shock, decreased in the remnant of the potential core, and increased close to the wall. The effect of the shock was to move mixing away from the wall, to increase the thickness of the lower boundary layer (as seen in the Schlieren), and to counteract the gradient-induced spreading of the mixing into the injectant. In contrast to the Station 4 profiles of Figure 22, the turbulence was concentrated into a small height band. Oddly, the potential core seems more intact with the shock interaction, but the turbulence levels were still higher than those in the ambient injection case. The Favre-averaged velocity shown in Figure 31 on page 165 was not greatly affected by the shock.

Chapter 6

DISCUSSION

A few of the most important uncertainties which may apply unevenly to different runs are listed here. Although the heights appeared to be measured to 0.02 cm, the Station 2 unheated profile of Figure 19 is one example where the discrepancies appear too large. A change in slope would improve the agreement since the outer flow probably should not have changed that much. Another example is the location of the splitter plate wake at Station 1 in Figure 25. A different problem was the inexact duplication of flow conditions. As stated before the free-stream Mach number in the heated-injection case was 3.5 percent lower than in the unheated case, and the free-stream turbulence levels were slightly higher. Furthermore, there were small total temperature variations from run to run, especially between the unheated and the heated cases.

The two aspects of hot wire use considered were this method's suitability for making measurements in heated and unheated flows and its implementation

as a near real-time component of wind tunnel operations. Studies have shown that hot wires operated at a single high overheat require a constant total temperature in order to measure the turbulent mass flux [27,28]. If any temperature variations are present, the multiple overheat method (or a dual wire method) is required.

There were some uncertainties associated with the hot-wire measurements. In the case of heated injection the temperature loading of the wire at each fixed wire temperature changed. The differences in the calibration curves for different overheats illustrates the possible effects of a change in τ. The effects are felt most strongly at the lowest wire temperatures. This could reduce measurements of both $(\rho u)'$ and $\overline{\rho u}$ in heated flow. As an example, Station 1 in Figure 19 shows a 33 percent lower mass flux in flow heated only 40 percent higher. This occurs despite $\rho u \propto \frac{1}{\sqrt{T_t}}$ and could be significant if the other uncertainties had little effect here. In agreement with theory, Smith found a fifteen percent drop in mass flux [23].

Walker and Walker estimate that approximately 90 percent of the turbulent kinetic energy in the flow can be resolved by wires with cutoff frequencies of 100 kHz (Figure 32 on page 166 [21]). This is the measured cutoff frequency of the lowest overheat of this anemometer operating in supersonic flow [18]. The estimate is based on a theoretical spectral distribution of isotropic turbulence. This frequency limit could result in an underestimation of turbulence intensity by up to ten percent, but would apply approximately evenly to all cases. One solution is to improve the freequency response of the hot wire. Another

possibility is to perform a test to estimate the roll-off rate of the turbulence spectrum. The use of a high-pass filter during hot-wire measurements, at several cutoff frequencies below 100 kHz, would produce a curve relating the resolution of turbulent kinetic energy by the wire to that portion of the frequency spectrum above the the cutoff frequency of the filter. These values could be extrapolated beyond the cutoff frequency of the hot-wire circuit, itself. This would be an estimation of the turbulence energy above 100 kHz. A correction factor could then be calculated with which to multiply the turbulence intensities measured by the circuit.

The nonlinear response of the hot wire voltage to the Reynolds number, another possible source of inaccuracies in turbulent regions, probably was not a factor. Figure 33 on page 167 and Figure 34 on page 168 are plots of mass flux intensity versus y/H found using the multiple overheat technique and a single overheat technique. The use of redundant overheats allows measurements of T_t fluctuations. An assumption of a linear hot wire reponse to mass flux changes is inherent in taking the logarithmic derivative of eq. (4.2), however. That was necessary to form the turbulence matrix and is discussed in Appendix B. The use of a single high overheat does not assume linearity. Its reduction assumes that there are no temperature fluctuations, but rms total temperature fluctuations would artificially increase it. Therefore, this curve represent a maximum value of the mass flux turbulence. The agreement is excellent except in the slot and free-stream flows in figure 34. The agreement in the unheated injection case verifies the validity of the multiple overheat method when temperature

fluctuations are small. The discrepancy in the slot might be expected due to reduced temperature loading, as discussed earlier. The lower maximum turbulence values found by the single overheat in the free stream were unexpected. Since the wire was calibrated in such an unheated flow, the two curves should match. The lower wire temperature settings (which are the most sensitive to temperature fluctuations) elevated the turbulence levels indicated by the multiple overheat method. One possibility mentioned by Bradshaw is dirt contamination [29]. This would not change the cold resistance (which did not change significantly in the wires checked for this) but would cause a drop in response at lower overheats.

This problem has yet to be fully understood, but a possible improvement of heated flow measurements is calibration of the wire in the flow to be tested [28]. This was done with all of the wires, but the temperature profile was not duplicated for the wires used in the heated case. Another answer, which must be verified by the above method, is the use of the more complete form of eq. (4.2).

$$\mathrm{Nu}_i = (a_i\sqrt{\mathrm{Re}} + b_i) \times (1 - C\tau) \tag{6.1}$$

Kovásznay used this to collapse all of his curves for different overheats onto the same line [14]. It may also work if the wire is used in conditions where the temperature is significantly different from those used in calibration. This means the calculation of another constant for each wire, however. Furthermore, the curves do not collapse together with this modification, but this may be the only choice if the probe cannot be calibrated in a flow duplicating the total

temperature profile. Finally, these changes may prove unnecessary if the discrepancies are due to probe contamination or another factor.

Much progress has been made toward the production of a high-speed reduction system for hot wire data. The programs listed in appendix C are simple to operate but relatively slow. The major limitation of the system is the speed and memory size of the computer. The small scatter in some of the data can be greatly reduced by taking more samples. This will require a faster sampling rate so that the flow at each height can be sampled before it changes in the mean (which can effect the coefficients in the turbulence matrix). Program Ave.FOR takes six minutes to run under current procedures on the PC, and the other programs require 0.5 minute each. Larger sample arrays will increase these times. Also, the roughly one megabyte of data (in ASCII form) for each traverse makes it impossible to look at raw data quickly since this exceeds the memory of both the computer and a 5 1/4 inch diskette. These reduction problems will be solved by a recently-purchased computer, which has a larger memory and clock speed.

Chapter 7

CONCLUSIONS

Both the heated and unheated injection streams have limited interaction with the main flow because turbulence spreads more slowly into supersonic streams of higher Mach number than into those of lower Mach number. In addition, the shear layer initially turned slightly downward. Increasing the injectant temperature by 40 percent does not appear to affect the spread of the lower region mixing zone (ie. shear/boundary layer, secondary stream, and lower boundary layer) into the outer flow. On the contrary it enhanced the turbulent mixing in the lower region, itself, by involving a greater portion of that flow in the mixing process. This is reasonable, since the large temperature and density gradients caused by heating the injectant are below most of the shear layer. Interestingly, the increased turbulence occurs despite the lower velocity gradient caused by heating the injectant. Although the maximum mass flux turbulence levels were not greatly affected by heating the injectant, mixing was greatly

enhanced in the slot flow by Station 4; and the turbulence scale in the pictures increased substantially. In general, shock interaction increased the level of turbulence and thickened the shear layer. The Favre-averaged velocity, $\overline{u''}$, showed the same trends as the rms mass flux and total temperature. The shock had little effect on this value, however.

The data presented are accurate mean and turbulence measurements in the case of unheated injection, up to the frequency measured. Small problems still remain for the heated case. This study of heated air injection is an intermediate step in a long-term project to study supersonic injection and mixing. Further projects planned or completed include combinations of normal and parallel injection, angled injection, and heated injection. Once the difficulties with large temperature variations are solved and the frequency response is improved (or compensated for), this hot-wire method can be used to measure turbulence accurately in all of these cases.

Chapter 8

APPENDICES

APPENDIX A

Dimensional Profiles

These plots correspond to the nondimensional figures referred to in Chapters 5 and 6 in the text. They are in SI units.

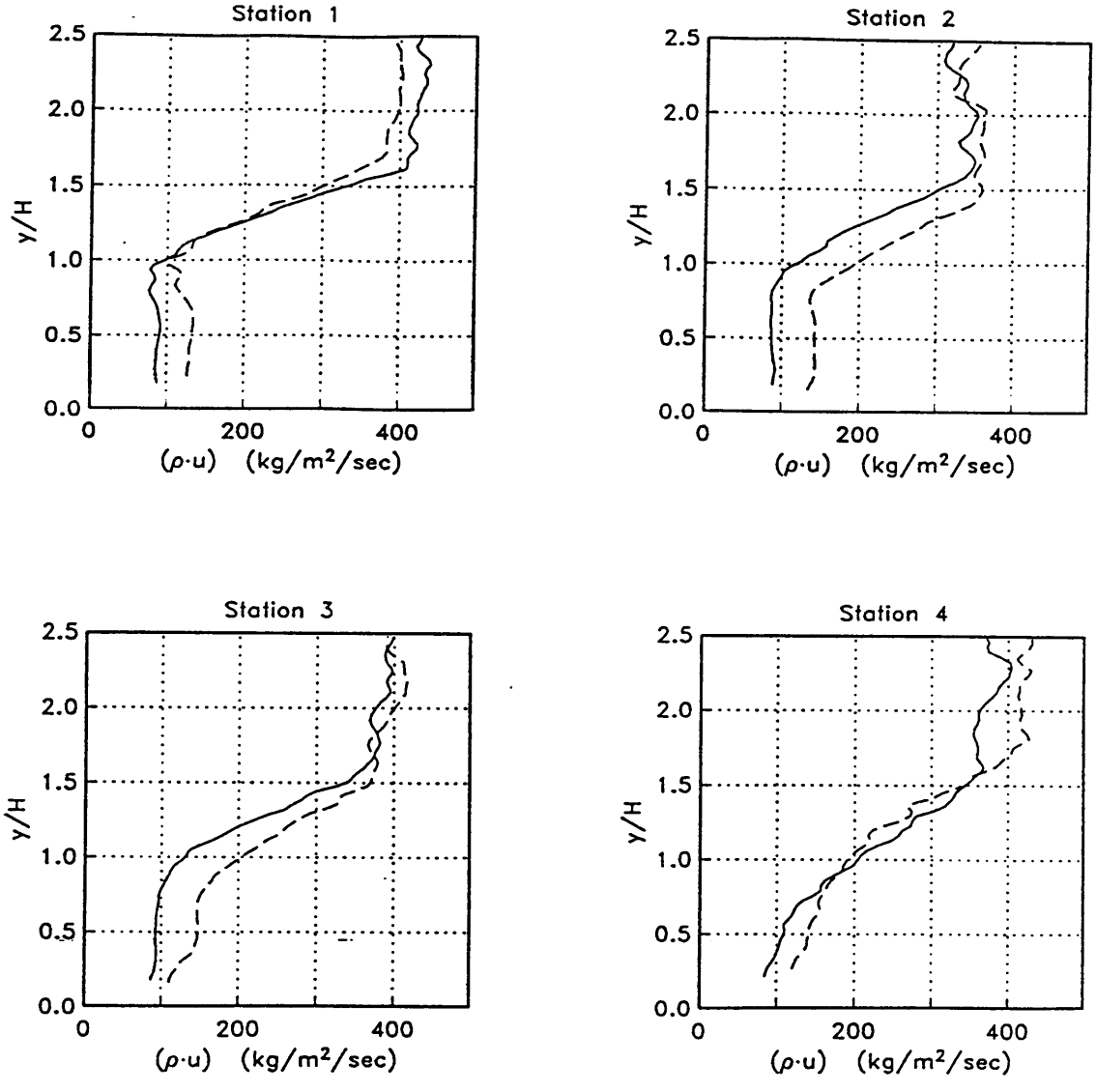

Cold Flow = Dashed Lines

Heated Flow = Solid Lines

Mean Mass Flux Profiles

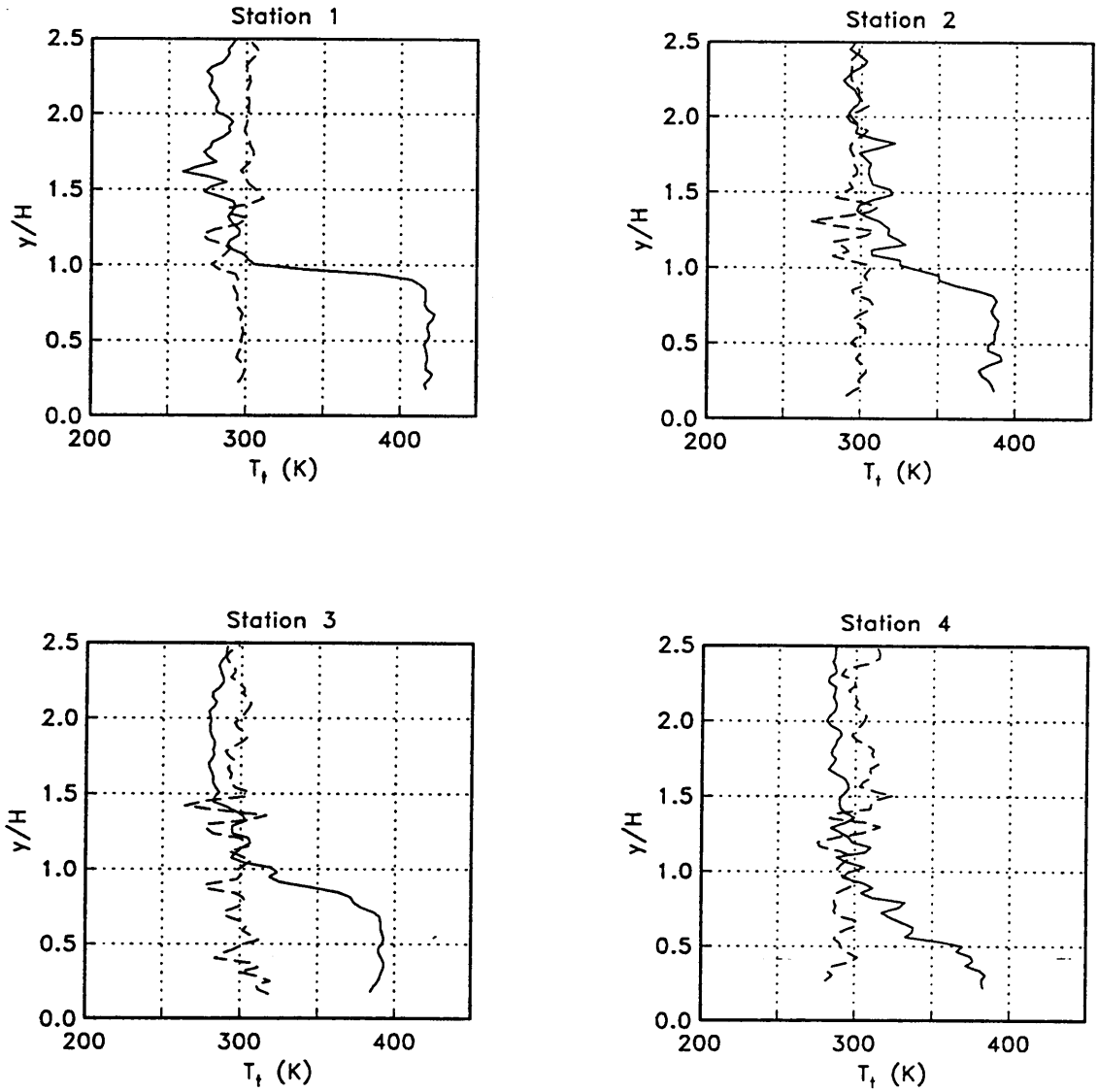

Cold flow = dashed lines

Heated flow = solid lines

Profiles of Mean Total Temperature

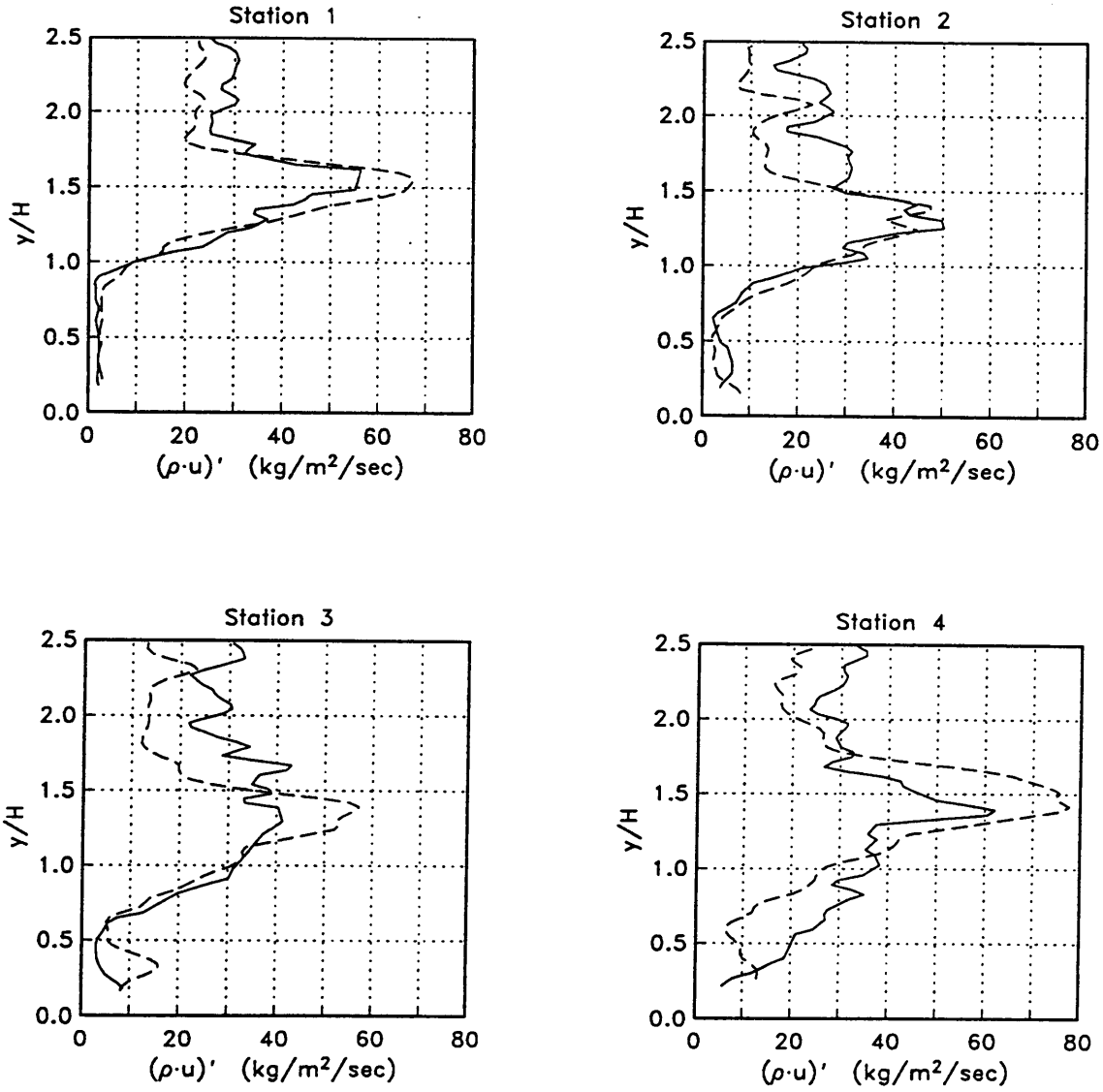

Cold Flow = Dashed Lines

Heated Flow = Solid Lines

Turbulent Mass Flux Intensity Profiles

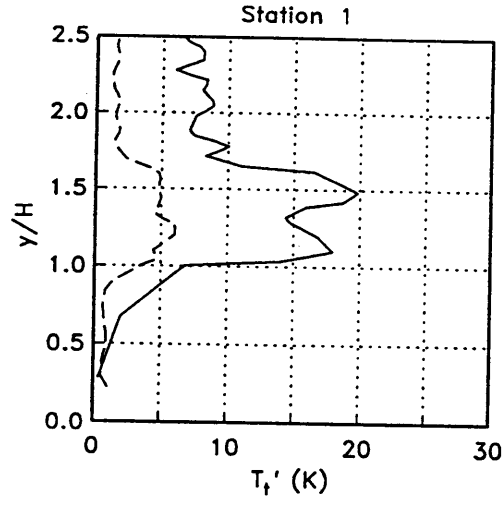

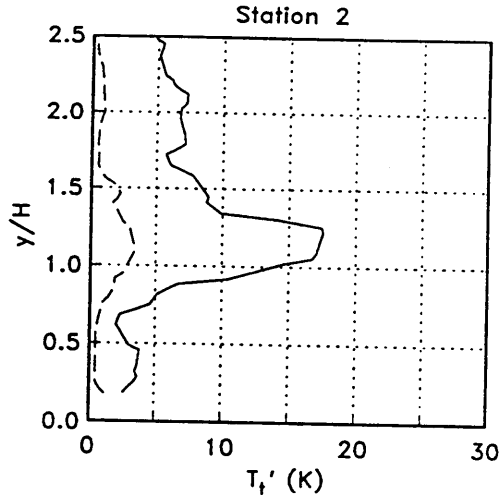

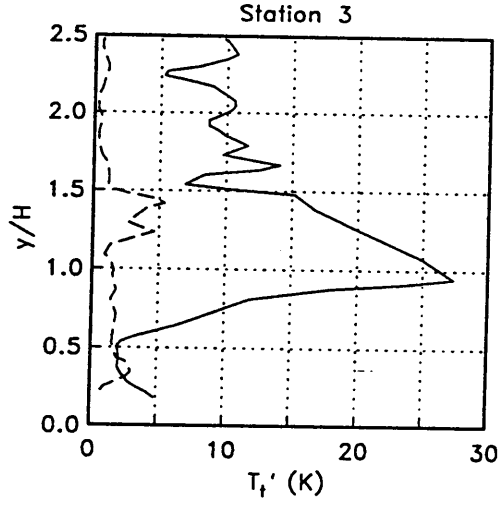

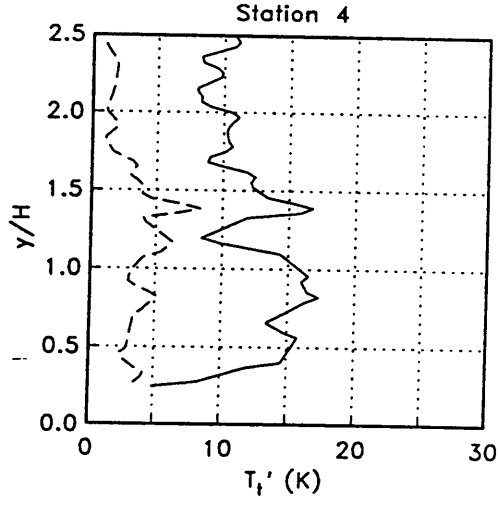

Cold Flow = Dashed Lines

Heated Flow = Solid Lines

Turbulent Temperature Intensity Profiles

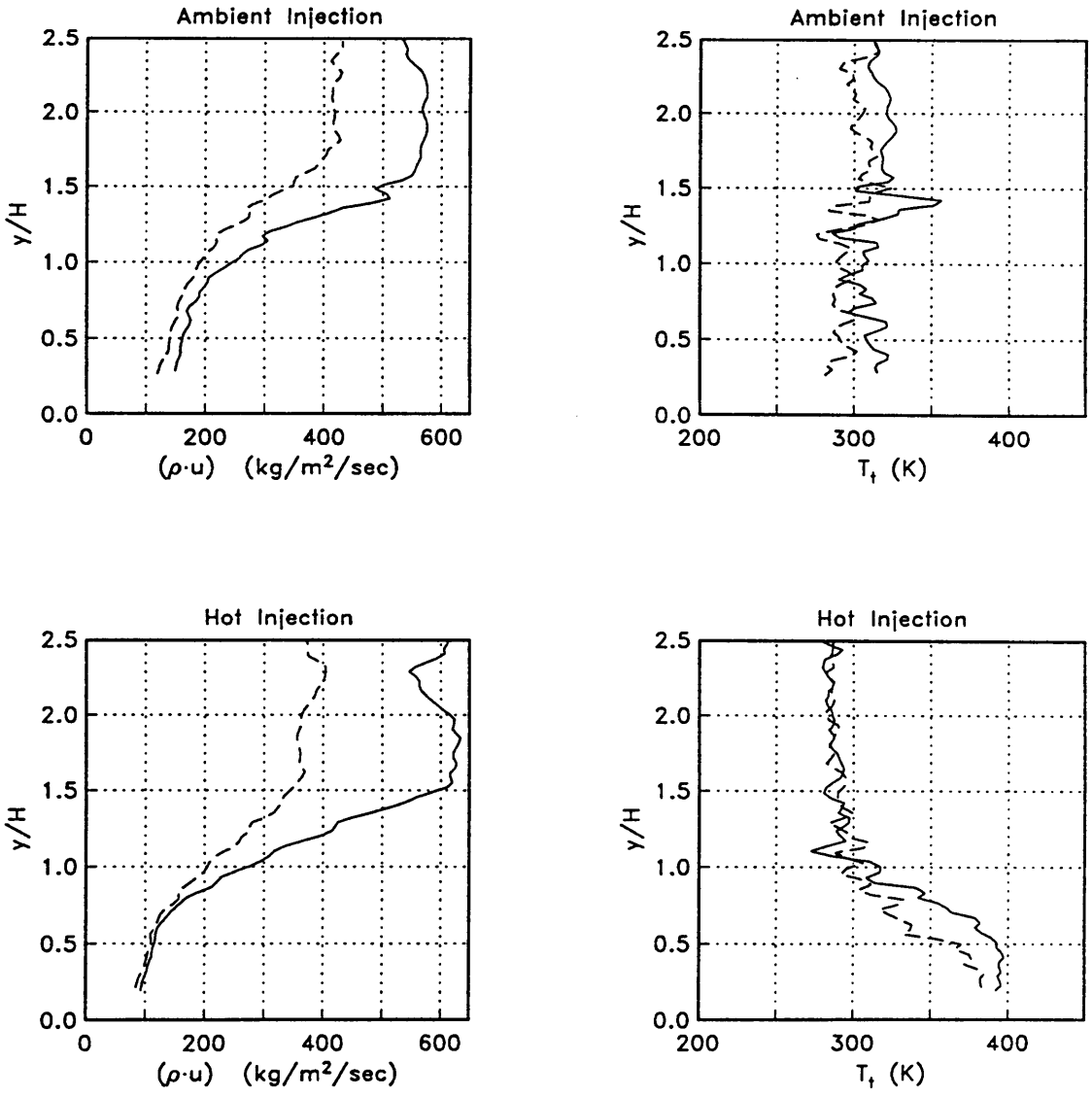

Shockless Flow = Dashed Lines

Shock Interaction Flow = Solid Lines

Mean Profile Changes Induced by Shock Impingement (Stn. 4)

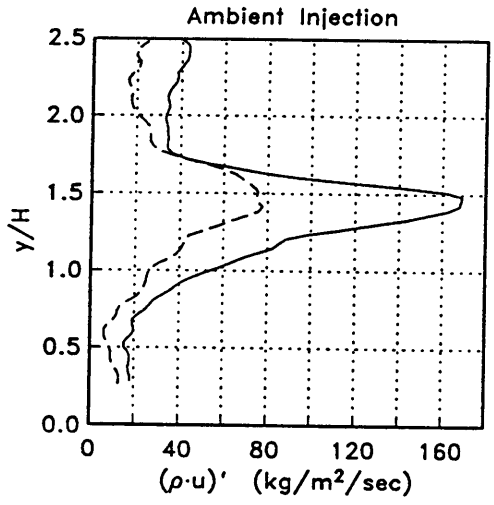

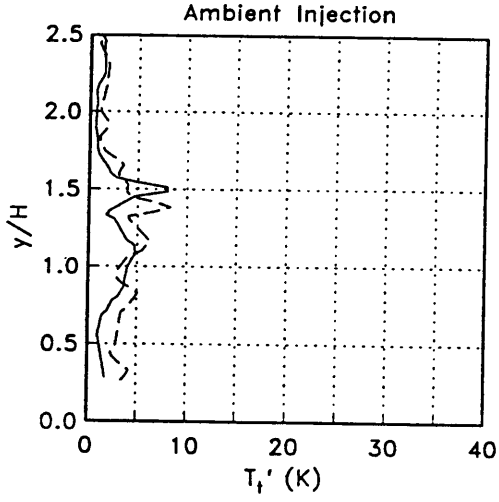

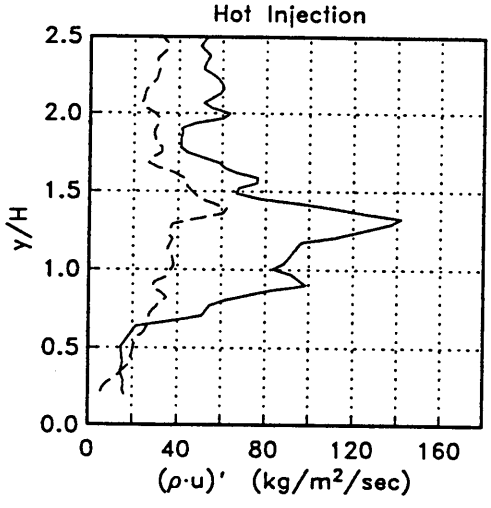

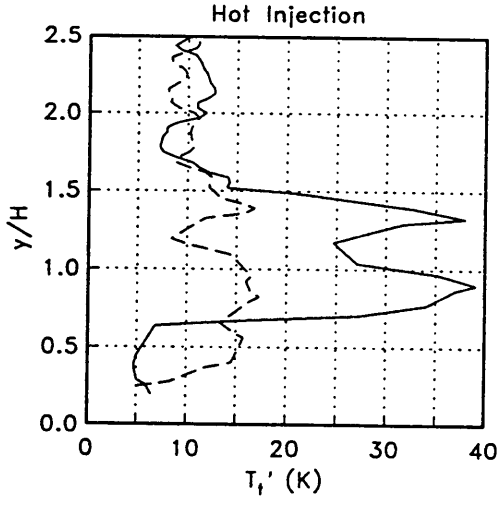

Shockless Flow = Dashed Lines

Shock Interaction Flow = Solid Lines

Turbulence Profile Changes Induced by Shock Impingement (Stn. 4)

APPENDIX B

Nonlinear Hot-Wire Effects

The following is a plot of nondimensional voltage ($\sqrt{\text{Nu}} \propto$Voltage) versus nondimensional mass flux. The fourth-order curve is derived from equation (4.2). In this representative example, the curve corresponds to the second overheat of hot wire B. As stated in Chapter 4, the formation of the turbulence matrix requires taking the logarithmic derivative of Equation (4.2). This approximation is shown as a straight line tangent to the actual relationship. From the shear layer at Station 2 in the unheated case, a value of the mean Reynolds Number was found. The straight line approximation extends for one standard deviation (of a normal distribution) on both sides of this value. This encompasses approximately 68 percent of the 159 data points around the mean. The curves do not match, but Figure 32, discussed in Chapter 6, demonstrates that the assumption of linearity produces excellent results. Therefore, this approximation does not introduce any significant error.

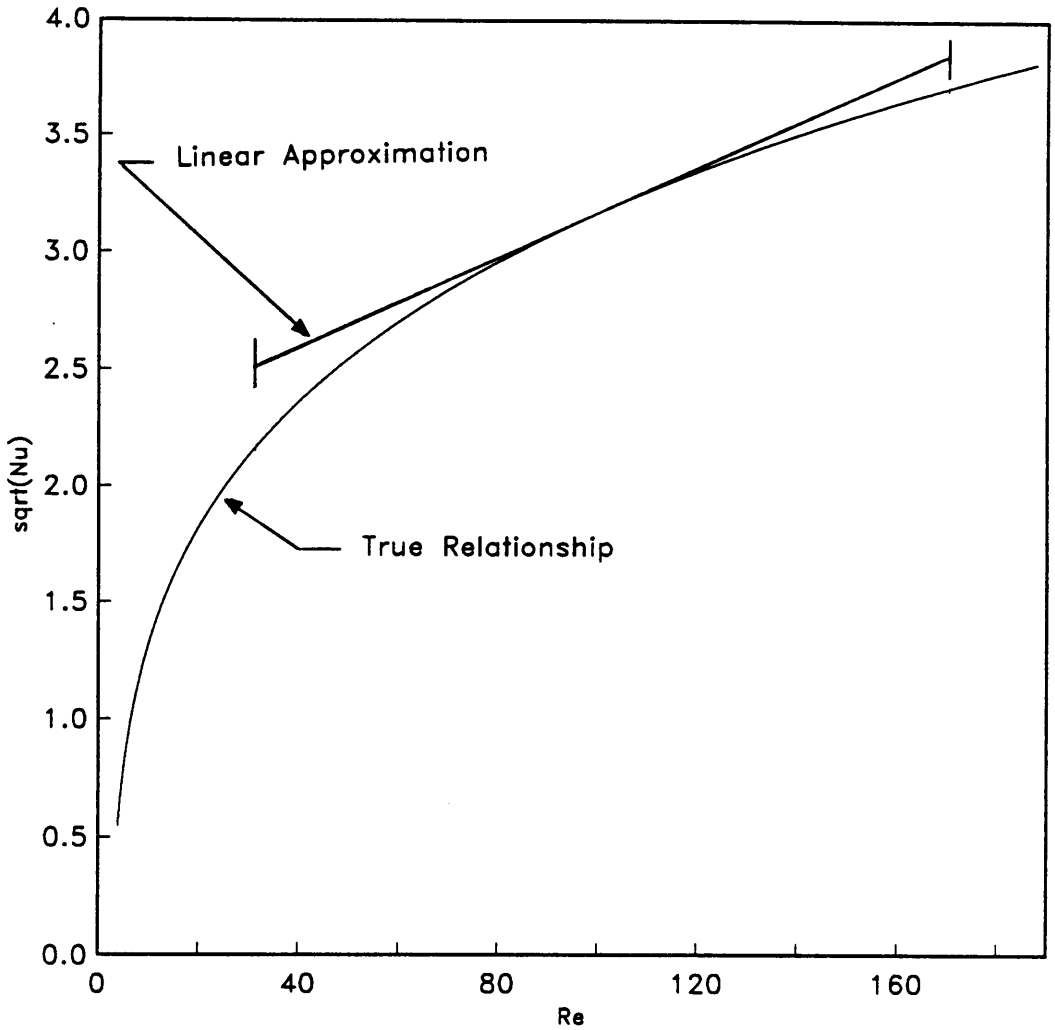

Nonlinear Response of Hot-Wire Voltages to Mass Flux Changes

APPENDIX C

Program Listings

Program Hwstep.FOR runs the wind tunnel. Ave.FOR computes averages and variances for the hot-wire data and calculates the average temperature, pressure, and height of each station. Calib.FOR forms calibration constants for each wire. Mean.FOR and Rms.FOR calculate the mean and turbulent mass flux and total temperature, respectively.

Program 1. Hwstep.FOR

```
      PROGRAM HWSTEP
C THIS PROGRAM TAKES DATA EITHER WHILE PROBE IS TRAVERSED OR FIXED
C link with libraries: das16for, numer
C
      INTEGER*2 IHOUR0,IHOUR1,IMIN0,IMIN1,ISEC0,ISEC1,IHUND0,
     $          DACN,RTNFLG,DATOUT,DATARRAY(10000),BASEADDR,
     $          STARTC,MODE,ENDCH,NOS,IPAR,DMALEV,CNT1,CNT2,
     $          INTLEV,IHUND1,DAT0(9),DACN0,hwch,idy,noshw,
     $          datahw(1431),cnt1hw,cnt2hw,modehw
      REAL MAXPSI,SECS,VOLT,TIME0,TIME1,TIMDIF,sechw
      character*6 fname(5)
      character*42    pgm(3),pgm1,pgm2,pgm3,pgm4
      character*2     exe1,exe2,exe3,exe4,exe5,exe6,exe7,exe8,exe9,exe10
c       data    pgm1    / 'V400 D200 Z1 R1                              ' /
c       data    pgm2    / 'V400 D200 Z0 R1                              ' /
        data    pgm3    / 'V100 D200 Z1 R1 Z0 R1                        ' /
        data    pgm4    / 'V10 D200 Z1 R1 Z0 R1                         ' /
        data    exe1    / 'Y1' /
        data    exe2    / 'Y2' /
        data    exe3    / 'Y3' /
        data    exe4    / 'Y4' /
        data    exe5    / 'Y5' /
        data    exe6    / 'Y6' /
        data    exe7    / 'Y7' /
        data    exe8    / 'Y8' /
        data    exe9    / 'Y9' /
        data    exe10   / 'x' /
      DATA DAT0 /4095,3391,2882,2403,2006,1553,988,475,0/
      call cinit
      open(1,file='c:hw.dat',status='new',form='binary')
C
      write(*,*)'INSURE STEPPER POWER IS ON AND STEPPER RESET'
C
      write(*,*)' input traverse up command'
      read(*,'(A)')pgm(1)
      write(*,*)' input traverse down command'
      read(*,'(A)')pgm(2)
      write(*,*)' need to traverse to an initial position first'
      write(*,*)'   (0 yes , 1 no) ?'
      read(*,'(i2)') iflag
      if (iflag.eq.0) then
          trup = 2.0
          write(*,*)' input initial traverse up command'
          read(*,'(a)') pgm(3)
          call outpgm (pgm(3))
         else
          trup = 3.0
          call outpgm (pgm(1))
      end if
C
      WRITE(*,*)'INPUT PRESSURE'
      READ(*,*)MAXPSI
      write(*,*)'INPUT # OF TRAVERSE STATIONS (INCLUDING INITIAL)'
      READ(*,*)IDY

      IOV = 9
      SHUTD = 24.0
      TVAL = 0.00000
C
      DACN = 1
      DACN0 = 0
      BASEADDR = #300
      DMALEV = 3
      INTLEV = 2
      CALL LOCATE(15,2)
      MODE = 18
```

```
      modehw = 19
      RTNFLG = 0
C
      CALL ADINIT(BASEADDR,DMALEV,INTLEV,RTNFLG)
      IF (RTNFLG.NE.0) GOTO 200
C
      CALL DIGOUT(0)
   10 CALL CLRSCN(7,0)
      CALL LOCATE(5,5)
C
      WRITE(*,*)'DEFAULT TIME PARAMETERS ARE AS FOLLOWS:'
      WRITE(*,*)'  '
      WRITE(*,*)TVAL,' VALVE OPENS AT T=0'
      WRITE(*,*)TRUP,' SECONDS TRAVERSE UP'
      WRITE(*,*)SHUTD,' SECONDS DIGITAL OUTPUTS OFF'
      CALL LOCATE(15,5)
      WRITE(*,*)'WANT TO CHANGE PARAMETERS? ENTER (1) IF YES'
      READ(*,'(F2.0)')CHA
      IF(CHA.NE.1.) GO TO 20
C
      CALL CLRSCN(7,0)
      CALL LOCATE(5,5)
      WRITE(*,*)'TIME IS SET AT ZERO WHEN WIND TUNNEL VALVE OPEN'
      WRITE(*,*)'  '
      WRITE(*,*)'ENTER TIME FOR TRAVERSE UP'
      READ(*,*)TRUP
      WRITE(*,*)'ENTER TIME FOR TUNNEL SHUTDOWN'
      READ(*,*)SHUTD
      WRITE(*,*)'  '
      WRITE(*,*)'TIMES OK AS ENTERED?  ENTER (2) TO CORRECT.'
      READ(*,'(F2.0)')CORR
      IF(CORR.EQ.2.)GOTO 10
C
C  SET UP A/D SAMPLING PARAMETERS
   20 CALL CLRSCN (7,0)
      CALL LOCATE (4,0)
      write(*,'(a\)')' enter hw channel (first or last channel) ='
      read(*,'(i2)')hwch
      WRITE(*,'(A\)')' ENTER THE START CHANNEL  for other data = '
      READ(*,'(I2)')STARTC
      WRITE(*,'(A\)')' ENTER THE END CHANNEL for other data = '
      READ(*,'(I2)')ENDCH
C
C      ******  SET SAMPLE RATE  ********
  250 CALL CLRSCN(7,0)
      CALL LOCATE (0,0)
        WRITE(*,*)' SET SAMPLE RATE  for hot-wire . . . '
        WRITE(*,*)
        WRITE(*,*)'     RATE IS ESTABLISHED BY DIVIDING THE CLOCK RATE'
        WRITE(*,*)'     (1 MHZ) BY THE PRODUCT OF THE TWO COUNTS.     '
        WRITE(*,*)'     AS AN EXAMPLE:'
        WRITE(*,*)'  '
        WRITE(*,*)'     HIGH COUNT = 10, LOW COUNT = 10 '
        WRITE(*,*)'     SAMPLE RATE = (1000000/(10*10)) = 10000 '
        WRITE(*,*)'           SAMPLES PER SECOND PER CHANNEL'
        WRITE(*,*)'  '
        WRITE(*,'(A\)')' ENTER THE LOW COUNT    =  '
        READ(*,'(I6)')CNT1HW
        WRITE(*,'(A\)')' ENTER THE HIGH COUNT   =  '
        READ(*,'(I6)')CNT2HW
      write(*,'(a\)')' enter secs at each overheat ratio ='
      read(*,*)sechw
      srhw = 1000000./FLOAT(CNT1HW*CNT2HW)
      noshw = int(sechw * srhw + 0.5)
      WRITE(*,*)
      WRITE(*,*)' THE COUNT SELECTION AS ENTERED WILL PROVIDE...'
```

```
      WRITE(*,*)'  '
      WRITE(*,*)'    ',SRHW,' SAMPLES PER SECOND PER CHANNEL'
      WRITE(*,*)'FOR '
      WRITE(*,*)'    ',SECHW,' SECONDS PER OVERHEAT WITH'
      WRITE(*,*)'    ',NOSHW,' POINTS PER OVERHEAT'
      WRITE(*,*)' IF PARAMETERS OK, PRESS RETURN.  IF NO, ENTER 1'
      READ(*,'(I2)')IPAR
      IF(IPAR.EQ.1)GOTO 250
  666 CALL CNTMO1 (2,CNT1HW)
      CALL CNTMO2 (2,CNT2HW)
C
  252 call clrscn(7,0)
      call locate(0,0)
      write(*,*)' set sample rate for other measurements . . .'
      write(*,'(a\)')' enter low count = '
      read(*,'(i6)')cnt1
      write(*,'(a\)')' enter high count = '
      read(*,'(i6)')cnt2
      sr = 1000000./float(cnt1*cnt2)
      write(*,'(a\)')' enter # of data points per channel per station ='
      READ(*,*)nos
      secs = nos/sr
      write(*,*)'count selection as entered will provide '
      write(*,*)'    ',sr,' samples per second per channel for'
      write(*,*)'    ',secs,' seconds per station'
      write(*,*)' if ok, press return.  if not, enter 1'
      read(*,'(i2)')ipar
      if (ipar.eq.1) goto 252
C
      WRITE(*,*)'ENTER (1) WHEN READY TO START'
      READ(*,'(F1.0)')BEGIN
      IF(BEGIN.NE.1.)GOTO 10
      CALL CLRSCN(7,0)
      CALL LOCATE(10,10)
      IHOUR0=0
      IMIN0=0
      ISEC0=0
      IHUND0=0
      IHOUR1=0
      IMIN1=0
      ISEC1=0
      IHUND1=0
      TIME0=0
      TIME1=0
C
      WRITE(*,*)'  *******   TIMER ENABLED  *******'
C
      CALL GTIME(IHOUR0,IMIN0,ISEC0,IHUND0)
      TIME0 = IHOUR0*3600.+IMIN0*60.+ISEC0+IHUND0/100.
      VOLT = MAXPSI/10.
      DATOUT = INT(VOLT/2.96E-3)
      CALL DAOUT(DACN,DATOUT,RTNFLG)
      WRITE(*,*)'VALVE ON'
      CALL DIGOUT(1)
   39 CALL GTIME(IHOUR1,IMIN1,ISEC1,IHUND1)
      TIME1 = IHOUR1*3600.+IMIN1*60.+ISEC1+IHUND1/100.
      TIMDIF = TIME1 - TIME0
      IF(TIMDIF.LT.TRUP)GOTO 39
      if (iflag.eq.0) then
           write(*,*)' ** initial traverse up **'
           call outexe(exe1)
           call outexe(exe10)
  944      call gtime(ihour1,imin1,isec1,ihund1)
           time1 = ihour1*3600.+imin1*60.+isec1+ihund1/100.
           timdif = time1 - time0
           if(timdif.lt.trup+1.0)goto 944
```

```
          call outpgm (pgm(1))
      end if
C
      WRITE(*,*)' TRAVERSE UP'
      WRITE(*,*)
C
      inc = 0
      nconv = nos * (endch - startc + 1)
      do 777 iy = 1,idy
         in = 0
         in2 = 1
         call daout(dacn0,dat0(in2),rtnflg)
         if(rtnflg.ne.0)goto 200
         DO 99 N2 = 1 , iov
           CALL ADCONV(modehw,hwch,hwch,noshw,datahw(1+IN),RTNFLG)
           IF(RTNFLG.NE.0) GO TO 200
           in2 = in2 + 1
           call daout(dacn0,dat0(in2),rtnflg)
           IN = IN + noshw
   99    CONTINUE

         call outexe(exe1)
         call cntmo1(2,cnt1)
         call cntmo2(2,cnt2)
         write(1) datahw
C
         call adconv(mode,startc,endch,nos,datarray(1+inc),rtnflg)
         if(rtnflg.ne.0)goto 200
         inc = inc + nconv
C
         call cntmo1(2,cnt1hw)
         call cntmo2(2,cnt2hw)
C
  777 CONTINUE
C
      call outexe (exe10)
      write(*,*)' delay to allow echo'
      tdown = trup + idy * (iov * sechw + secs)
   32 call gtime(ihour1,imin1,isec1,ihund1)
      time1 = ihour1*3600. + imin1*60. + isec1 + ihund1/100.
      timdif = time1 - time0
      if(timdif.lt.tdown+1.) goto 32
C
      call outpgm (pgm(2))
C
      close(1)
C
      WRITE(*,*)'TRAVERSE DOWN'
        call outexe (exe1)
        call outexe (exe10)
   29 CALL GTIME(IHOUR1,IMIN1,ISEC1,IHUND1)
      TIME1 = IHOUR1*3600.+IMIN1*60.+ISEC1+IHUND1/100.
      TIMDIF = TIME1 - TIME0
      IF(TIMDIF.LT.SHUTD)GOTO 29
      CALL DIGOUT(0)
      WRITE(*,*)'ALL DIGITAL OUTPUTS OFF'
      WRITE(*,*)
C
      write(*,*)'WRITING TO FILES . . .'
      nch = endch - startc + 1
      fname(1) = 'b:dat1'
      fname(2) = 'b:dat2'
      fname(3) = 'b:dat3'
      fname(4) = 'b:dat4'
      fname(5) = 'b:dat5'
      do 23 j = 1 , nch
```

```
        open(j,file=fname(j),status='new', form ='binary')
        in2 = j
        do 13 i = 1 , nos * idy
             write(j) datarray(in2)
             in2 = in2 + nch
   13   continue
        close (j)
   23 continue
      GO TO 188
C
  200 CALL CLRSCN(7,0)
      CALL DIGOUT(0)
      CALL LOCATE(2,2)
      WRITE(*,*)'** THERE HAS BEEN AN ERROR NUMBER ',RTNFLG
      WRITE(*,*)
      WRITE(*,'(A\)')' HIT <ENTER> TO RETURN TO MAIN MENU '
      READ(*,'(I2)')IERR
  188 CONTINUE
         END

C --- outpgm
        subroutine      outpgm (pgm)
        character*42    pgm
          do 100 i = 1,42
            call cout (pgm(i:i))
  100     continue
          call cout (13)
          return
        end

C --- outexe
        subroutine      outexe (exe)
        character*2     exe
          do 100 i = 1,2
            call cout (exe(i:i))
  100     continue
          return
        end
```

Program 2. Ave.FOR

```
$debug
C  Program to average hot-wire data (9 / 25 / 88).
C  AVE.FOR
C  Section to average data and find mean squares - from HWAVG.FOR
C  avecold4.for
c  from avecold2.for - uses earlier switching in channels and removes
c    some of the scatter in the data
c
C  Number of samples per overheat at given height

      INTEGER*2 DATARRAY(50085),N,J,K,DATA(560,3), small,count(9,35)
      INTEGER*4 IV,ISUM,NOS,i,isq(9,35)
      REAL AV(9,35),XN, AVE(35,3),M,sq(9,35),test(9,35)
      CHARACTER*14 FNAME(4)
      CHARACTER*3 RUN
      CHARACTER*5 NAME1
      CHARACTER*7 NAME2, NAME3*8

      N = 159
      NOS = (9*N)*35

      WRITE(*,*) 'Enter run number'
      READ(*,3) RUN
      WRITE(*,*) 'Enter the LVDT slope (cm/V)'
      READ(*,*) M
      WRITE(*,*) 'Enter the y-intercept relative to the floor'
      READ(*,*) B
      FNAME(1) = 'a:hw.' // RUN
    3 FORMAT(A3)

      open(1, file = fname(1), status = 'old', form = 'binary')
      DO 10 I = 1,NOS
         READ(1) DATARRAY(I)
   10 CONTINUE
      CLOSE(1)
c   calculation of average voltage and mean square voltage/average
c      voltage at each height and overheat

      DO 40 J = 1,35

         DO 30 I = 2,9

         do 30 ii = 1,2
            isum2 = 0.0
            ISUM = 0
            kount = 0
            iflag1 = 0
            iflag2 = 0

            DO 20 K = 2,N-1


               IV = DATARRAY( (N-0)*(I-1) + 9*N*(J-1) + K)
c              if(ii.eq.2.and.abs(float(iv)-av(i,j)).ge.2.97*sigma )
c    #                goto 20
               if(ii.eq.2) then
                  if(small.eq.iv.and.iflag1.le.0) then
                     iflag1 = iflag1 + 1
                     goto 20
                  end if
                  if(large.eq.iv.and.iflag2.le.0) then
                     iflag2 = iflag2 + 1
                     goto 20
                  end if
               end if
```

```
                kount = kount +1
                isum  = isum + iv
                isum2 = isum2 + iv*iv

                if(ii.eq.1) then
                   if(k.eq.2) then
                      small = iv
                      large = iv
                   end if
                   if(iv.lt.small) small = iv
                   if(iv.gt.large) large = iv
                end if

   20        CONTINUE
c            write(*,*) kount
             AV(I,J) = FLOAT(ISUM)/float(kount)
             isq(i,j) = isum2
             count(i,j) = float(kount)

                sigma = float(isum2)/float(kount -1)
     1                -av(i,j)*av(i,j)*float(kount)/float(kount-1)
                if(sigma.le.0.0) sigma = 0.0
                test(i,j) = sigma
                sigma = sqrt(sigma)

   30    CONTINUE

   40 CONTINUE

      FNAME(1) = 'b:hwav.'//RUN
      OPEN(2, FILE = FNAME(1), STATUS = 'unknown')
      DO 17 K = 1,35
         WRITE(2,4) (count(J,K), J = 2,9)
         WRITE(2,1) (AV(J,K), J = 2,9)
   17 CONTINUE
      CLOSE(2)

    1 format(1x,8f9.3)
    4 format(1x,8i9)

      fname(2) = 'b:hwsq.' // run
    2 FORMAT(8i10)
      OPEN(1, FILE = FNAME(2), STATUS = 'unknown')
      DO 53 K = 1,35
         WRITE(1,1) (test(J,K), J = 2,9)
         WRITE(1,2) (isq(J,K), J = 2,9)
   53 CONTINUE
      CLOSE(1)

C*************************
C   Calculate averages of Pt, Tt, and LVDT taken during hw run
C   From ave.for
C    560 SAMPLES, 16 AT EACH OF 35 STATIONS

c     goto 777
      NOS2 = 560
      NCH = 3

      FNAME(1) = 'a:dat1.'// RUN
      FNAME(2) = 'a:dat2.'// RUN
      FNAME(3) = 'a:dat3.'// RUN

      OPEN(1, file = fname(1), status = 'OLD', form = 'BINARY')
      DO 11 I = 1,NOS2
         READ(1) DATA(I,1)
   11 CONTINUE
```

```
      CLOSE(1)
      OPEN(2, file = fname(2), status = 'OLD', form = 'BINARY')
      DO 14 I = 1,NOS2
         READ(2) DATA(I,2)
   14 CONTINUE
      CLOSE(2)
      OPEN(3, file = fname(3), status = 'OLD', form = 'BINARY')
      DO 16 I = 1,NOS2
         READ(3) DATA(I,3)
   16 CONTINUE
      CLOSE(3)
      lim = 35
      DO 41 J = 1,3

         DO 31 I = 1,lim

            isum = 0
            DO 21 K = 1,16
               iv = data(16*(i-1)+k,j)
               if(k.eq.1) then
                  small = iv
                  large = iv
               end if
               if(iv.lt.small) small = iv
               if(iv.gt.large) large = iv
               isum = isum + iv
   21       CONTINUE
            ave(i,j) = float(isum - large - small)/14.0


            IF(J.EQ.2) THEN
c              LVDT
               AVE(I,J) = AVE(I,J)/409.5*M + B

            ELSE IF(J.EQ.3) THEN
c              Pt1 calibration date (8 /23/88)
               AVE(I,J) = AVE(I,J)*20./409.5 + .13

            ELSE
c              Tt1 calibration date (6 /23/88)
               AVE(I,J) = AVE(I,J)*.07920392 -26.94829 + 273.15
            END IF

   31    CONTINUE

   41 CONTINUE

      NAME3 = 'b:ptlav.'
      FNAME(1) = NAME3// RUN
      NAME3 = 'b:ttlav.'
      FNAME(2) = NAME3// RUN
      OPEN(2, FILE = FNAME(1), STATUS = 'unknown')
      DO 19 J = 1,lim
         WRITE(2,7) AVE(J,3), AVE(J,2)
   19 CONTINUE
      CLOSE(2)
      OPEN(2, FILE = FNAME(2), STATUS = 'unknown')
      DO 22 J = 1,lim
         WRITE(2,7) AVE(J,1), AVE(J,2)
   22 CONTINUE
      CLOSE(2)
    7 FORMAT( 2(1X,E14.7) )

  777 STOP
      END
```

Program 3. Calib.FOR

```
c234567
c * * * * * * * * * * * * * * * * * * * * * * * * * * * * * * * * * * * *
c *                                                                       *
c *  program  CALIB.F  calculates the nusselt number and reynolds  *
c *                                                                       *
c *        number to find calibration curves  ( nu vs. re )               *
c *                                                                       *
c *                    Randy Hyde    (11/29/88 )                          *
c *                                                                       *
c *              calibration runs always in cold flow                     *
c *                                                                       *
c * * * * * * * * * * * * * * * * * * * * * * * * * * * * * * * * * * * *
c   input : 1 rhou file
c           1 hwsq file
c           1 Ttlav file

      real*4 ttl(35), yl(35), nu(35,8), sqre(35), a(8), b(8)
      real*4 r(70), n(70,8), lo2, lo3, twire(8)
      character*12 fname, run*3, stn*4 , name(8)*1, wire*3
      integer*2 iflag(35)
      common // ttl,yl,run,stn
      data name /'1','2','3','4','5','6','7','8'/

c  nn = the number of the highest useful overheat
      nn = 7
      k = 0

      write(*,*) ' input the run number'
      read(*,33) run
      write(*,*) 'input the station number'
      read(*,3) stn
    3 format(a4)
   33 format(a3)

c   heights of low turbulence regions in profiles
c      top of injected flow: hi1
c      pair around shear layer (lo height, hi height): lo2, hi2
c      bottom of free stream: lo3

c  these correspond to the 85 psi case from the spring
c        hi1 = 1.27
c        lo2 = 4.064
c        hi2 = 6.0
c        lo3 = 6.0
c        hi1 = 1.0
c        lo2 = 2.0
c        hi2 = 2.5
c        lo3 = 6.0
c  these correspond to the 95 psi cases from spring and summer
c    use summer profile with fall hotwire runs
         hi1 = .84963
         lo2 = 1.76149
         hi2 = 2.41681
         lo3 = 3.71729

c  program calculates Nusselt numbers and Reynolds numbers at all
c   heights (Nu & sqRe), then picks out values in low turbulence
c   regions (n & r)
      call reynold(sqre,iflag,nn)
      call nusselt(nu,twire,nn)

c   pick out low turbulence regions

      do 5 i = 1,35
c        remove specific points due to oil impact
c        if(i.eq.9.or.i.eq.19) goto 5
```

```
c       if(i.eq.11.or.i.eq.14.or.i.eq.16.or.i.eq.17) goto 5
c       if(i.eq.2) goto 5

c  removals for hot-wire E.1
        if(i.eq.13.or.i.eq.20) goto 5
        if(i.eq.11.or.i.eq.14.or.i.eq.16.or.i.eq.17) goto 5
c  removals for hot-wire E.2
        if(i.eq.9.or.i.eq.19) goto 5
        if(i.eq.14.or.i.eq.16.or.i.eq.17) goto 5
        if(i.eq.2) goto 5
c  removals for hot-wire D.2
        if(i.eq.11.or.i.eq.14.or.i.eq.21.or.i.eq.23) goto 5
        if(i.eq.2.or.i.eq.3) goto 5
        if( (   (yl(i).lt.hil.and.iflag(i).eq.0).or.
     #          ( yl(i).gt.lo2.and.yl(i).lt.hi2).or.
     #                    yl(i).gt.lo3 )   .and.yl(i).gt..0003 ) then
           k = k + 1
           r(k) = sqre(i)
           write(*,*) i,k,yl(i),r(k)
           do 6 j = 1,nn
              n(k,j) = nu(i,j)
    6      continue
        end if
    5 continue

c   least squares curve fit ->  Nu(i,j) = a(j)*sqre(i) + b(j)
      do 20 j = 1,nn

         sum1 = 0.0
         sum2 = 0.0
         sum3 = 0.0
         sum4 = 0.0

         do 10 i = 1,k
            x = r(i)
            sum1 = sum1 + x*x
            sum2 = sum2 + x
            sum3 = sum3 + x * n(i,j)
            sum4 = sum4 + n(i,j)
   10    continue

         b(j) = (sum3/sum1 - sum4/sum2) / (sum2/sum1 - float(k)/sum2)
         a(j) = sum4/sum2 - float(k)*b(j)/sum2
   20 continue

c  store calibration constants of given wire along with wire
c   overheat temperatures in degrees K and degrees F
      write(*,*) 'Enter wire name'
      read(*,33) wire

      write(*,*) '     a          b'
      fname = 'fit.' // wire
      open(1,file = fname, status = 'unknown')
      do 41 j = 1,nn
         write(1,102) twire(j), ( twire(j) - 273.15 )*1.8 + 32.
         write(1,100) a(j), b(j)
         write(*,*) a(j), b(j)
   41 continue
      close(1)
      write(*,*)

c   output - scattered data to fit lines to
c   the following two files are just plots of the least squares fits

      do 37 j = 1,nn
```

```
         fname = 'revnu'// name(j)  // '.' //wire
         open(1,file = fname,status = 'unknown')
         write(1,106) k

         do 40 i = 1,k
            write(1,101) r(i),n(i,j)
   40 continue

      close(1)
   37 continue

  100 format(2(1x,e14.7))
  101 format(2(1x,f7.4))
  102 format(2(1x,f8.4))
  106 format(i2)
    4 format(i3)

c   plotter files - calibration lines

      do 50 j = 1,nn
         write(1,666)
  666 format('4')

         fname = 'line'// name(j) // '.' // wire
         open(1,file = fname,status = 'unknown')

         do 45 i = 5,11,2
            y = a(j)*float(i) + b(j)
            write(1,*) i, y
   45 continue
         close(1)

   50 continue

      stop
      end

      subroutine reynold(sqre,iflag,nn)
c234567
c * * * * * * * * * * * * * * * * * * * * * * * * * * * * * * * * * * * *
c *                                                                       *
c *                    routine to calculate re                            *
c *                                                                       *
c *                          ( 8/09/88 )                                  *
c *                                                                       *
c * * * * * * * * * * * * * * * * * * * * * * * * * * * * * * * * * * * *
c   English unit calculation

      integer*2 n,i,k,iflag(35)
      real y1(35), tt1(35), rhou(1000), y2(1000), mu, m
      real sqre(35)
      character*12 fname
      character*3 run, stn*4, run2*5
      common // tt1,y1,run,stn

c   calculation of re using data from hw runs and mean flow runs -
c     -uses averaged data

c   note that y1 is in centimeters

c  this section reads in values of Tt1 and y1 from Dr. Walker's spring
c   files
    3 format(a3)
c     write(*,*) 'enter the name of the averaged file'
c     read(*,*) run2
c     fname = run2//'.avg'
```

```
c     open(2,file = fname, status = 'old')
c     read(2,*)
c     read(2,*)
c     read(2,*)
c     read(2,*)
c     read(2,*) m, b
c     read(2,*)
c     do 21 i = 1,35
c     il and a are dummies
c     read(2,*) il,a,ttl(i),yl(i)
c     spring calibration
c     ttl(i) = ttl(i)*.1402 - 27.94 + 273.15
c     write(*,*) ttl(i)
c     yl(i) = yl(i) *m +b
c  21 continue
c     close(2)

   this reads in Ttl and yl from files that are already reduced
      fname = 'ttlav.' // run
      open(2, file = fname,status = 'old')
      do 11 i = 1,35
         read(2,*) ttl(i), yl(i)
   11 continue
      close(2)
 1000 format( 2(1x,e14.7) )

c  reads in rho-u profiles from mean flow measurements
      fname = 'rhou.' // stn
      open(1, file = fname, status = 'old')
      read(1,*) nmean
      do 13 i = 1,nmean
         read(1,*) rhou(i), y2(i)
   13 continue
      close(1)

c   interpolate mean flow data and calculate sqre
c   mu(lb-sec/ft2), d(ft), T(K)

      d = 1.6404e-5
      write(*,*)
      do 79 i = 1,35
            iflag(i) = 0
         if (yl(i).le.y2(1)) then
            iflag(i) = 1
c           write(*,*) iflag(i),i
            goto 79
         end if
         kl = 0
         do 77 k = 1,nmean
            kl = kl + 1
            if (yl(i).le.y2(k)) goto 78
   77    continue
         yl(i) = .0002
   78    c     = ( yl(i)-y2(kl-1) )/( y2(kl)-y2(kl-1) )
         ru    = rhou(kl-1) + c*( rhou(kl) - rhou(kl-1) )

         mu    = 3.584851e-07 * (ttl(i)/273.1)**1.5 * 383.7 /
     1           (ttl(i)+110.6)
c        write(*,*) '    i             ru             d              mu'
c        write(*,*) i,ru,d,mu
         sqre(i) = sqrt( ru*d/mu )
         write(*,*) iflag(i),i,yl(i),sqre(i)
   79 continue

      return
      end
```

```
      subroutine nusselt(nu,twire,nn)
c234567
c * * * * * * * * * * * * * * * * * * * * * * * * * * * * * * * * * * * *
c *                                                                       *
c *             routine nu calculates the nusselt number                  *
c *                                                                       *
c *                            ( 8/16/88 )                                *
c *                                                                       *
c * * * * * * * * * * * * * * * * * * * * * * * * * * * * * * * * * * * *
c   calculations in metric units
c   all properties are stagnation values

      dimension tt1(35), in(35,8), kount(35,8)
      character*3 run, stn*4, fname*12
      real*4 l, iwire2, nu(35,8),  kt
      real*4 r3(8),tt1(35), vout(35,8), y1(35), rwire(8), twire(8)
      common // tt1, y1,run,stn

c   highest overheat is inoperative - last two resists are same

c  r3 is the series of resistances that the hot wire circuit
c   steps through to create the sequence of overheats
c     data r3 /4.74,4.94.5.22,5.53,5.88,6.28,6.74,7.28 /
c     fall sequence
      data r3 /4.94,4.94,5.22,5.53,5.88,6.28,6.74,6.74 /
 1000 format( 2(1x,e14.7) )

      pi = acos(-1.0)
      r2 = 7.54
c  rwire = (r2+r3) - r1 - rcircuit

c   hotwire length in meters
      l = 1.25 / 1000.

c  series resistance with hotwire depends on probe holder:
c      single or dual
c  leads resistance (prongs) is 0.5 ohms
c  rcircuit = 0.48 + 0.5 (IN SPRING 88 DATA)
c  rcircuit = 0.46 + 0.5 (IN FALL 88 DATA)
      do 10 i = 1,nn
         rwire(i) = r3(i) - .46 - 0.5
   10 continue

c   read in hotwire files for station 2

    3 format(a3)
    4 format(a8)
      fname = 'hwsq.' // run
      write(*,4) fname

C  reads in squared value of hw voltage
c  in spring data, number of samples is 156 - first and last - hi - lo
c        = 152
c  in fall data, number of samples is 159 - first and last - hi - lo
c        = 155
c  averaged of squared voltage gives average of squared current
      open(1, file = fname, status = 'old')
      do 20 j = 1,35
c     write(*,*) j
         read(1,*)
         read(1,*) (in(j,i), i = 1,nn)
         do 31 i = 1,nn
            vout(j,i) = float( in(j,i) )/154.
   31    continue
   20 continue
```

```
      close(1)

c   temperature in c   (tref = 20 c )
      write(*,*) 'enter wire resistance at 20 c'
      read(*,*) rwref

      write(*,*) 'Wire temperatures (F):'
      write(*,*)
      do 50 i = 1,nn
         twire(i) = 20.0 + ( rwire(i) - rwref ) / rwref / .0036 + 273.15
         write(*,*) ( twire(i) - 273.15 )*1.8 + 32.0
   50 continue

      write(*,*)
c * * * * * * * * * * * * * * * * * * * * * * * * * * * * * * * * * * * * *
c   - kt is thermal conductivity of air at stagnation conditions
c   - use ttl for flow total temp since it is measured with the hotwire
c   - 409.5 is the digital equivalent of 1 volt
c   - 1.065595716 is 1/gain of output circuit that changes vt on the
c     bridge to vout in the metrabyte (8/12/88)

c              iwire**2*rwire
c     Nu = --------------------
c           pi*lwire*deltaT*Kt

      do 80 i = 1,35

         tt = ttl(i)
         kt = (  ( -0.2553166e-07*tt + 0.9216215e-04 )*tt +
     #                  .6001070e-03  )
         do 79 j = 1,nn
            iwire2 = vout(i,j)*(1.065595716/( r2 + r3(j) ) / 409.5)**2
            nu(i,j) = iwire2*rwire(j)/( pi*l*(twire(j)-tt)*kt )

   79 continue
      write(*,*) (nu(i,j), j=1,nn)
   80 continue
      return
      end
c * * * * * * * * * * * * * * * * * * * * * * * * * * * * * * * * * * * * *
c * * * * * * * * * * * * * * * * * * * * * * * * * * * * * * * * * * * * *
```

Program 4. Mean.FOR

```
C * * * * * * * * * * * * * * * * * * * * * * * * * * * * * * * * * * * * * * * *
C *                                                                               *
C *   Program MEAN.F finds Re and Tt from hotwire data                 *
C *                                                                               *
C *                                                                               *
C *                          (11/ 30 / 88 )                                       *
C *                                                                               *
C * * * * * * * * * * * * * * * * * * * * * * * * * * * * * * * * * * * * * * * *
C234567890123456789012345678901234567890123456789012345678901234567890123456789012

      real*4 tt1(35), y1(35),z(35,8), vout2(35,8),kount(35,8)
      real*4 tt2(704), y2(704), tt(35), t2(35), minf2
      real*4 sqre(35), a(8), b(8), twire(8), t(35), mu, m, minf
      character*3 fname*12, fname1*12,run, wire, stn, run2*5

c  n = number of highest overheat
      n = 7
c   required quantities:
c      inputs
c       - a, b
c       - l, pi, r3
c       - tt1, ,tt2, iwire
c      calculations
c       - kt, mu
c       - tw, y/H
c      output
c       - sqrt(re)
c       - rhou
c       -Tt

c * * * * * * * * * * * * * * * * * * * * * * * * * * * * * * * * * * * * * * * *
c *                                INPUT                                        *
c * * * * * * * * * * * * * * * * * * * * * * * * * * * * * * * * * * * * * * * *
      write(*,*) ' input the run number'
      read(*,3) run
      write(*,*) 'enter the lowest overheat'
      read(*,*) n1
      write(*,*) ' input the wire number'
      read(*,3) wire
    3 format(a3)

      fname = 'fit.' // wire
      open(1,file = fname, status = 'old')
      do 41 j = 1,n
         read (1,*) twire(j)
         read (1,*) a(j), b(j)
   41 continue
      close(1)

  100 format(/2(1x,e14.7))
  207 format(2(1x,e14.7))
  101 format(2(1x,f7.1))

c   note that y1 is in centimeters

c  reads averaged files of fall data **********************************
        fname = 'ttlav.' // run
        open(2, file = fname,status = 'old')
        do 11 i = 1,35
           read(2,*) tt1(i), y
           y1(i) = y/2.54/0.475
   11   continue
        close(2)
c ******************************************************************************

c  reads averaged files of spring data ********************************
```

```
c     write(*,*) 'enter the name of the averaged file'
c     read(*,*) run2
c     fname = run2//'.avg'
c     open(2,file=fname,status = 'old')
c     read(2,*)
c     read(2,*)
c     read(2,*)
c     read(2,*)
c     read(2,*) m, b1
c     read(2,*)
c     do 222 i = 1,35
c     read(2,*) i1,a1,tt1(i),y
c     spring calibration
c     tt1(i) = tt1(i)*.1402 - 27.94 + 273.15
c     y1(i) = (y * m + b1)/2.54/0.475
c 222 continue
c     close(2)
c **************************************************************************

c    read n tt2
       write(*,*) 'enter 1 if flow is cold'
       read(*,*) k2
       if(k2.eq.1) then
          do 12 i = 1,35
             tt(i) = tt1(i)
    12    continue
          goto 13
       end if

       write(*,*) 'enter the name of tt2 file'
       read(*,777) fname1
   777 format(a12)
       open(1,file = fname1,status = 'old')
       read(1,*) nmean
       do 23 i = 1,nmean
          read(1,*) tt2(i), y2(i)
c         convert y2 from half-inches to y/H
          y2(i) = y2(i) /2.0/0.475
    23 continue
       close(1)

       do 79 i = 1,35
          if(y1(i).le.y2(1)) goto 79
          k1 = 0
          do 77 k = 1,nmean
             k1 = k1 + 1
             if(y1(i).le.y2(k) ) goto 78
    77 continue
       tt(i) = tt1(i)
       goto 79
    78 c = ( y1(i) - y2(k1-1) )/( y2(k1) - y2(k1-1) )
       tt(i) = tt2(k1-1) + c*(tt2(k1)-tt2(k1-1) )
    79 continue

c    read in hotwire files for station 2

     4 format(a8)
    13    fname = 'hwsq.' // run
          write(*,4) fname
          open(1, file = fname, status = 'old')
          do 20 i = 1,35
             read(1,*)
             read(1,*) (vout2(i,j), j = 1,8)
             do 31 j = n1,n
c  number of samples is fixed in spring (152) and fall (155)
                vout2(i,j) = vout2(i,j)/154.0
```

```
   31    continue
   20    continue
         close(1)


      call nu(a,b,vout2,z,twire,tt,n1,n)
      call solver(z,a,b,twire,sqre,t,t2,n1,n)

c234567
c * * * * * * * * * * * * * * * * * * * * * * * * * * * * * * * * * * * *
c *                              output                                   *
c * * * * * * * * * * * * * * * * * * * * * * * * * * * * * * * * * * * *

c d in feet
      d = 1.6404e-5
         fname = 'meanre.'//run
         open(1, file = fname, status = 'unknown')
         do 102 j = 3,35
            write(1,207) sqre(j), y1(j)
  102    continue
         close(1)

c  mu and d are in english units
         fname = 'meanrue.'//run
         open(1, file = fname, status = 'unknown')
         do 107 j = 3,35
            mu = 3.584851e-07*(tt(j)/273.1)**1.5*383.7/
     #           (tt(j)+110.6)
            write(1,207) sqre(j)**2*mu/d, y1(j)
  107    continue
         close(1)

c  multiply slug/ft/ft/sec by 157.0408 to obtain kg/m/m/sec
         fname = 'meanrum.'//run
         open(1, file = fname, status = 'unknown')
         do 109 j = 3,35
            mu = 3.584851e-07*(tt(j)/273.1)**1.5*383.7/
     #           (tt(j)+110.6)
            write(1,207) sqre(j)**2*mu/d*157.0408, y1(j)
  109    continue
         close(1)

c  normalize rho-u profile by free-stream value

         write(*,*) 'enter the total pressure, ptinf, in psi'
         read(*,*) ptinf
c        minf = 3.016
c        minf2 = minf*minf
c        r = 286.8
c  r is J/kg/deg K
c  multiply lb/in/in by 6894.864 to obtain N/m/m
c        g = 1.4
c        f = 1.0 + (g-1)/2.0 * minf2
         fname = 'meanrun.'//run
         open(1, file = fname, status = 'unknown')
         do 108 j = 3,35
c           rhoinf = ptinf*6894.864/f**(1.0/(g-1)) / r / tt1(j)
c           uinf   = minf*sqrt(g*r*tt1(j)/f)
            mu     = 3.584851e-07*(tt(j)/273.1)**1.5*383.7/
     #             (tt(j)+110.6)
c           write(1,207) sqre(j)**2*mu/d*157.0408/rhoinf/uinf,
c    #                   y1(j)
            write(1,207) sqre(j)**2*mu/d/( 61.379*ptinf/95.)*
     #                 sqrt(tt1(j)*1.8),
     #                   y1(j)
  108    continue
```

```
         close(1)

         write(*,*) 'enter jet temperature in deg F'
         read(*,*) tjet
         tjet = (tjet + 459.67)/1.8
         fname = 'meanttn.' // run
         open(1,file = fname, status = 'unknown')
         do 14 k = 3,35
            theta = (t(k)-tt1(k)) / (tjet-tt1(k))
            write(1,207) theta, y1(k)
   14    continue
         close(1)

c  Tt in deg K
         fname = 'meanttm.' // run
         open(1,file = fname, status = 'unknown')
         do 114 k = 3,35
            write(1,207) t(k), y1(k)
  114    continue
         close(1)

c  Tt in deg R
         fname = 'meantte.' // run
         open(1,file = fname, status = 'unknown')
         do 115 k = 3,35
            write(1,207) t(k)*1.8, y1(k)
  115    continue
         close(1)

c  Ttinf in deg K
         fname = 'ttinf.' // run
         open(1,file = fname, status = 'unknown')
         do 116 k = 3,35
            write(1,207) tt1(k), y1(k)
  116    continue
         close(1)
      stop
      end

      subroutine nu(a,b,vout2,z,twire,tt,n1,nn)
c234567
c * * * * * * * * * * * * * * * * * * * * * * * * * * * * * * * * * * * * *
c * routine to calculate z, the variable term in the right hand sides *
c *                                                                       *
c * * * * * * * * * * * * * * * * * * * * * * * * * * * * * * * * * * * * *
      real*4  vout2(35,8), rwire(8),kt, tt(35)
      real*4  l, iwire2, r3(8), twire(8)
      real*4  a(8), b(8), z(35,8)

c   calculations in metric units

c   all properties are stagnation values

c   highest overheat is inoperative - last two resists are same

c     data r3 /4.74,4.94.5.22,5.53,5.88,6.28,6.74,7.28 /
      data r3 /4.94,4.94,5.22,5.53,5.88,6.28,6.74,6.74 /
 1000 format( 2(1x,e14.7) )

      pi = acos(-1.0)
      r2 = 7.54

c   hotwire length in meters
      l = 1.25 / 1000.
c  series resistance with hotwire in second leg is
c         0.48 in spring
```

```
c     and  0.46 in fall
c  leads resistance (prongs) is 0.5 ohms
      do 10 i = nl,nn
         rwire(i) = r3(i) - .46 - 0.5
   10 continue

      write(*,*)
c * * * * * * * * * * * * * * * * * * * * * * * * * * * * * * * * * * * * *
c   - kt is thermal conductivity of air at stagnation conditions
c   - use tt1 for flow total temperature in cold flow since it applies
c     to given hotwire run
c   - use tt2 in the slot in hot-injection runs where tt1 is completely
c     invalid
c   - 409.5 is the digital equivalent of 1 volt
c   - 1.065595716 is 1/gain of output circuit that changes vt on the
c     bridge to vout in the metrabyte (8/12/88)
c   - mean(Ei**2) --> mean(Vwire**2) --> mean(iw**2*rw**2) -->
c     mean(c**2*vout**2*rw**2) --> c**2*rw**2*mean(vout**2) -->
c     c**2 * rw**2 * sum(vout**2)/(number of samples -1)
c   - 159-4 samples at 35 heights and 8 overheats (IN FALL)
c   - METRIC UNITS

         do 79 i = 1,35

            kt = (  ( -0.2553166e-07*tt(i) + 0.9216215e-04 )*tt(i) +
     a                        .6001070e-03  )
c           write(*,*) kt
            do 79 j = nl,nn
c              iwire2 = iwire**2
               iwire2 = vout2(i,j)*(1.065595716/( r2 + r3(j) )
     #              / 409.5 )**2
               z(i,j) = iwire2*rwire(j)/ ( a(j)*pi*l*kt
     #                 *twire(j) ) - b(j)/a(j)
   79    continue

      return
      end

      subroutine solver(z,a,b,twire,sqre,t,t2,nl,n)
c  * * * * * * * * * * * * * * * * * * * * * * * * * * * * * * * * * * * *
c  *        inverts matrix and at each height solves Ax=b                 *
c  * * * * * * * * * * * * * * * * * * * * * * * * * * * * * * * * * * * *

      implicit real*8 (a-i,o-z)
      integer*2 i
      real*8  x(8), y(8)
      real*4  sqre(35), a(8), b(8), t(35), z(35,8), twire(8),t2(35)

c   3 x 3 matrix inverted analytically (ie. cofactors,adjoint,etc.)

      a11 = 0.0
      a21 = 0.0
      a31 = 0.0
      a12 = 0.0
      a22 = 0.0
      a32 = 0.0
      a13 = 0.0
      a23 = 0.0
      a33 = 0.0

      a11 = -float(n-nl+1)

c  build matrix
      do 10 i = nl,n
         write(*,*) ' a = ',a(i),' b = ', b(i), ' twire = ',twire(i)
c        change units of temp to 1000's of degrees to improve
```

```
c           condition of matrix
          x(i) = 1.0d0/dble( twire(i)/1000.)
          y(i) = dble(b(i))/( dble(twire(i))/1000.0d0*dble(a(i)) )
          a12 = a12 + y(i)
          a13 = a13 + x(i)
          a22 = a22 + y(i)*y(i)
          a23 = a23 + x(i)*y(i)
          a33 = a33 + x(i)*x(i)
   10 continue

       a21 = -a12
       a31 = -a13
       a32 =  a23

c      write(*,*)
c      write(*,* ) '                          - A -'
c      write(*,100) a11,a12,a13
c      write(*,100) a21,a22,a23
c      write(*,100) a31,a32,a33

c     computes cofactors for adjoint matrix

       c11 = a22*a33 - a23*a32
       c21 = a13*a32 - a12*a33
       c31 = a12*a23 - a22*a13
       c12 = a31*a23 - a21*a33
       c22 = a11*a33 - a31*a13
       c32 = a21*a13 - a11*a23
       c13 = a21*a32 - a31*a22
       c23 = a31*a12 - a11*a32
       c33 = a11*a22 - a21*a12

c      write(*,*)
c      write(*,* ) '                      A inverse * det(A)'
c      write(*,100) c11,c21,c31
c      write(*,100) c12,c22,c32
c      write(*,100) c13,c23,c33

c    computes determinant

       deta = a11*c11 + a21*c21 + a31*c31
c      write(*,*) 'deta = ',deta

c    multiply A by A-inverse as a check to get the identity matrix

       i11 = (a11*c11 + a12*c12 + a13*c13) / deta
       i12 = (a11*c21 + a12*c22 + a13*c23) / deta
       i13 = (a11*c31 + a12*c32 + a13*c33) / deta
       i21 = (a21*c11 + a22*c12 + a23*c13) / deta
       i22 = (a21*c21 + a22*c22 + a23*c23) / deta
       i23 = (a21*c31 + a22*c32 + a23*c33) / deta
       i31 = (a31*c11 + a32*c12 + a33*c13) / deta
       i32 = (a31*c21 + a32*c22 + a33*c23) / deta
       i33 = (a31*c31 + a32*c32 + a33*c33) / deta

       write(*,*)
       write(*,* ) '                        identity'
c      write(*,100) i11,i12,i13
c      write(*,100) i21,i22,i23
c      write(*,100) i31,i32,i33

  100 format(3(2x,e14.7))

c    computes x = A^(-1) * b

c    beta1 = sqrt(Re),  beta2 = Tt,  beta3 = Tt*sqrt(Re)
```

```
      do 30 j = 1,35
         b1 = 0.0
         b2 = 0.0
         b3 = 0.0
         do 20 i = n1,n
            b1  =  b1 - dble(z(j,i))
            b2  =  b2 - y(i)*dble(z(j,i))
            b3  =  b3 - x(i)*dble(z(j,i))
   20    continue
            sqre(j) = ( c11*b1 + c21*b2 + c31*b3 ) / deta
c           beta2 = ( c12*b1 + c22*b2 + c32*b3 ) / deta
c  there is less scatter in Tt using beta3/beta1 instead of beta2
c     - unknown reason
            beta3 = ( c13*b1 + c23*b2 + c33*b3 ) / deta
            t(j) = beta3/sqre(j)*1000.0d0
   30 continue

      return
      end
c *************************************************************************
c *************************************************************************
```

Program 5. RMS.FOR

```
C * * * * * * * * * * * * * * * * * * * * * * * * * * * * * * * * * * * * * *
C *                                                                           *
C *    Program RMS.F finds rhou' and Tt' from hotwire data                    *
C *                                                                           *
C *                Randy Hyde       ( 1/ 07 / 89 )                            *
C *                                                                           *
C * * * * * * * * * * * * * * * * * * * * * * * * * * * * * * * * * * * * * *
C234567890123456789012345678901234567890123456789012345678901234567890123456789012

      real*4  y1(35)
      real*4 sqre(35), a(8), b(8), twire(8), t(35), m(35)
      real*4 vav(35,8), vms2(35,8), ratio2(35,8)
      real*4 mrms(35), trms(35), mest(35)
      character*3 fname*12, run, wire

c   required quantities:
c       - a, b
c       - tw
c       - ttbar, sq(Re)bar (from mean.f)
c * * * * * * * * * * * * * * * * * * * * * * * * * * * * * * * * * * * * * *
c *                              INPUT                                        *
c * * * * * * * * * * * * * * * * * * * * * * * * * * * * * * * * * * * * * *
      write(*,*) ' input the run number'
      read(*,3) run
      write(*,*) 'enter the lowest overheat'
      read(*,*) n1
      n = 7
      write(*,*) ' input the wire number'
      read(*,3) wire
    3 format(a3)

c  read in wire temperatures and calibration constants ***************
      fname = 'fit.' // wire
      open(1,file = fname, status = 'old')
      do 41 j = 1,n
         read(1,*)     twire(j)
         read (1,*)  a(j), b(j)
   41 continue
      close(1)

  100 format(2(1x,e14.7))

c   note that y1 is in slot heights of 0.475 inches

c  following three files were generated by mean.f ********************
         fname = 'meanre.' // run
         open(2, file = fname,status = 'old')
         do 18 i = 3,35
            read(2,*) sqre(i), y1(i)
   18    continue
         close(2)

         fname = 'meanttm.' // run
         open(2, file = fname,status = 'old')
         do 23 i = 3,35
            read(2,*) t(i)
   23    continue
         close(2)

         fname = 'meanrum.' // run
         open(2, file = fname,status = 'old')
         do 24 i = 3,35
            read(2,*) m(i)
   24    continue
         close(2)
```

```
c   read in hotwire files for station 2 ********************************

          fname = 'hwsq.' // run
          write(*,*) fname
          open(1, file = fname, status = 'old')
          do 20 i = 1,35
             read(1,*) (vms2(i,j), j = 1,8)
             read(1,*)
   20     continue
          close(1)

          fname = 'hwav.' // run
          write(*,*) fname
          open(1, file = fname, status = 'old')
          do 21 i = 1,35
             read(1,*)
             read(1,*) (vav(i,j), j = 1,8)
   21     continue
          close(1)

c    calculate (e'/Ebar)^2
          do 22 i = 1,35
             do 22 j = 1,8
                ratio2(i,j) = vms2(i,j)/(vav(i,j)*vav(i,j) )
   22     continue

c         fname = 'ratio.'//run
c         open(1, file = fname, status = 'unknown')
c         do 42 j = 1,8
c         write(1,*)
c         write(1,44)
c         do 42 i = 1,35
c            write(1,*) i, ratio2(i,j)
c            write(1,*) (ratio2(i,j), j = 1,n)
c  42     continue
c         close(1)
   43 format(8f9.6)
c  44 format('35')

      call solver(z,a,b,twire,sqre,t,num,ratio2,
     #            mrms,trms,mest,nl,n)

c234567
c * * * * * * * * * * * * * * * * * * * * * * * * * * * * * * * * * * * *
c *                              output                                   *
c * * * * * * * * * * * * * * * * * * * * * * * * * * * * * * * * * * * *

c  outputs rms mass flux in metric units
          fname = 'mrmsm.'//run
          open(1, file = fname, status = 'unknown')
          do 102 j = 3,35
             if(mrms(j).le.0.000001) goto 102
             write(1,100) mrms(j)*m(j), y1(j)
  102     continue
          close(1)

c  divide kg/m/m/sec by 157.0408 to obtain slug/ft/ft/sec
          fname = 'mrmse.'//run
          open(1, file = fname, status = 'unknown')
          do 104 j = 3,35
             if(mrms(j).le.0.000001) goto 104
             write(1,100) mrms(j)*m(j)/157.0408, y1(j)
  104     continue
          close(1)

c  outputs rms mass flux divided by mean mass flux
```

```
      fname = 'mrmsn.'//run
      open(1, file = fname, status = 'unknown')
      do 103 j = 3,35
         if(mrms(j).le.0.000001) goto 103
         write(1,100) mrms(j), y1(j)
103   continue
      close(1)

c  outputs rms temperature in degrees C (or K)
      fname = 'trmsm.' // run
      open(1,file = fname, status = 'unknown')
      do 114 k = 3,35
         if(trms(k).le.0.000001) goto 114
         write(1,100) trms(k)*t(k), y1(k)
114   continue
      close(1)

c  outputs rms temperature in degrees F (or R)
      fname = 'trmse.' // run
      open(1,file = fname, status = 'unknown')
      do 115 k = 3,35
         if(trms(k).le.0.000001) goto 115
         write(1,100) trms(k)*t(k)*1.8, y1(k)
115   continue
      close(1)

c  outputs rms temperature divided by mean temperature
      fname = 'trmsn.' // run
      open(1,file = fname, status = 'unknown')
      do 14 k = 3,35
         if(trms(k).le.0.000001) goto 14
         write(1,100) trms(k), y1(k)
 14   continue
      close(1)

c  outputs rms mass flux divided by mean mass flux which is
c    calculated with overheat 7 (as a check fo the maximum
c    possible value of m'/mbar
      fname = 'mrmsn2.' // run
      open(1,file = fname, status = 'unknown')
      do 52 k = 3,35
         write(1,100) mest(k), y1(k)
 52   continue
      close(1)

      stop
      end

c234567
c * * * * * * * * * * * * * * * * * * * * * * * * * * * * * * * * * * * *
c *                                                                       *
c * * * * * * * * * * * * * * * * * * * * * * * * * * * * * * * * * * * *
      subroutine solver(z,a,b,twire,sqre,t,num,ratio2,
     #                  mrms,trms,mest,n1,n)
      implicit real*8 (a-i,o-z)
      integer*2 i
      real*4  ratio2(35,8), twire(8)
      real*4   sqre(35), a(8), b(8), t(35), z(35,8)
      real*4   mrms(35), trms(35), mest(35)
c   calculations in english units except temperature (K)
c   all properties are stagnation values except rho and u

c * * * * * * * * * * * * * * * * * * * * * * * * * * * * * * * * * * * *
c   - use tt1 in cold-injection runs since it is virtually the same
c     as tt2 and applies to the corrent hotwire run
c   - use tt2 in  heated slot-injection runs where tt1 does not apply
```

```
c          ----------------      ----------------
c   -        {  Vm       } 2       {  Vw       } 2
c            {    rms    }         {    rms    }      m = metrabyte
c            { -------- }     =    { -------- }      w = wire
c            {  Vm       }         {  Vw       }
c            {    mean   }         {    mean   }
c
c   - 159 samples at 35 heights and n overheats in FALL
c   - 156 samples at 35 heights and 7 overheats in SPRING
c         (eight overheat is same as seventh in spring/not fall)
c * * * * * * * * * * * * * * * * * * * * * * * * * * * * * * * * * * * *
c *          inverts matrix and at each height solves Ax=b                *
c * * * * * * * * * * * * * * * * * * * * * * * * * * * * * * * * * * * *

c   3 x 3 matrix inverted analytically (ie. cofactors, adjoint, etc. )

         do 200 j = 3,35
            a11 = 0.0
            a21 = 0.0
            a31 = 0.0
            a12 = 0.0
            a22 = 0.0
            a32 = 0.0
            a13 = 0.0
            a23 = 0.0
            a33 = 0.0
            b1 = 0.0
            b2 = 0.0
            b3 = 0.0

c  build matrix and right hand side
            do 11 i = n1,n
c            write(*,*) ' a = ',a(i),' b = ', b(i), ' twire = ',twire(i)

      f = 1.0d0/( 4.0d0*(1.d0 + dble(b(i))/dble(a(i))/dble(sqre(j)) )  )
      g = -dble(t(j)) /( 2.0d0* (dble(twire(i)) - dble(t(j)) )  )
               a12 = a12 + f*f*g*g
               a11 = a11 + f**4
               a13 = a13 + 2.0d0*f*f*f*g
               a22 = a22 + g**4
               a23 = a23 + 2.0d0*g*g*g*f
               b1  =  b1 + f*f*dble(ratio2(j,i))
               b2  =  b2 + g*g*dble(ratio2(j,i))
               b3  =  b3 + 2.0d0*f*g*dble(ratio2(j,i))

c  calculate m'/mbar = 1/fsub7*(e'/Ebar) as a check
      if(i.eq.n) then
        mest(j) = dble(sqrt( ratio2(j,i) )) / f
      end if
c   assumes Tt' equals zero
c   the highest overheat is used since it is least sensitive
c       to any Tt' value there actually is

   11       continue

            a33 = 4.0d0*a12
            a21 = a12
            a31 = a13
            a32 = a23

c           write(*,*)
c           write(*,* ) '                          - A -'
c           write(*,100) a11,a12,a13
c           write(*,100) a21,a22,a23
c           write(*,100) a31,a32,a33
```

```
c     compute cofactors for adjoint matrix

              c11 = a22*a33 - a23*a32
              c21 = a13*a32 - a12*a33
              c31 = a12*a23 - a22*a13
              c12 = a31*a23 - a21*a33
              c22 = a11*a33 - a31*a13
              c32 = a21*a13 - a11*a23
              c13 = a21*a32 - a31*a22
              c23 = a31*a12 - a11*a32
              c33 = a11*a22 - a21*a12

c             write(*,*)
c             write(*,* ) '                          A inverse*det(A)'
c             write(*,100) c11,c21,c31
c             write(*,100) c12,c22,c32
c             write(*,100) c13,c23,c33

c     compute determinant

              deta = a11*c11 + a21*c21 + a31*c31
c             write(*,*) 'deta = ',deta

c     multiply A by A-inverse as a check to get the identity matrix
c             i11 = (a11*c11 + a12*c12 + a13*c13) / deta
c             i12 = (a11*c21 + a12*c22 + a13*c23) / deta
c             i13 = (a11*c31 + a12*c32 + a13*c33) / deta
c             i21 = (a21*c11 + a22*c12 + a23*c13) / deta
c             i22 = (a21*c21 + a22*c22 + a23*c23) / deta
c             i23 = (a21*c31 + a22*c32 + a23*c33) / deta
c             i31 = (a31*c11 + a32*c12 + a33*c13) / deta
c             i32 = (a31*c21 + a32*c22 + a33*c23) / deta
c             i33 = (a31*c31 + a32*c32 + a33*c33) / deta
c             write(*,*)
c             write(*,* ) '                        identity'
c             write(*,100) i11,i12,i13
c             write(*,100) i21,i22,i23
c             write(*,100) i31,i32,i33
  100 format(3(2x,e14.7))


c     computes x = A^(-1) * b

c     beta1 = (mp/mbar)2,  beta2 = (Tp/Tbar)^2,  beta3 = (mTp/mTbar)^2

c                mrms(j) = dsqrt( ( c11*b1 + c21*b2 + c31*b3 ) / deta )
                 beta1 = ( c11*b1 + c21*b2 + c31*b3 ) / deta
                 if(beta1.le.0.0d0) beta1 = 0.0d0
                 mrms(j) = dsqrt(beta1)
                 beta2 = ( c12*b1 + c22*b2 + c32*b3 ) / deta
                 if(beta2.le.0.0d0) beta2 = 0.0d0
                 trms(j) = dsqrt(beta2)
c                beta3 = ( c13*b1 + c23*b2 + c33*b3 ) / deta
  200 continue
      return
      end
c ***************************************************************************
c ***************************************************************************
```

APPENDIX D

Tables of Nondimensional Values

These tables correspond to the plots discussed in Chapters 5 and 6. Zeros listed in the table correspond to negative values removed from the plots. These values are not smoothed. Apply a 3-point binomial filter to the mean mass flux and the total temperature values to obtain the plotted values. Apply a 5-point binomial filter to the rms mass flux and the total temperature values to obtain the plotted values. The columns are as follows:

- y/H, H = 0.475 in.
- $\frac{\overline{(\rho u)}}{(\rho u)_\infty}$
- Local Temperature
  - $\frac{\overline{T}_t}{T_{t_\infty}}$, Unheated
  - $\theta = \frac{\overline{T}_t - T_{t_\infty}}{T_{t_j} - T_{t_\infty}}$, Heated
- $\frac{(\rho u)'}{\overline{(\rho u)}}$
- $\frac{T_t'}{\overline{T}_t}$

Table 1. Profile Data at Station 1 - Unheated

y/H	rho u	T	(rho u)'	T'
0.225	0.3196	0.9758	0.02716	0.004851
0.260	0.3225	1.0055	0.01834	0.002098
0.290	0.3206	0.9940	0.02173	0.002124
0.321	0.3300	1.0057	0.01484	0.000000
0.355	0.3272	0.9981	0.01848	0.000000
0.387	0.3217	0.9780	0.01552	0.000842
0.420	0.3280	0.9909	0.01580	0.000000
0.453	0.3324	0.9999	0.02310	0.003278
0.486	0.3318	0.9942	0.02667	0.004357
0.516	0.3342	1.0019	0.01543	0.000000
0.548	0.3368	0.9982	0.01661	0.000000
0.581	0.3387	1.0124	0.02147	0.002215
0.614	0.3364	0.9875	0.02224	0.003173
0.647	0.3376	1.0010	0.02334	0.002614
0.680	0.3351	1.0099	0.01691	0.000000
0.714	0.3235	0.9970	0.02338	0.002357
0.746	0.3118	0.9847	0.02127	0.000000
0.768	0.3019	0.9967	0.02424	0.002230
0.808	0.2867	0.9972	0.02106	0.000000
0.840	0.2708	0.9907	0.02744	0.001745
0.874	0.2794	0.9847	0.04441	0.005184
0.906	0.3108	0.9939	0.05578	0.004943
0.940	0.2961	1.0241	0.06861	0.003582
0.974	0.2407	0.9388	0.06615	0.000000
1.007	0.2356	0.9309	0.09562	0.015022
1.039	0.3115	0.9760	0.12740	0.018942
1.072	0.3358	0.9654	0.13153	0.017097
1.103	0.3270	0.9901	0.09728	0.012995
1.137	0.3358	0.9986	0.12257	0.013343
1.170	0.3550	0.9158	0.13704	0.000000
1.204	0.4053	0.9255	0.17713	0.026627
1.237	0.4547	0.9493	0.14260	0.000000
1.269	0.4983	0.9974	0.19495	0.025760
1.311	0.5737	1.0559	0.20385	0.011806
1.343	0.5530	0.9274	0.19240	0.012080
1.376	0.5897	0.9559	0.21805	0.023058
1.408	0.6564	1.0144	0.19851	0.000000
1.441	0.7284	1.0702	0.22057	0.008896
1.473	0.7148	1.0024	0.24550	0.025834
1.505	0.7822	1.0566	0.20262	0.004839
1.538	0.7841	0.9823	0.21980	0.025759
1.569	0.8428	1.0225	0.20597	0.010333
1.600	0.8598	0.9946	0.19690	0.019356
1.631	0.8855	0.9903	0.16783	0.016912
1.662	0.9256	1.0081	0.12782	0.008939
1.696	0.9532	1.0222	0.10832	0.008236
1.729	0.9679	1.0234	0.06808	0.000000
1.762	0.9687	1.0281	0.05778	0.004604
1.793	0.9626	1.0147	0.04530	0.003075
1.824	0.9616	1.0155	0.05474	0.006032
1.855	0.9726	1.0220	0.04932	0.004544
1.887	0.9566	0.9954	0.05993	0.007561
1.919	0.9889	1.0152	0.05675	0.005632
1.950	0.9890	1.0139	0.05503	0.004081
1.982	0.9960	1.0118	0.05674	0.005814
2.016	1.0074	1.0214	0.05094	0.004039
2.050	0.9997	1.0132	0.05996	0.006475
2.083	1.0113	1.0260	0.06154	0.005854
2.114	1.0030	1.0165	0.05974	0.005743
2.149	0.9994	1.0167	0.05179	0.004281
2.181	1.0049	1.0155	0.04393	0.000000
2.215	1.0136	1.0307	0.05051	0.003101
2.249	1.0116	1.0223	0.05265	0.005082
2.284	1.0055	1.0219	0.05036	0.003014

2.319	1.0063	1.0206	0.05987	0.005837
2.355	0.9951	1.0074	0.06085	0.006676
2.401	1.0273	1.0520	0.06084	0.004508
2.435	0.9936	1.0073	0.05633	0.004896
2.471	0.9972	1.0241	0.05259	0.004297
2.507	0.9867	1.0044	0.06326	0.007340
2.542	1.0009	1.0250	0.05801	0.005214
2.578	0.9948	1.0166	0.05203	0.004186
2.616	0.9841	1.0119	0.05408	0.003426
2.653	0.9906	1.0185	0.05005	0.003801
2.689	0.9928	1.0190	0.05820	0.005511
2.722	0.9953	1.0200	0.05897	0.005692
2.758	0.9955	1.0174	0.04445	0.001579
2.795	0.9951	1.0182	0.05805	0.005076
2.829	0.9847	1.0068	0.05565	0.006773
2.864	1.0007	1.0327	0.05484	0.004682
2.901	1.0014	1.0246	0.05503	0.004572
2.936	0.9953	1.0162	0.05083	0.004190
2.972	1.0023	1.0249	0.04739	0.002460
3.006	0.9975	1.0196	0.05124	0.002210
3.041	0.9932	1.0211	0.05553	0.005529
3.078	0.9849	1.0157	0.05509	0.005020
3.112	0.9837	1.0104	0.06036	0.006685
3.147	0.9874	1.0100	0.05529	0.005175
3.184	0.9932	1.0148	0.05594	0.004774
3.220	0.9937	1.0190	0.06366	0.007096
3.255	0.9816	0.9997	0.05559	0.004954
3.289	0.9946	1.0092	0.05269	0.000000
3.324	1.0021	1.0100	0.05680	0.005578
3.358	1.0190	1.0313	0.05335	0.003718
3.392	1.0079	1.0214	0.06167	0.005745
3.425	1.0080	1.0252	0.06516	0.006469
3.461	0.9961	1.0065	0.06902	0.007418
3.499	0.9979	1.0161	0.06145	0.005018
3.532	0.9702	0.9909	0.06625	0.009628

Table 2. Profile Data at Station 2 - Unheated

y/H	rho u	T	(rho u)'	T'
0.155	0.3741	0.9718	0.06504	0.000000
0.186	0.3788	0.9647	0.06174	0.006405
0.219	0.3991	1.0387	0.03717	0.001194
0.250	0.3966	0.9676	0.02463	0.001433
0.270	0.4004	1.0098	0.02245	0.001881
0.312	0.4000	1.0101	0.02132	0.000000
0.344	0.4024	1.0278	0.01711	0.000000
0.376	0.3998	0.9988	0.01505	0.000000
0.399	0.3960	0.9798	0.01607	0.000000
0.440	0.3994	1.0190	0.02415	0.001691
0.474	0.3982	1.0015	0.02130	0.000000
0.505	0.3960	0.9736	0.00435	0.000000
0.538	0.3962	0.9939	0.01719	0.000000
0.567	0.4008	1.0293	0.02157	0.000000
0.599	0.3987	1.0164	0.02502	0.001674
0.631	0.3990	1.0174	0.02572	0.001414
0.662	0.3932	0.9725	0.02193	0.000000
0.695	0.3893	1.0128	0.04841	0.003624
0.724	0.3818	1.0349	0.05232	0.002205
0.760	0.3751	1.0284	0.06466	0.004049
0.793	0.3839	1.0600	0.06610	0.001474
0.825	0.3863	0.9765	0.08870	0.000000
0.857	0.4019	0.9816	0.11369	0.010849
0.887	0.4350	1.0406	0.11465	0.004940
0.920	0.4570	1.0230	0.11864	0.006134
0.952	0.4944	1.0293	0.13181	0.003978
0.985	0.5196	1.0144	0.11487	0.000000
1.018	0.5579	1.0807	0.12415	0.000000
1.050	0.5733	0.9891	0.12128	0.000000
1.081	0.5993	0.9178	0.16320	0.020815
1.112	0.6381	1.0032	0.14462	0.007673
1.143	0.6701	1.0518	0.13394	0.000000
1.175	0.6705	0.8258	0.13896	0.000000
1.218	0.7764	1.1188	0.15906	0.000000
1.249	0.7577	0.9924	0.17950	0.013263
1.282	0.8181	1.0144	0.16133	0.005673
1.313	0.8011	0.7331	0.07654	0.000000
1.343	0.9145	1.0804	0.14236	0.000000
1.373	0.8962	0.9504	0.16228	0.010228
1.404	0.9763	1.0946	0.13501	0.000966
1.434	0.9823	1.0168	0.13076	0.007247
1.466	0.9868	0.9016	0.09857	0.013530
1.498	1.0036	0.9811	0.08056	0.000000
1.531	1.0025	0.9919	0.07756	0.004025
1.562	0.9792	0.9836	0.06289	0.002917
1.592	0.9589	0.9657	0.04568	0.004512
1.623	0.9778	1.0167	0.03823	0.001177
1.654	0.9808	0.9917	0.03433	0.001917
1.686	0.9966	0.9993	0.03750	0.002077
1.716	1.0010	0.9868	0.03652	0.002083
1.747	1.0094	1.0046	0.03554	0.000000
1.780	0.9927	0.9778	0.03922	0.000000
1.813	0.9875	0.9916	0.04116	0.002292
1.843	0.9841	0.9938	0.03107	0.000000
1.875	0.9887	1.0049	0.02677	0.000000
1.909	1.0050	1.0530	0.02929	0.000753
1.941	0.9929	1.0015	0.02944	0.000000
1.974	1.0021	0.9945	0.03834	0.003671
2.006	1.0003	0.9701	0.04069	0.004236
2.042	1.0114	1.0093	0.04471	0.002762
2.074	0.9875	1.0659	0.08921	0.003683
2.111	0.8912	0.9963	0.06711	0.000000
2.144	0.8741	1.0213	0.02418	0.000000
2.179	0.8841	1.0194	0.02000	0.000000

2.213	0.9017	0.9999	0.01981	0.000000
2.248	0.9125	1.0085	0.02369	0.000000
2.293	0.9020	0.9566	0.03157	0.003010
2.330	0.9201	1.0042	0.03018	0.001195
2.368	0.9246	0.9499	0.02776	0.002487
2.402	0.9534	0.9941	0.02703	0.000000
2.438	0.9777	1.0045	0.02994	0.001001
2.472	0.9843	0.9867	0.02488	0.000000
2.506	0.9988	0.9879	0.02407	0.000000
2.540	1.0058	0.9700	0.02745	0.000689
2.574	1.0278	0.9898	0.02721	0.001086
2.608	1.0325	0.9772	0.03173	0.002013
2.645	1.0345	0.9717	0.02858	0.001648
2.679	1.0485	0.9826	0.02721	0.000000
2.714	1.0564	0.9692	0.02675	0.000000
2.748	1.0670	0.9808	0.02905	0.000475
2.783	1.0820	1.0198	0.02873	0.000000
2.816	1.0645	0.9663	0.02554	0.000000
2.852	1.0774	1.0093	0.02630	0.000874
2.886	1.0863	1.0158	0.03256	0.002166
2.924	1.0689	0.9416	0.03148	0.003414
2.958	1.0877	0.9699	0.03227	0.002671
2.993	1.1318	1.0189	0.03732	0.001818
3.028	1.1282	1.0105	0.03473	0.002209
3.061	1.1256	0.9989	0.02660	0.000000
3.095	1.1183	0.9868	0.02960	0.000000
3.130	1.1265	1.0158	0.02744	0.000886
3.162	1.1157	0.9895	0.03315	0.002883
3.197	1.1180	1.0071	0.02497	0.000000
3.232	1.1163	1.0193	0.02272	0.000000
3.269	1.1153	1.0137	0.02401	0.000000
3.303	1.1147	1.0015	0.02999	0.002031
3.337	1.1182	1.0126	0.02759	0.001510
3.371	1.1098	0.9897	0.02483	0.000772
3.406	1.1125	0.9813	0.02593	0.001225

Table 3. Profile Data at Station 3 - Unheated

y/H	rho u	T	(rho u)'	T'
0.163	0.2813	1.0772	0.07195	0.000000
0.194	0.2862	1.0731	0.07229	0.000000
0.223	0.2888	0.9863	0.08294	0.003486
0.252	0.3097	1.1428	0.09038	0.000270
0.282	0.3143	1.0341	0.11764	0.006637
0.310	0.3199	0.9755	0.14060	0.013227
0.342	0.3528	1.0551	0.12179	0.004280
0.373	0.3752	1.1247	0.09531	0.000000
0.404	0.3559	0.8413	0.08884	0.023125
0.436	0.3807	1.0320	0.04896	0.000858
0.467	0.3756	0.9955	0.03962	0.000000
0.495	0.3747	0.9918	0.03043	0.000000
0.527	0.3838	1.0971	0.03954	0.000512
0.557	0.3762	1.0392	0.03678	0.000000
0.589	0.3725	0.9876	0.03454	0.000000
0.619	0.3787	1.0767	0.04335	0.000000
0.652	0.3704	0.9885	0.01538	0.000000
0.683	0.3761	1.0180	0.05878	0.000000
0.715	0.3743	0.9372	0.10623	0.015440
0.745	0.3878	1.0415	0.08446	0.001413
0.777	0.3924	1.0362	0.07166	0.000000
0.806	0.4067	1.0114	0.11605	0.006065
0.838	0.4289	1.0549	0.11698	0.002183
0.868	0.4252	0.9252	0.13872	0.012985
0.895	0.4368	0.8902	0.12086	0.000000
0.931	0.4813	1.0838	0.14217	0.002312
0.964	0.4931	1.0125	0.13681	0.002963
0.987	0.5067	1.0028	0.15659	0.010517
1.027	0.5410	1.0420	0.15011	0.000000
1.056	0.5609	1.0539	0.15941	0.002625
1.088	0.5890	1.0536	0.14903	0.002428
1.120	0.5990	0.9474	0.11777	0.000000
1.152	0.6357	1.0658	0.15261	0.003021
1.204	0.6900	1.0941	0.17819	0.000787
1.236	0.6706	0.8140	0.22183	0.048267
1.266	0.7490	1.0898	0.17605	0.001461
1.296	0.7149	0.7755	0.18099	0.001705
1.326	0.8178	1.1246	0.17304	0.000000
1.357	0.8460	1.1152	0.16691	0.000000
1.389	0.8372	0.9465	0.18138	0.017894
1.419	0.8432	0.8801	0.17801	0.026057
1.451	0.8994	0.8855	0.14298	0.024409
1.481	0.9551	1.1053	0.09797	0.000740
1.511	0.9421	1.0216	0.09157	0.006218
1.540	0.9532	1.0057	0.06445	0.002197
1.570	0.9531	1.0069	0.05968	0.004720
1.600	0.9592	0.9889	0.04983	0.004563
1.632	0.9760	1.0172	0.05021	0.003294
1.663	0.9635	0.9960	0.05569	0.003875
1.694	0.9399	0.9808	0.05332	0.004464
1.718	0.9486	1.0464	0.04292	0.000830
1.754	0.9268	0.9749	0.03755	0.003001
1.785	0.9385	0.9969	0.03195	0.000000
1.814	0.9561	1.0094	0.03205	0.000655
1.845	0.9721	1.0375	0.03073	0.001259
1.875	0.9860	1.0463	0.03276	0.001515
1.906	0.9944	1.0434	0.03325	0.001079
1.937	1.0003	1.0249	0.03380	0.001902
1.970	1.0053	1.0034	0.03502	0.003252
2.001	1.0211	1.0438	0.03345	0.000758
2.032	1.0275	1.0351	0.03183	0.000740
2.064	1.0455	1.0557	0.03171	0.001281
2.096	1.0554	1.0575	0.03354	0.000856
2.128	1.0564	1.0601	0.03415	0.001326

2.160	1.0495	1.0211	0.03188	0.002288
2.194	1.0692	1.0623	0.02859	0.000000
2.237	1.0538	1.0106	0.04109	0.002263
2.271	1.0556	0.9596	0.04940	0.004767
2.305	1.0755	1.0309	0.06309	0.003608
2.337	1.0189	0.9893	0.06168	0.002884
2.370	1.0101	1.0000	0.04010	0.002671
2.406	0.9941	0.9699	0.03223	0.001567
2.440	1.0011	0.9941	0.03225	0.002181
2.475	0.9977	1.0083	0.03370	0.002173
2.510	1.0060	1.0393	0.03457	0.002032
2.545	1.0024	1.0351	0.03559	0.001854
2.579	1.0020	1.0120	0.03307	0.001111
2.610	1.0019	0.9990	0.03282	0.001838
2.644	0.9928	0.9928	0.03191	0.001950
2.680	1.0092	1.0479	0.03601	0.001749
2.712	0.9934	1.0097	0.03279	0.002015
2.748	0.9939	1.0261	0.03501	0.001083
2.781	1.0038	1.0653	0.03467	0.000900
2.816	0.9849	1.0196	0.03139	0.001489
2.850	0.9770	1.0199	0.03305	0.001050
2.884	0.9815	1.0237	0.03478	0.001932
2.917	0.9800	1.0154	0.02950	0.000342
2.952	0.9823	1.0099	0.03074	0.001270
2.985	0.9828	1.0233	0.03564	0.002490
3.019	0.9769	1.0138	0.03262	0.002044
3.054	0.9764	1.0323	0.02727	0.000000
3.087	0.9787	1.0519	0.03227	0.001326
3.120	0.9720	1.0392	0.02978	0.001081
3.155	0.9677	1.0214	0.03095	0.001423
3.188	0.9692	1.0242	0.02962	0.000417
3.221	0.9676	1.0359	0.03126	0.000853
3.253	0.9729	1.0367	0.03437	0.001654
3.286	0.9763	1.0254	0.03058	0.000000
3.321	0.9855	1.0430	0.03526	0.002106

Table 4. Profile Data at Station 4 - Unheated

y/H	rho u	T	(rho u)'	T'
0.266	0.2821	0.9073	0.10475	0.010243
0.304	0.3094	1.0072	0.11129	0.014161
0.333	0.2955	0.9123	0.10603	0.017253
0.365	0.3180	0.9527	0.09856	0.016928
0.396	0.3337	1.0170	0.06059	0.000000
0.426	0.3405	1.0232	0.06436	0.001326
0.458	0.3378	0.9962	0.07734	0.009053
0.490	0.3379	0.9571	0.06784	0.010977
0.522	0.3505	1.0119	0.05397	0.000000
0.550	0.3347	0.9316	0.05367	0.000000
0.581	0.3591	0.9921	0.03884	0.000000
0.610	0.3550	0.9702	0.04203	0.000000
0.642	0.3752	1.0351	0.03655	0.000000
0.673	0.3840	1.0440	0.07543	0.000000
0.703	0.3616	0.9355	0.07975	0.011116
0.736	0.3770	0.9857	0.09119	0.014561
0.767	0.3859	0.9704	0.05741	0.000000
0.797	0.3937	0.9726	0.10459	0.013866
0.827	0.4007	0.9704	0.14433	0.025791
0.856	0.4070	0.9772	0.12218	0.011599
0.889	0.4261	0.9949	0.13611	0.012103
0.920	0.4553	1.0498	0.14403	0.010551
0.952	0.4392	0.9961	0.12585	0.000000
0.984	0.4551	0.9857	0.14266	0.005085
1.015	0.4667	0.9719	0.13319	0.000000
1.045	0.4852	1.0037	0.15130	0.000000
1.072	0.4900	0.9904	0.15649	0.015811
1.104	0.5232	1.0364	0.19865	0.018998
1.135	0.5398	1.0079	0.17165	0.000000
1.167	0.5125	0.9224	0.19451	0.022258
1.197	0.5322	0.9376	0.20770	0.031081
1.228	0.5652	0.9810	0.15544	0.000000
1.258	0.6209	1.0561	0.19428	0.000000
1.296	0.6767	1.0701	0.23146	0.008281
1.326	0.6721	1.0639	0.22745	0.005592
1.354	0.6468	0.9160	0.24154	0.017083
1.384	0.6467	0.9059	0.31642	0.060615
1.415	0.7689	1.1168	0.24361	0.006398
1.446	0.7483	1.0226	0.25072	0.020520
1.476	0.7681	1.0122	0.21597	0.004550
1.507	0.9020	1.1725	0.21791	0.000000
1.529	0.8064	1.0077	0.22619	0.020665
1.565	0.8675	1.0360	0.19970	0.010411
1.594	0.8821	1.0029	0.18228	0.007338
1.624	0.9538	1.0712	0.17404	0.009466
1.654	0.9388	1.0484	0.16000	0.014275
1.685	0.9543	1.0186	0.13048	0.011862
1.714	0.9968	1.1030	0.11063	0.005181
1.748	0.9633	1.0360	0.08563	0.007075
1.779	1.0123	1.0543	0.06285	0.000000
1.810	1.0508	1.0656	0.06612	0.001656
1.840	1.0233	1.0438	0.05838	0.002524
1.872	1.0088	1.0237	0.06192	0.004955
1.903	1.0037	1.0035	0.06775	0.009143
1.935	0.9969	1.0167	0.06193	0.005430
1.967	1.0135	1.0291	0.05761	0.006192
2.001	1.0103	1.0489	0.04906	0.003473
2.034	0.9927	1.0352	0.04459	0.001633
2.068	1.0190	1.0673	0.04081	0.000000
2.099	0.9664	0.9721	0.04526	0.005912
2.133	1.0289	1.0788	0.03612	0.000000
2.166	0.9727	0.9871	0.05459	0.009061
2.200	1.0182	1.0288	0.03276	0.001104
2.234	1.0046	1.0005	0.03888	0.000000

2.270	1.0714	1.0762	0.03277	0.000000
2.304	0.9881	0.9540	0.05670	0.011466
2.348	0.9894	0.9833	0.06266	0.006470
2.381	1.0167	1.0521	0.03931	0.000000
2.413	1.0360	1.0655	0.04202	0.002032
2.445	1.0487	1.0659	0.04934	0.002440
2.479	1.0448	1.0518	0.05872	0.004540
2.515	1.0383	1.0633	0.06750	0.004324
2.547	1.0312	1.0736	0.06313	0.001640
2.583	0.9972	1.0581	0.06484	0.004357
2.616	1.0097	1.0812	0.05060	0.002874
2.646	0.9809	1.0448	0.03783	0.000000
2.680	0.9974	1.0639	0.03801	0.001354
2.713	1.0061	1.0733	0.04138	0.002190
2.746	0.9993	1.0740	0.03638	0.001259
2.780	0.9860	1.0568	0.04189	0.002588
2.813	0.9975	1.0612	0.04102	0.001984
2.848	0.9943	1.0717	0.03536	0.000000
2.882	0.9946	1.0663	0.03731	0.002045
2.913	0.9824	1.0620	0.03548	0.001051
2.946	0.9890	1.0593	0.04151	0.002799
2.980	0.9910	1.0595	0.04216	0.003322
3.012	1.0313	1.1070	0.03984	0.001721
3.045	1.0111	1.0797	0.04232	0.002932
3.078	1.0286	1.0865	0.03961	0.001710
3.114	1.0118	1.0392	0.03877	0.000000
3.148	1.0141	1.0549	0.04000	0.002512
3.181	1.0239	1.0493	0.04449	0.003149
3.213	1.0212	1.0452	0.04351	0.003654
3.248	1.0165	1.0473	0.04008	0.002601
3.280	0.9831	0.9970	0.04259	0.003319
3.316	1.0672	1.1030	0.03946	0.001309
3.348	1.0323	1.0475	0.03907	0.001802
3.383	1.0458	1.0511	0.04232	0.002912
3.415	1.0565	1.0636	0.04192	0.002536

Table 5. Profile Data at Station 4 With Shock Interaction - Unheated

y/H	rho u	T	(rho u)'	T'
0.285	0.3666	1.0550	0.11525	0.003722
0.315	0.3700	1.0379	0.13749	0.010070
0.343	0.3734	1.0545	0.09870	0.000000
0.374	0.3812	1.0640	0.11669	0.000000
0.405	0.3880	1.1207	0.10575	0.000000
0.438	0.3866	1.0024	0.11703	0.000000
0.469	0.3900	1.0594	0.12131	0.001738
0.500	0.3939	1.0359	0.08806	0.000000
0.531	0.3984	1.0054	0.07518	0.000000
0.560	0.4103	1.0725	0.11547	0.002033
0.589	0.4220	1.0732	0.10403	0.000000
0.621	0.4271	1.0955	0.12666	0.000000
0.650	0.4195	1.0475	0.10590	0.000000
0.681	0.4106	0.9689	0.09234	0.004276
0.713	0.4222	0.9965	0.13726	0.009833
0.745	0.4486	1.0870	0.13261	0.000000
0.776	0.4615	1.0622	0.14889	0.004013
0.806	0.4631	0.9918	0.14208	0.013422
0.836	0.4797	1.0489	0.14773	0.000000
0.868	0.4938	1.0670	0.19770	0.011558
0.900	0.4992	0.9150	0.17229	0.000000
0.931	0.5276	1.0195	0.19438	0.013307
0.962	0.5596	1.0558	0.19378	0.000000
0.993	0.5873	0.9990	0.22614	0.012069
1.024	0.6198	1.0796	0.21551	0.000000
1.055	0.6359	1.0302	0.25770	0.013959
1.083	0.6595	1.0157	0.25418	0.020651
1.113	0.7116	1.0840	0.22801	0.000000
1.143	0.7380	1.0970	0.28756	0.010242
1.174	0.7157	0.9927	0.30892	0.021404
1.206	0.7428	0.8627	0.23954	0.000000
1.236	0.8086	1.1679	0.31278	0.000000
1.267	0.8599	0.8881	0.29168	0.000000
1.306	0.9504	1.1454	0.35207	0.003174
1.334	1.0051	1.1053	0.35497	0.004588
1.363	1.0521	1.0336	0.34485	0.007340
1.393	1.1678	1.2399	0.34568	0.000000
1.424	1.2448	1.2007	0.33528	0.000000
1.455	1.2287	1.1327	0.31058	0.001667
1.486	1.1828	0.9567	0.36418	0.044671
1.514	1.2156	0.9926	0.36779	0.038156
1.545	1.2962	1.1194	0.24943	0.005477
1.575	1.3344	1.0937	0.20280	0.006651
1.603	1.3441	1.0683	0.16969	0.009217
1.632	1.3500	1.0682	0.13257	0.004454
1.665	1.3594	1.0737	0.11970	0.007558
1.695	1.3681	1.0705	0.08568	0.003064
1.726	1.3682	1.0818	0.06828	0.002552
1.757	1.3658	1.0528	0.06389	0.003938
1.788	1.3718	1.0896	0.05614	0.001442
1.819	1.3801	1.0780	0.05859	0.003523
1.850	1.3882	1.1005	0.06558	0.002767
1.881	1.3924	1.1102	0.05408	0.001286
1.913	1.3908	1.1009	0.06133	0.002433
1.945	1.3871	1.1080	0.06134	0.002582
1.978	1.3781	1.0763	0.05451	0.000000
2.011	1.3718	1.0947	0.05774	0.001302
2.045	1.3731	1.0825	0.06469	0.003188
2.078	1.3815	1.0991	0.06082	0.002693
2.103	1.3887	1.0997	0.05754	0.001861
2.142	1.3882	1.0914	0.05995	0.002354
2.177	1.3870	1.0919	0.05888	0.002219
2.212	1.3821	1.0748	0.06821	0.003663
2.246	1.3739	1.0488	0.07172	0.006583

2.280	1.3628	1.0840	0.06355	0.003985
2.315	1.3405	1.0235	0.06564	0.004947
2.360	1.3173	1.0569	0.09362	0.006001
2.392	1.3106	1.0402	0.07232	0.003163
2.425	1.3155	1.0837	0.08099	0.004788
2.459	1.3074	1.0338	0.08532	0.005600
2.492	1.2950	1.0507	0.07997	0.005342
2.526	1.2998	1.0649	0.05744	0.000393
2.560	1.3072	1.0885	0.06221	0.002510
2.593	1.3058	1.0553	0.05650	0.002961
2.627	1.2991	1.1012	0.05768	0.001871
2.658	1.2851	1.0619	0.05878	0.003652
2.691	1.2764	1.0690	0.04791	0.000000
2.724	1.2830	1.0621	0.05158	0.003482
2.758	1.2984	1.0832	0.05575	0.002703
2.792	1.3049	1.0911	0.05531	0.002658
2.826	1.3070	1.0529	0.05522	0.003631
2.859	1.3297	1.0856	0.05507	0.002109
2.892	1.3529	1.1085	0.05049	0.001022
2.926	1.3565	1.0862	0.04931	0.001815
2.959	1.3650	1.0687	0.06345	0.004507
2.991	1.3915	1.0951	0.05427	0.002443
3.024	1.4163	1.0913	0.04782	0.001739
3.057	1.4357	1.0818	0.04904	0.002096
3.091	1.4613	1.0941	0.05681	0.003041
3.126	1.4735	1.0933	0.05460	0.002888
3.159	1.4617	1.0352	0.05110	0.000000
3.192	1.4563	1.0213	0.04789	0.000000
3.223	1.4646	1.0435	0.05176	0.002947
3.256	1.4640	1.0310	0.05352	0.003676
3.290	1.4688	1.0173	0.06745	0.007194
3.323	1.4830	1.0664	0.05571	0.003375
3.357	1.4833	1.0306	0.05201	0.000000
3.389	1.4861	1.0434	0.04710	0.000000
3.423	1.4948	1.0450	0.05380	0.002452

Table 6. Profile Data at Station 1 - Heated

y/H	rho u	T	(rho u)'	T'
0.182	0.2072	1.0116	0.03431	0.000000
0.215	0.2104	0.9825	0.01286	0.000000
0.249	0.2038	1.0009	0.02074	0.000000
0.282	0.2008	1.0933	0.03350	0.000223
0.313	0.2072	0.9493	0.00000	0.000000
0.347	0.2051	1.0067	0.02085	0.000000
0.378	0.2056	1.0365	0.02183	0.000000
0.410	0.2067	0.9554	0.00000	0.000000
0.444	0.2123	1.0712	0.03040	0.000000
0.477	0.2118	0.9069	0.00000	0.000000
0.510	0.2167	1.0790	0.02735	0.000000
0.545	0.2203	0.9859	0.00000	0.000000
0.578	0.2182	1.0278	0.01564	0.000000
0.611	0.2137	0.9946	0.01501	0.000000
0.643	0.2137	1.0259	0.01553	0.000000
0.676	0.2098	1.0935	0.03391	0.000267
0.708	0.2056	0.9724	0.02352	0.000000
0.742	0.1957	0.9967	0.02010	0.000000
0.775	0.1849	1.0104	0.00000	0.000000
0.809	0.1766	0.9763	0.00000	0.000000
0.842	0.1901	1.0296	0.00000	0.000000
0.873	0.2069	0.9492	0.00336	0.000000
0.905	0.1996	0.9507	0.03387	0.000000
0.940	0.1794	0.8442	0.02238	0.000000
0.971	0.1784	0.3714	0.00000	0.000000
1.006	0.2439	-.0470	0.09583	0.011971
1.037	0.2677	0.1699	0.18639	0.048968
1.070	0.2664	0.0428	0.04268	0.000000
1.103	0.2812	-.0020	0.27148	0.093822
1.136	0.3040	-.0187	0.00000	0.000000
1.166	0.3626	-.0370	0.00000	0.000000
1.199	0.3982	0.0681	0.18253	0.034504
1.231	0.4148	0.0591	0.12049	0.000000
1.287	0.5427	-.0122	0.24216	0.062488
1.320	0.5493	-.0410	0.14198	0.036423
1.354	0.5794	0.0176	0.04978	0.000000
1.387	0.6334	0.0161	0.21827	0.058730
1.420	0.6782	0.0433	0.20414	0.055909
1.453	0.7129	-.0456	0.03255	0.000000
1.486	0.7514	-.1520	0.24998	0.095901
1.520	0.8397	-.1480	0.00000	0.000000
1.552	0.8073	0.0821	0.00000	0.000000
1.585	0.9176	-.0710	0.00000	0.000000
1.620	0.9991	-.3144	0.15921	0.071323
1.653	0.9486	-.1679	0.09759	0.034637
1.686	0.9833	0.0446	0.00000	0.000000
1.719	0.9535	-.1363	0.03578	0.011799
1.751	1.0204	-.1258	0.09570	0.045140
1.783	0.9913	-.0516	0.08714	0.038005
1.817	0.9879	-.0938	0.08065	0.036248
1.850	0.9652	-.0468	0.03160	0.016780
1.884	0.9653	0.0949	0.07783	0.027035
1.917	0.9927	-.0953	0.06037	0.026246
1.951	0.9674	0.1222	0.00000	-0.000000
1.982	1.0202	-.0369	0.04865	0.023601
2.015	0.9848	-.0348	0.06638	0.030478
2.049	0.9988	-.0788	0.07771	0.034967
2.081	1.0004	0.0007	0.07118	0.029328
2.113	1.0109	-.0585	0.07144	0.031233
2.149	1.0063	-.0528	0.06663	0.029013
2.183	1.0356	-.0776	0.04004	0.022684
2.216	1.0209	-.0875	0.09433	0.042960
2.248	1.0136	0.0073	0.05526	0.023970
2.280	1.0149	-.1525	0.00000	0.009227

2.311	1.0371	-.0169	0.06263	0.027305
2.344	1.0399	-.0387	0.09217	0.038274
2.396	0.9971	0.0226	0.04595	0.017238
2.430	0.9941	-.0899	0.09059	0.036537
2.462	1.0276	-.0054	0.06124	0.024395
2.495	1.0096	0.0336	0.02781	0.009696
2.527	1.0189	-.0529	0.09219	0.036066
2.557	1.0133	0.0343	0.06561	0.026225
2.590	0.9930	0.0445	0.04357	0.015762
2.624	0.9942	0.0616	0.07719	0.026900
2.656	0.9921	-.0298	0.08137	0.031129
2.690	0.9914	0.0486	0.04904	0.018718
2.724	0.9569	0.0577	0.06969	0.024928
2.756	0.9263	0.0200	0.07156	0.020163
2.789	0.9095	0.0018	0.10152	0.039352
2.821	0.9042	-.0030	0.06731	0.023328
2.852	0.9083	0.0358	0.06333	0.023252
2.887	0.9237	0.0158	0.04722	0.021232
2.921	0.9271	0.0295	0.09754	0.034487
2.956	0.9160	0.0127	0.05690	0.021116
2.988	0.9403	-.0548	0.07664	0.032494
3.022	0.9420	0.0320	0.05460	0.022000
3.054	0.9423	-.0126	0.07110	0.029680
3.086	0.9436	0.0268	0.05293	0.020710
3.117	0.9603	0.0098	0.04174	0.017549
3.151	0.9450	0.0055	0.08978	0.033397
3.183	0.9489	0.0795	0.05897	0.021003
3.216	0.9500	0.0216	0.07515	0.028986
3.248	0.9450	0.0099	0.04000	0.016675
3.282	0.9439	-.0785	0.06425	0.029316
3.313	0.9619	0.0019	0.03831	0.019915
3.343	0.9738	-.0123	0.04611	0.021610
3.373	0.9643	0.0561	0.05508	0.020670
3.403	0.9772	-.0474	0.05698	0.024111
3.435	0.9906	-.0139	0.07234	0.030813

Table 7. Profile Data at Station 2 - Heated

y/H	rho u	T	(rho u)'	T'
0.189	0.2515	0.8070	0.03137	0.004931
0.222	0.2595	0.7692	0.06398	0.010321
0.255	0.2527	0.7996	0.03023	0.004509
0.291	0.2686	0.7123	0.11104	0.015969
0.326	0.2586	0.6793	0.00000	0.006220
0.360	0.2558	0.7500	0.04474	0.006623
0.392	0.2516	0.8781	0.00000	0.000000
0.425	0.2505	0.8750	0.00000	0.000000
0.458	0.2490	0.7168	0.08664	0.017118
0.490	0.2492	0.7453	0.03206	0.006207
0.522	0.2458	0.8510	0.00000	0.000000
0.553	0.2519	0.7628	0.00000	0.000000
0.589	0.2425	0.8385	0.00000	0.000000
0.623	0.2466	0.7901	0.02750	0.002309
0.654	0.2447	0.8751	0.01485	0.000000
0.687	0.2504	0.7621	0.02987	0.005391
0.721	0.2487	0.8008	0.06762	0.008860
0.755	0.2464	0.7828	0.08557	0.014320
0.788	0.2452	0.8395	0.00000	0.000000
0.820	0.2438	0.8016	0.10222	0.013732
0.850	0.2594	0.7382	0.00000	0.000000
0.886	0.2635	0.5826	0.07550	0.011123
0.920	0.2887	0.4063	0.17617	0.026429
0.954	0.2831	0.5421	0.00000	0.000000
0.988	0.3043	0.4296	0.12679	0.000000
1.021	0.3817	0.0676	0.26191	0.064516
1.054	0.3534	0.4773	0.27518	0.037427
1.088	0.4145	0.0191	0.28774	0.078690
1.122	0.4750	-.1172	0.12574	0.000000
1.157	0.4050	0.6264	0.18493	0.000000
1.191	0.4995	0.0535	0.00000	0.000000
1.224	0.5069	0.2845	0.18036	0.023779
1.259	0.5182	0.1738	0.36747	0.092713
1.310	0.6565	0.1069	0.22161	0.033928
1.345	0.6742	-.0486	0.16386	0.022565
1.380	0.6876	-.0268	0.13905	0.000000
1.415	0.7652	-.0626	0.20108	0.030113
1.450	0.8051	0.0308	0.17586	0.033380
1.486	0.8551	0.1400	0.06226	0.000000
1.520	0.8517	0.2393	0.06183	0.000000
1.553	0.9341	-.0935	0.00000	0.000000
1.589	0.9587	0.1289	0.12771	0.027872
1.623	0.9765	-.0307	0.00000	0.000000
1.656	0.9938	0.0353	0.08002	0.012992
1.692	0.9965	0.0582	0.00000	0.000000
1.727	0.9972	0.0023	0.07473	0.016680
1.763	0.9552	-.0097	0.10444	0.024560
1.795	0.9498	-.0496	0.09415	0.024287
1.829	0.9057	0.4080	0.00000	0.000000
1.860	0.9732	-.1029	0.08527	0.027239
1.895	0.9744	0.0154	0.02639	0.000000
1.926	0.9857	-.0584	0.03627	0.000000
1.960	0.9832	0.0242	0.08071	0.019479
1.994	1.0071	-.0689	0.00000	0.000000
2.026	1.0115	-.0681	0.07943	0.023461
2.058	0.9572	-.0364	0.09834	0.023105
2.089	0.9623	-.0047	0.02974	0.000000
2.120	0.9439	0.0162	0.10620	0.029735
2.151	0.9437	-.0253	0.07458	0.019564
2.182	0.9565	-.0160	0.07255	0.019587
2.212	0.9664	-.0347	0.07980	0.022779
2.244	0.9534	-.1310	0.07730	0.023284
2.277	0.9287	0.0108	0.05627	0.000000
2.308	0.8935	-.0690	0.04618	0.000000

2.340	0.8718	0.0657	0.03379	0.000000
2.370	0.8713	0.0737	0.05562	0.008567
2.419	0.8744	-.0392	0.09070	0.024499
2.449	0.9131	-.0965	0.05705	0.016402
2.481	0.9037	-.0421	0.07207	0.021106
2.513	0.9090	0.0110	0.05309	0.007090
2.546	0.9465	-.1729	0.07817	0.018424
2.577	0.9378	-.0140	0.07340	0.019070
2.610	0.9450	-.0282	0.05158	0.011057
2.640	0.9726	-.0367	0.05198	0.013161
2.672	0.9762	0.0713	0.00000	0.000000
2.703	0.9935	0.0059	0.00000	0.000000
2.736	0.9977	0.0892	0.06293	0.016437
2.768	1.0128	0.0319	0.03633	0.009387
2.801	1.0279	-.0230	0.05973	0.005491
2.835	1.0292	0.0539	0.10170	0.024904
2.866	1.0314	0.0197	0.09798	0.022431
2.897	1.0534	-.0475	0.10442	0.028910
2.929	1.0551	-.0346	0.09864	0.024816
2.963	1.0758	-.0623	0.04336	0.000000
2.996	1.0475	0.0359	0.11712	0.027420
3.028	1.0860	-.1235	0.00000	0.000000
3.060	1.0870	-.0570	0.10527	0.027123
3.093	1.0844	-.0013	0.10858	0.028332
3.128	1.0966	0.0565	0.02429	0.003196
3.161	1.1313	0.0098	0.08421	0.023154
3.191	1.0726	0.0415	0.09915	0.024617
3.224	1.1127	0.0525	0.03180	0.000000
3.256	1.0781	0.0723	0.09139	0.022479
3.289	1.0890	0.1218	0.06641	0.012264
3.322	1.0995	-.0978	0.02016	0.010188
3.355	1.0751	-.1190	0.06529	0.015192
3.389	1.0786	0.1257	0.06722	0.009717
3.421	1.0752	-.0824	0.06212	0.021202
3.451	1.0544	-.0260	0.00000	0.000000

Table 8. Profile Data at Station 3 - Heated

y/H	rho u	T	(rho u)'	T'
0.180	0.2197	0.7151	0.11012	0.013503
0.213	0.2327	0.7355	0.09404	0.012158
0.245	0.2390	0.7684	0.06314	0.007914
0.277	0.2387	0.7737	0.04651	0.006659
0.311	0.2422	0.7769	0.04435	0.006900
0.343	0.2456	0.8009	0.04150	0.006235
0.376	0.2404	0.7870	0.02582	0.003274
0.407	0.2425	0.7898	0.03573	0.006185
0.440	0.2383	0.7591	0.00000	0.000000
0.473	0.2401	0.7591	0.03809	0.006438
0.506	0.2407	0.7930	0.02039	0.003430
0.540	0.2402	0.8052	0.04246	0.004579
0.576	0.2415	0.7756	0.07462	0.009923
0.611	0.2426	0.7821	0.02514	0.000000
0.645	0.2427	0.7687	0.08545	0.006375
0.677	0.2496	0.7887	0.07732	0.000000
0.711	0.2513	0.7614	0.00000	0.000000
0.745	0.2495	0.6668	0.00000	0.000000
0.778	0.2518	0.6128	0.00000	0.000000
0.811	0.2703	0.6764	0.23547	0.034779
0.845	0.2697	0.5518	0.00000	0.000000
0.878	0.2824	0.4773	0.23031	0.053610
0.912	0.2943	0.2091	0.28010	0.068446
0.945	0.2903	0.2240	0.32805	0.099749
0.977	0.3312	0.2634	0.13717	0.000000
1.010	0.3483	0.3287	0.00000	0.000000
1.041	0.3328	0.0570	0.00000	0.000000
1.074	0.3744	0.0191	0.31138	0.115401
1.108	0.4307	0.0947	0.00000	0.000000
1.141	0.4578	0.0716	0.00000	0.000000
1.174	0.4808	0.1573	0.00000	0.000000
1.206	0.5225	0.1833	0.15610	0.000000
1.237	0.5379	0.0187	0.00000	0.000000
1.287	0.6154	-.0295	0.15210	0.027060
1.319	0.6997	0.1884	0.00000	0.000000
1.352	0.6666	0.0359	0.00000	0.000000
1.383	0.7426	0.0816	0.22115	0.061581
1.416	0.7412	0.0172	0.06119	0.000000
1.447	0.7549	-.0961	0.06154	0.000000
1.479	0.8597	-.0490	0.20164	0.075010
1.509	0.9002	0.0028	0.06337	0.027076
1.540	0.8814	-.0457	0.12366	0.009815
1.574	0.9233	-.0654	0.00000	0.000000
1.604	0.9361	-.0271	0.07092	0.023460
1.636	0.9452	-.0569	0.12434	0.050743
1.669	0.9770	-.0541	0.14477	0.064912
1.701	0.9607	-.0748	0.09172	0.042021
1.731	0.9777	-.0562	0.03690	0.017593
1.761	0.9960	-.0073	0.08862	0.039960
1.791	0.9696	-.0761	0.11796	0.055113
1.824	0.9832	-.0081	0.07307	0.029843
1.854	0.9646	-.0396	0.05726	0.030949
1.886	0.9485	-.0511	0.09928	0.045901
1.919	0.9562	-.0459	0.02997	0.017637
1.951	0.9420	-.0630	0.06614	0.035153
1.982	0.9716	-.0361	0.05906	0.031366
2.014	0.9664	-.0425	0.08565	0.039887
2.045	0.9888	-.0635	0.08004	0.037400
2.075	0.9976	-.0307	0.07832	0.038414
2.106	1.0316	0.0222	0.07745	0.037540
2.138	1.0012	-.0563	0.05597	0.029930
2.170	1.0053	-.0259	0.07491	0.033286
2.203	0.9952	0.0109	0.07401	0.036580
2.237	1.0328	0.0404	0.00000	0.000815

2.267	1.0164	0.0115	0.03387	0.020624
2.296	0.9985	0.0439	0.05979	0.026310
2.347	1.0049	-.0708	0.08067	0.038373
2.378	1.0050	-.0238	0.10347	0.043881
2.411	1.0206	0.0015	0.06633	0.029373
2.442	1.0285	-.0196	0.08959	0.038086
2.477	1.0368	0.0132	0.08378	0.036621
2.508	1.0342	-.0013	0.05970	0.026682
2.541	1.0225	0.0158	0.06451	0.028961
2.573	1.0162	0.0127	0.02907	0.017485
2.605	1.0234	0.0216	0.09565	0.040066
2.638	0.9936	-.0400	0.08766	0.041919
2.671	0.9877	0.0633	0.09005	0.034933
2.707	1.0018	0.0139	0.09014	0.038638
2.735	0.9888	-.0265	0.09289	0.041816
2.775	1.0276	-.0024	0.07224	0.032955
2.809	1.0211	0.0000	0.11071	0.047341
2.842	0.9944	-.0101	0.02662	0.016989
2.874	0.9851	0.0120	0.09005	0.038406
2.901	0.9905	0.0122	0.07071	0.031672
2.942	1.0044	0.0205	0.06719	0.032822
2.975	0.9882	-.0111	0.08215	0.041338
3.010	1.0036	0.0131	0.05824	0.027957
3.046	1.0000	-.0097	0.08492	0.039390
3.081	0.9819	-.0369	0.08200	0.038898
3.113	1.0052	0.0474	0.08476	0.034694
3.147	0.9968	0.0151	0.06970	0.032247
3.182	0.9825	0.0217	0.07600	0.033964
3.208	0.9759	-.0125	0.06974	0.031117
3.251	0.9771	0.0131	0.09783	0.042620
3.286	0.9692	0.0097	0.07961	0.037864
3.320	0.9685	0.0122	0.08245	0.035917
3.354	0.9573	-.0438	0.07516	0.037842
3.385	0.9750	0.0335	0.08197	0.035841
3.418	0.9657	0.0117	0.03975	0.022982

Table 9. Profile Data at Station 4 - Heated

y/H	rho u	T	(rho u)'	T'
0.215	0.2279	0.7731	0.04565	0.000000
0.245	0.2434	0.7354	0.09441	0.006598
0.275	0.2421	0.7789	0.07932	0.012464
0.305	0.2534	0.7281	0.08278	0.000000
0.335	0.2749	0.8730	0.00000	0.000000
0.368	0.2697	0.5007	0.24551	0.056477
0.399	0.2836	0.7962	0.13765	0.015778
0.431	0.2913	0.7402	0.00000	0.000000
0.464	0.2820	0.5071	0.00000	0.000000
0.498	0.3112	0.7207	0.00000	0.000000
0.529	0.3066	0.6617	0.00000	0.000000
0.562	0.2880	0.0805	0.21077	0.083608
0.593	0.3200	0.5405	0.19944	0.031039
0.625	0.3333	0.3539	0.00000	0.000000
0.658	0.3322	0.3045	0.25887	0.037837
0.692	0.3518	0.3373	0.22166	0.040877
0.724	0.3505	0.0792	0.14903	0.000000
0.758	0.4183	0.3704	0.00000	0.000000
0.790	0.4352	0.4568	0.23826	0.046703
0.822	0.4324	0.1045	0.22609	0.067084
0.855	0.4263	0.0232	0.26341	0.054503
0.888	0.4881	0.2969	0.09151	0.000000
0.922	0.4934	0.0985	0.17224	0.042051
0.956	0.5572	0.0090	0.18255	0.064660
0.992	0.5565	-.0405	0.00000	0.000000
1.027	0.5635	0.2754	0.18308	0.000000
1.063	0.6021	0.0455	0.00000	0.000000
1.095	0.6128	-.1829	0.20861	0.076770
1.128	0.6923	0.2890	0.08511	0.000000
1.161	0.7151	0.2017	0.16816	0.009462
1.194	0.6933	0.0246	0.14698	0.026905
1.228	0.7613	0.0849	0.14101	0.000000
1.262	0.7735	0.0649	0.00000	0.000000
1.291	0.7098	-.1496	0.10044	0.000000
1.325	0.8752	0.0671	0.13342	0.026884
1.358	0.8694	0.0878	0.25902	0.077394
1.391	0.8847	-.0173	0.16824	0.044822
1.422	0.9297	0.0040	0.19473	0.069510
1.454	0.8817	-.0042	0.11927	0.026636
1.487	0.9614	-.0181	0.00000	0.000000
1.521	0.9452	0.0153	0.16594	0.058918
1.554	0.9824	0.0577	0.06998	0.018713
1.587	0.9966	0.0201	0.16678	0.064722
1.619	1.0220	0.0407	0.08167	0.028084
1.651	1.0087	-.0154	0.10367	0.044703
1.681	0.9674	-.0832	0.03972	0.020619
1.715	1.0039	-.0220	0.08655	0.033175
1.747	0.9832	0.0106	0.09162	0.033170
1.780	0.9949	-.0550	0.10912	0.046507
1.812	0.9724	-.0310	0.06549	0.029293
1.843	0.9753	0.0016	0.00000	0.000000
1.875	0.9719	-.0236	0.08497	0.038626
1.906	0.9854	0.0342	0.08524	0.035849
1.938	0.9981	0.0326	0.07906	0.033340
1.968	0.9842	-.0428	0.09463	0.042595
2.000	0.9940	-.0404	0.09107	0.043841
2.033	0.9998	-.0551	0.05951	0.027508
2.066	1.0284	0.0169	0.05316	0.024577
2.098	1.0345	-.0141	0.07127	0.032913
2.130	1.0696	0.0188	0.07243	0.031812
2.155	1.0461	-.0247	0.04146	0.014887
2.193	1.0747	-.0049	0.09132	0.041332
2.224	1.1050	0.0323	0.07566	0.032401
2.255	1.0930	-.0420	0.06210	0.031983

2.287	1.1003	-.0451	0.09978	0.043391
2.320	1.1161	0.0346	0.06039	0.022813
2.359	1.0840	-.0434	0.07876	0.024129
2.391	1.0120	-.0920	0.08592	0.036449
2.423	1.0364	-.0157	0.10504	0.040647
2.454	1.0360	-.0857	0.08991	0.038037
2.484	1.0377	-.0214	0.09502	0.039994
2.516	0.9955	-.0556	0.08129	0.035374
2.548	1.0252	-.0367	0.06808	0.032633
2.580	1.0685	-.0393	0.07919	0.030610
2.614	1.0556	0.0057	0.06159	0.026043
2.646	1.0139	-.0962	0.08142	0.038702
2.678	1.0661	0.0318	0.10855	0.041757
2.709	1.0308	-.0132	0.00000	0.011957
2.740	1.0268	-.0382	0.07768	0.034081
2.774	1.0195	-.0586	0.06317	0.032119
2.803	1.0273	-.0059	0.05031	0.028000
2.837	1.0179	-.0483	0.08611	0.037601
2.870	1.0085	-.0386	0.04724	0.021604
2.904	1.0088	-.0244	0.06948	0.030630
2.934	1.0286	-.0105	0.05283	0.022450
2.967	1.0064	-.0591	0.07209	0.031562
3.000	1.0152	-.0053	0.06468	0.027413
3.032	1.0146	-.0616	0.04458	0.022499
3.064	1.0237	-.0286	0.08595	0.034407
3.100	1.0298	0.0560	0.05790	0.024165
3.133	1.0311	0.0236	0.03755	0.017000
3.169	1.0039	-.0449	0.07057	0.036567
3.202	1.0289	0.0063	0.08744	0.035814
3.235	1.0060	-.0217	0.07421	0.037011
3.268	1.0262	0.0090	0.09242	0.036362
3.302	1.0081	-.0058	0.07942	0.035370
3.337	1.0008	-.0252	0.06598	0.032712
3.372	1.0165	0.0014	0.06855	0.031434
3.406	1.0131	-.0095	0.06016	0.028598

Table 10. Profile Data at Station 4 With Shock Interaction - Heated

y/H	rho u	T	(rho u)'	T'
0.197	0.2554	0.7018	0.21656	0.015877
0.229	0.2611	0.7660	0.11260	0.000000
0.256	0.2645	0.7644	0.19728	0.018870
0.288	0.2735	0.6841	0.16047	0.009724
0.316	0.2833	0.7967	0.15101	0.000000
0.348	0.2861	0.7183	0.11455	0.000000
0.379	0.2941	0.7349	0.16680	0.009405
0.412	0.3047	0.7762	0.11534	0.000000
0.445	0.3073	0.7637	0.17808	0.015995
0.477	0.3118	0.7075	0.00000	0.000000
0.509	0.3209	0.7445	0.08816	0.000000
0.541	0.3237	0.7313	0.00000	0.000000
0.572	0.3256	0.6113	0.00000	0.000000
0.606	0.3333	0.6827	0.00000	0.000000
0.637	0.3517	0.5562	0.09490	0.014512
0.670	0.3718	0.8296	0.26203	0.003658
0.704	0.3902	0.3224	0.45852	0.127108
0.735	0.4153	0.6367	0.00000	0.000000
0.769	0.4417	0.4246	0.44306	0.102725
0.801	0.4665	0.3538	0.11824	0.000000
0.832	0.5124	0.3738	0.00000	0.000000
0.867	0.5777	0.5389	0.43337	0.070118
0.899	0.6025	0.0292	0.53801	0.190434
0.933	0.6249	0.1250	0.00000	0.000000
0.969	0.6880	0.2987	0.40418	0.092763
1.003	0.7531	0.1059	0.15757	0.000000
1.038	0.8090	0.3322	0.37258	0.090732
1.072	0.8458	-.1256	0.00000	0.000000
1.105	0.8700	-.0999	0.00000	0.000000
1.138	0.9197	-.0715	0.00000	0.000000
1.172	1.0007	0.1488	0.25682	0.031871
1.205	1.0833	0.0183	0.20511	0.000000
1.237	1.1373	-.0223	0.00000	0.000000
1.292	1.1726	0.0541	0.36917	0.111850
1.326	1.2499	0.0403	0.46422	0.163302
1.358	1.3419	-.0552	0.07225	0.000000
1.390	1.4239	-.0522	0.35771	0.132991
1.422	1.4960	0.0931	0.12938	0.000000
1.454	1.5433	-.1542	0.11712	0.000000
1.487	1.6142	-.0480	0.14939	0.052329
1.520	1.6882	-.1316	0.04322	0.016496
1.554	1.7138	-.0329	0.16776	0.072161
1.586	1.7037	-.0138	0.13871	0.052119
1.619	1.7046	-.0028	0.08235	0.030261
1.649	1.7262	0.0193	0.09755	0.038713
1.681	1.7304	-.0196	0.11133	0.045347
1.713	1.7166	-.0010	0.07235	0.023481
1.746	1.7139	-.0339	0.06991	0.024689
1.779	1.7243	-.0171	0.06868	0.027757
1.812	1.7388	-.1025	0.00000	0.000000
1.847	1.7462	-.0065	0.04983	0.017875
1.875	1.7269	-.0175	0.08775	0.036396
1.905	1.7081	-.1014	0.05749	0.025683
1.936	1.7133	0.0049	0.04970	0.019350
1.969	1.7166	-.0434	0.12227	0.049032
2.000	1.6959	-.0173	0.12218	0.047799
2.032	1.6621	-.0565	0.07716	0.033114
2.066	1.6317	-.0128	0.06617	0.029045
2.098	1.6038	-.1271	0.12081	0.058916
2.129	1.5781	0.0231	0.08091	0.032198
2.160	1.5570	-.1081	0.12920	0.058263
2.191	1.5482	0.0124	0.09817	0.035276
2.224	1.5467	-.0118	0.09812	0.040778
2.255	1.5306	-.0446	0.11267	0.048384

2.287	1.4984	-.0567	0.08588	0.037173
2.319	1.5301	-.0554	0.07156	0.035264
2.375	1.6315	-.1233	0.13234	0.056197
2.407	1.6733	0.0002	0.05021	0.016611
2.438	1.6673	0.0342	0.10269	0.034239
2.469	1.6818	-.0418	0.06818	0.027132
2.499	1.6895	-.1649	0.10014	0.047328
2.531	1.6813	-.0126	0.08538	0.034078
2.563	1.6822	-.0043	0.07833	0.031527
2.594	1.6933	-.1129	0.10275	0.047214
2.628	1.7052	-.0042	0.06099	0.023924
2.662	1.7187	-.0239	0.05514	0.015363
2.692	1.7218	-.0866	0.04713	0.022815
2.723	1.7182	-.0230	0.08344	0.033591
2.755	1.7221	-.0274	0.09687	0.038451
2.786	1.7275	-.0461	0.07684	0.032799
2.819	1.7392	-.0610	0.08547	0.034276
2.852	1.7581	-.0587	0.06223	0.025694
2.886	1.7789	-.0594	0.08159	0.035263
2.918	1.8123	-.0088	0.06951	0.024992
2.951	1.8418	-.0102	0.04854	0.022015
2.983	1.8512	-.1060	0.04008	0.023026
3.016	1.8583	-.0335	0.05643	0.024743
3.048	1.8660	0.0046	0.04174	0.016233
3.081	1.8754	-.0051	0.05386	0.021808
3.115	1.8845	-.0462	0.10558	0.042052
3.151	1.8823	-.0432	0.02512	0.010798
3.185	1.8860	-.0665	0.09409	0.042519
3.216	1.8133	-.2160	0.32986	0.164877
3.249	1.6170	0.5262	0.16550	0.018961
3.285	1.4535	-.3208	0.09136	0.019653
3.319	1.3842	-.0214	0.14839	0.059911
3.354	1.3543	-.0478	0.11894	0.054811
3.388	1.3387	-.0380	0.10673	0.046943
3.423	1.3285	-.0213	0.07056	0.032415

APPENDIX E

Tables of Dimensional Values (SI Units)

These tables correspond to the plots of Appendix A. Zeros in these tables correspond to negative values removed from the plots. These values are not smoothed. Apply a 3-point binomial filter to the mean mass flux and the total temperature values to obtain the plotted values. Apply a 5-point binomial filter to the rms mass flux and the total temperature values to obtain the plotted values. The columns are as follows:

- y/H, H = 0.475 in.
- $\overline{(\rho u)}$ $(\frac{kg}{m^2 sec})$
- $\overline{T}_t$ (K)
- $(\rho u)'$ $(\frac{kg}{m^2 sec})$
- T_t' (K)
- T_{t_∞} (K)

Table 1. Profile Data at Station 1 - Unheated

y/H	rho u	T(K)	(rho u)'	T'(K)	Tinf(K)
0.225	126.09	293.11	3.425	1.422	300.37
0.260	127.57	300.30	2.340	0.630	298.64
0.290	126.71	297.52	2.754	0.632	299.30
0.321	130.35	301.23	1.935	0.000	299.53
0.355	129.48	297.87	2.392	0.000	298.44
0.387	127.38	291.56	1.977	0.246	298.13
0.420	129.81	295.69	2.051	0.000	298.42
0.453	131.63	298.11	3.040	0.977	298.14
0.486	131.45	296.10	3.505	1.290	297.82
0.516	132.44	298.28	2.043	0.000	297.71
0.548	133.49	296.95	2.217	0.000	297.49
0.581	134.33	300.83	2.884	0.666	297.15
0.614	133.45	293.29	2.967	0.931	297.01
0.647	133.97	297.13	3.127	0.777	296.82
0.680	133.03	299.57	2.249	0.000	296.62
0.714	128.47	295.42	3.003	0.696	296.30
0.746	123.90	291.56	2.635	0.000	296.09
0.768	119.93	295.29	2.907	0.659	296.29
0.808	113.97	294.89	2.400	0.000	295.72
0.840	107.68	292.77	2.955	0.511	295.52
0.874	111.19	290.71	4.937	1.507	295.23
0.906	123.71	293.26	6.900	1.450	295.07
0.940	117.89	301.96	8.088	1.082	294.85
0.974	95.88	276.49	6.342	0.000	294.50
1.007	93.89	274.05	8.978	4.117	294.38
1.039	124.21	286.96	15.824	5.436	294.01
1.072	133.96	283.62	17.619	4.849	293.80
1.103	130.48	290.67	12.693	3.777	293.58
1.137	134.06	292.91	16.431	3.908	293.32
1.170	141.74	268.49	19.423	0.000	293.18
1.204	161.90	271.07	28.678	7.218	292.88
1.237	181.72	277.76	25.913	0.000	292.60
1.269	199.25	291.55	38.844	7.510	292.33
1.311	226.31	317.14	46.132	3.744	300.34
1.343	218.71	277.14	42.080	3.348	298.84
1.376	233.40	285.22	50.893	6.577	298.38
1.408	259.39	303.64	51.492	0.000	299.32
1.441	287.80	320.38	63.481	2.850	299.36
1.473	282.63	299.67	69.386	7.742	298.94
1.505	309.65	315.17	62.742	1.525	298.28
1.538	310.35	293.06	68.216	7.549	298.33
1.569	333.58	305.05	68.706	3.152	298.34
1.600	340.42	296.53	67.027	5.740	298.14
1.631	350.79	294.93	58.874	4.988	297.83
1.662	366.74	300.13	46.877	2.683	297.72
1.696	377.71	304.30	40.914	2.506	297.69
1.729	383.60	304.50	26.116	0.000	297.55
1.762	384.14	305.57	22.194	1.407	297.22
1.793	381.86	301.38	17.300	0.927	297.01
1.824	381.58	301.45	20.889	1.818	296.85
1.855	385.96	303.37	19.035	1.378	296.83
1.887	379.76	295.24	22.759	2.232	296.60
1.919	392.63	301.03	22.283	1.695	296.52
1.950	392.87	300.37	21.618	1.226	296.23
1.982	395.67	299.65	22.450	1.742	296.16
2.016	400.36	302.32	20.393	1.221	295.97
2.050	397.39	299.70	23.828	1.941	295.81
2.083	402.18	303.21	24.748	1.775	295.54
2.114	398.91	300.35	23.832	1.725	295.47
2.149	397.59	300.26	20.589	1.285	295.32
2.181	399.88	299.75	17.567	0.000	295.16
2.215	403.50	303.99	20.380	0.943	294.93
2.249	402.87	301.28	21.211	1.531	294.72
2.284	400.53	301.00	20.172	0.907	294.55

2.319	400.93	300.52	24.005	1.754	294.45
2.355	396.64	296.36	24.137	1.979	294.18
2.401	405.00	316.37	24.639	1.426	300.73
2.435	392.52	301.72	22.111	1.477	299.52
2.471	394.85	305.31	20.765	1.312	298.14
2.507	390.22	300.18	24.687	2.203	298.85
2.542	395.44	306.94	22.938	1.600	299.46
2.578	393.21	304.09	20.459	1.273	299.14
2.616	389.58	301.82	21.069	1.034	298.28
2.653	392.38	303.41	19.637	1.153	297.89
2.689	393.22	303.62	22.886	1.673	297.95
2.722	394.12	304.04	23.243	1.730	298.07
2.758	394.29	303.15	17.526	0.479	297.98
2.795	394.31	303.09	22.891	1.538	297.68
2.829	390.46	299.27	21.729	2.027	297.24
2.864	396.86	306.94	21.764	1.437	297.22
2.901	397.08	304.56	21.851	1.392	297.24
2.936	394.81	301.85	20.066	1.265	297.05
2.972	397.74	304.20	18.848	0.748	296.82
3.006	395.99	302.37	20.289	0.668	296.57
3.041	394.44	302.61	21.904	1.673	296.35
3.078	391.05	301.13	21.542	1.512	296.47
3.112	390.75	299.35	23.584	2.001	296.25
3.147	392.39	298.96	21.696	1.547	295.99
3.184	394.80	300.20	22.084	1.433	295.82
3.220	395.12	301.25	25.154	2.138	295.64
3.255	390.41	295.42	21.701	1.464	295.51
3.289	395.70	298.03	20.850	0.000	295.30
3.324	398.87	297.96	22.654	1.662	295.02
3.358	405.80	303.96	21.649	1.130	294.74
3.392	401.44	300.91	24.757	1.729	294.61
3.425	401.73	301.69	26.175	1.952	294.29
3.461	397.03	296.16	27.402	2.197	294.24
3.499	397.91	298.68	24.449	1.499	293.96
3.532	387.08	290.98	25.644	2.802	293.64

Table 2. Profile Data at Station 2 - Unheated

y/H	rho u	T(K)	(rho u)'	T'(K)	Tinf(K)
0.155	134.13	292.65	8.723	0.000	301.13
0.186	136.18	288.94	8.408	1.851	299.50
0.219	143.29	311.92	5.326	0.372	300.29
0.250	142.36	290.72	3.507	0.417	300.47
0.270	143.91	302.57	3.230	0.569	299.63
0.312	143.84	302.43	3.067	0.000	299.40
0.344	144.66	307.81	2.474	0.000	299.49
0.376	143.79	298.88	2.163	0.000	299.22
0.399	142.42	293.19	2.288	0.000	299.25
0.440	143.79	304.35	3.473	0.515	298.68
0.474	143.37	299.05	3.054	0.000	298.59
0.505	142.62	290.49	0.620	0.000	298.37
0.538	142.76	296.24	2.454	0.000	298.05
0.567	144.47	306.70	3.116	0.000	297.97
0.599	143.77	302.58	3.597	0.506	297.69
0.631	143.92	302.71	3.702	0.428	297.53
0.662	141.90	289.08	3.112	0.000	297.27
0.695	140.51	300.94	6.802	1.091	297.14
0.724	137.83	307.33	7.211	0.678	296.95
0.760	135.49	305.16	8.760	1.236	296.73
0.793	138.72	314.27	9.170	0.463	296.47
0.825	139.62	289.30	12.384	0.000	296.26
0.857	145.35	290.50	16.525	3.152	295.95
0.887	157.36	307.83	18.042	1.521	295.82
0.920	165.37	302.36	19.619	1.855	295.55
0.952	178.96	303.99	23.590	1.209	295.34
0.985	188.18	299.37	21.617	0.000	295.13
1.018	202.15	318.62	25.097	0.000	294.82
1.050	207.80	291.36	25.203	0.000	294.58
1.081	217.32	270.17	35.467	5.624	294.36
1.112	231.53	294.98	33.484	2.263	294.03
1.143	243.16	309.18	32.568	0.000	293.95
1.175	243.42	242.51	33.825	0.000	293.67
1.218	278.42	336.73	44.286	0.000	300.97
1.249	272.34	297.30	48.887	3.943	299.58
1.282	293.72	304.57	47.386	1.728	300.25
1.313	287.57	220.18	22.012	0.000	300.34
1.343	328.71	323.64	46.795	0.000	299.56
1.373	322.19	284.62	52.286	2.911	299.48
1.404	351.00	327.76	47.390	0.317	299.44
1.434	353.37	304.09	46.207	2.204	299.07
1.466	355.14	269.42	35.006	3.645	298.83
1.498	361.33	292.98	29.110	0.000	298.62
1.531	361.02	296.05	28.002	1.192	298.47
1.562	352.71	293.41	22.181	0.856	298.30
1.592	345.57	287.79	15.784	1.299	298.02
1.623	352.48	302.86	13.474	0.356	297.87
1.654	353.66	295.21	12.140	0.566	297.70
1.686	359.58	297.12	13.484	0.617	297.33
1.716	361.24	293.26	13.194	0.611	297.17
1.747	364.41	298.33	12.950	0.000	296.97
1.780	358.48	290.20	14.058	0.000	296.79
1.813	356.77	294.06	14.684	0.674	296.55
1.843	355.76	294.37	11.052	0.000	296.21
1.875	357.54	297.44	9.572	0.000	296.01
1.909	363.58	311.42	10.650	0.234	295.74
1.941	359.30	296.02	10.576	0.000	295.57
1.974	362.78	293.74	13.909	1.078	295.35
2.006	362.24	286.37	14.738	1.213	295.18
2.042	366.41	297.68	16.383	0.822	294.92
2.074	357.96	313.99	31.934	1.156	294.59
2.111	323.14	293.33	21.686	0.000	294.42
2.144	317.16	300.29	7.667	0.000	294.03
2.179	320.79	299.70	6.416	0.000	294.01

2.213	327.38	293.63	6.484	0.000	293.65
2.248	331.47	295.84	7.851	0.000	293.34
2.293	323.40	288.05	10.210	0.867	301.11
2.330	330.67	300.92	9.980	0.360	299.66
2.368	331.97	285.19	9.214	0.709	300.23
2.402	342.21	298.62	9.250	0.000	300.40
2.438	351.38	301.02	10.522	0.301	299.67
2.472	353.87	295.49	8.803	0.000	299.46
2.506	359.06	295.87	8.642	0.000	299.49
2.540	361.64	290.39	9.926	0.200	299.39
2.574	369.80	295.96	10.064	0.321	299.01
2.608	371.57	292.06	11.789	0.588	298.86
2.645	372.31	290.39	10.642	0.479	298.85
2.679	377.44	293.49	10.270	0.000	298.69
2.714	380.47	289.24	10.176	0.000	298.42
2.748	384.36	292.55	11.165	0.139	298.28
2.783	389.87	304.05	11.200	0.000	298.14
2.816	383.70	287.88	9.799	0.000	297.93
2.852	388.39	300.62	10.214	0.263	297.85
2.886	391.67	302.45	12.752	0.655	297.74
2.924	385.53	280.15	12.137	0.956	297.52
2.958	392.48	288.34	12.666	0.770	297.29
2.993	408.47	302.77	15.244	0.550	297.16
3.028	407.33	300.02	14.145	0.663	296.91
3.061	406.48	296.50	10.811	0.000	296.82
3.095	403.95	292.73	11.957	0.000	296.64
3.130	407.05	301.14	11.168	0.267	296.45
3.162	403.27	293.15	13.367	0.845	296.25
3.197	404.12	298.34	10.089	0.000	296.23
3.232	403.73	301.63	9.173	0.000	295.92
3.269	403.49	299.78	9.686	0.000	295.72
3.303	403.44	295.96	12.099	0.601	295.52
3.337	404.75	299.16	11.165	0.452	295.43
3.371	401.84	292.17	9.979	0.225	295.21
3.406	402.98	289.47	10.447	0.355	294.97

Table 3. Profile Data at Station 3 - Unheated

y/H	rho u	T(K)	(rho u)'	T'(K)	Tinf(K)
0.163	109.48	319.31	7.878	0.000	296.41
0.194	111.48	317.52	8.060	0.000	295.90
0.223	112.35	292.45	9.318	1.020	296.51
0.252	120.41	339.46	10.883	0.092	297.03
0.282	122.17	307.20	14.372	2.039	297.06
0.310	124.47	289.33	17.501	3.827	296.60
0.342	137.34	312.58	16.727	1.338	296.24
0.373	146.22	332.49	13.936	0.000	295.64
0.404	138.70	248.66	12.322	5.750	295.57
0.436	148.36	305.07	7.264	0.262	295.61
0.467	146.33	294.36	5.798	0.000	295.68
0.495	146.04	293.11	4.444	0.000	295.52
0.527	149.62	324.01	5.916	0.166	295.32
0.557	146.78	306.47	5.398	0.000	294.89
0.589	145.36	291.15	5.020	0.000	294.81
0.619	147.84	317.15	6.408	0.000	294.56
0.652	144.65	291.05	2.225	0.000	294.43
0.683	146.91	299.57	8.635	0.000	294.26
0.715	146.24	275.64	15.535	4.256	294.11
0.745	151.59	306.03	12.803	0.432	293.82
0.777	153.37	304.48	10.990	0.000	293.84
0.806	158.99	297.00	18.451	1.801	293.67
0.838	167.74	309.53	19.622	0.676	293.43
0.868	166.32	271.43	23.071	3.524	293.38
0.895	170.93	260.96	20.659	0.000	293.14
0.931	188.47	317.30	26.794	0.734	292.77
0.964	193.14	296.26	26.423	0.878	292.59
0.987	198.40	293.67	31.067	3.089	292.85
1.027	212.05	304.48	31.830	0.000	292.21
1.056	219.88	307.84	35.052	0.808	292.08
1.088	231.05	307.32	34.433	0.746	291.69
1.120	235.07	276.15	27.685	0.000	291.48
1.152	249.56	310.46	38.085	0.938	291.28
1.204	268.49	324.33	47.844	0.255	296.43
1.236	261.04	241.16	57.905	11.640	296.26
1.266	292.09	321.73	51.422	0.470	295.21
1.296	279.08	228.39	50.511	0.389	294.53
1.326	319.31	331.17	55.253	0.000	294.49
1.357	330.22	328.61	55.115	0.000	294.66
1.389	326.77	278.87	59.269	4.990	294.63
1.419	329.36	258.94	58.630	6.747	294.21
1.451	351.55	260.19	50.264	6.351	293.82
1.481	373.34	324.70	36.576	0.240	293.77
1.511	368.40	299.92	33.735	1.865	293.59
1.540	372.89	294.97	24.034	0.648	293.30
1.570	373.04	295.06	22.264	1.393	293.04
1.600	375.54	289.62	18.715	1.321	292.87
1.632	382.24	297.72	19.190	0.981	292.68
1.663	377.47	291.34	21.020	1.129	292.50
1.694	368.28	286.76	19.636	1.280	292.37
1.718	371.58	306.15	15.947	0.254	292.57
1.754	363.38	284.69	13.645	0.854	292.01
1.785	368.12	290.86	11.761	0.000	291.75
1.814	375.23	294.17	12.028	0.193	291.43
1.845	381.64	302.16	11.729	0.381	291.25
1.875	387.25	304.48	12.687	0.461	291.01
1.906	390.60	303.58	12.986	0.328	290.96
1.937	393.19	297.79	13.288	0.567	290.56
1.970	395.17	291.48	13.839	0.948	290.49
2.001	401.58	302.96	13.432	0.230	290.25
2.032	404.23	300.18	12.867	0.222	290.01
2.064	411.54	305.86	13.049	0.392	289.72
2.096	415.47	306.31	13.936	0.262	289.65
2.128	416.07	306.79	14.209	0.407	289.40

2.160	413.56	295.18	13.183	0.675	289.08
2.194	421.37	307.02	12.048	0.000	289.01
2.237	410.11	299.53	16.850	0.678	296.38
2.271	410.92	284.27	20.300	1.355	296.23
2.305	419.58	304.06	26.471	1.097	294.93
2.337	398.01	291.02	24.548	0.839	294.18
2.370	394.27	294.62	15.810	0.787	294.60
2.406	387.82	286.10	12.501	0.448	294.97
2.440	390.54	293.23	12.593	0.639	294.96
2.475	389.65	296.76	13.129	0.645	294.31
2.510	393.01	305.68	13.585	0.621	294.12
2.545	391.84	304.06	13.947	0.564	293.76
2.579	391.86	297.05	12.958	0.330	293.53
2.610	391.78	293.29	12.856	0.539	293.58
2.644	388.16	291.54	12.386	0.568	293.65
2.680	394.77	307.45	14.215	0.538	293.39
2.712	388.77	295.96	12.748	0.596	293.13
2.748	389.19	300.42	13.624	0.325	292.78
2.781	393.00	311.96	13.626	0.281	292.83
2.816	385.70	298.45	12.108	0.444	292.70
2.850	382.65	298.48	12.645	0.314	292.64
2.884	384.61	299.30	13.375	0.578	292.36
2.917	384.01	296.89	11.326	0.101	292.38
2.952	385.06	295.03	11.836	0.375	292.14
2.985	385.45	298.60	13.736	0.743	291.81
3.019	383.08	295.93	12.496	0.605	291.90
3.054	382.98	301.18	10.445	0.000	291.75
3.087	384.06	306.67	12.391	0.407	291.53
3.120	381.61	302.65	11.364	0.327	291.25
3.155	380.03	297.33	11.761	0.423	291.09
3.188	380.62	298.11	11.274	0.124	291.06
3.221	380.11	301.34	11.883	0.257	290.89
3.253	382.29	301.40	13.140	0.499	290.72
3.286	383.81	297.85	11.736	0.000	290.46
3.321	387.53	302.82	13.664	0.638	290.32

Table 4. Profile Data at Station 4 - Unheated

y/H	rho u	T(K)	(rho u)'	T'(K)	Tinf(K)
0.266	115.90	271.81	12.140	2.784	299.57
0.304	127.47	299.99	14.186	4.248	297.86
0.333	121.61	272.25	12.894	4.697	298.42
0.365	130.80	284.63	12.892	4.818	298.77
0.396	137.49	302.83	8.330	0.000	297.77
0.426	140.36	304.39	9.034	0.404	297.49
0.458	139.23	296.53	10.767	2.685	297.67
0.490	139.32	284.65	9.451	3.125	297.40
0.522	144.61	300.48	7.804	0.000	296.95
0.550	138.15	276.40	7.415	0.000	296.71
0.581	148.21	294.37	5.757	0.000	296.73
0.610	146.58	287.77	6.161	0.000	296.60
0.642	155.02	306.55	5.666	0.000	296.16
0.673	158.71	309.07	11.972	0.000	296.04
0.703	149.47	276.75	11.921	3.076	295.83
0.736	155.92	291.33	14.219	4.242	295.55
0.767	159.64	286.61	9.165	0.000	295.35
0.797	162.92	287.07	17.040	3.981	295.15
0.827	165.87	286.24	23.940	7.382	294.96
0.856	168.58	287.99	20.597	3.340	294.70
0.889	176.57	292.90	24.032	3.545	294.39
0.920	188.73	308.92	27.184	3.259	294.27
0.952	182.11	292.83	22.918	0.000	293.98
0.984	188.78	289.66	26.931	1.473	293.86
1.015	193.68	285.26	25.795	0.000	293.50
1.045	201.45	294.36	30.479	0.000	293.29
1.072	203.50	290.24	31.847	4.589	293.06
1.104	217.37	303.52	43.181	5.766	292.88
1.135	224.35	294.98	38.509	0.000	292.65
1.167	213.07	269.78	41.445	6.005	292.47
1.197	221.38	273.90	45.979	8.513	292.13
1.228	235.22	286.38	36.563	0.000	291.91
1.258	258.49	308.07	50.222	0.000	291.71
1.296	278.09	320.29	64.367	2.652	299.30
1.326	276.94	316.76	62.990	1.771	297.72
1.354	266.19	273.38	64.295	4.670	298.46
1.384	266.18	270.31	84.224	16.385	298.41
1.415	316.88	332.44	77.195	2.127	297.66
1.446	308.61	303.95	77.373	6.237	297.25
1.476	316.70	301.02	68.398	1.370	297.40
1.507	372.00	348.49	81.062	0.000	297.23
1.529	332.67	299.39	75.246	6.187	297.08
1.565	358.07	307.46	71.507	3.201	296.76
1.594	364.15	297.53	66.378	2.183	296.66
1.624	394.04	317.31	68.577	3.004	296.23
1.654	387.93	310.43	62.069	4.431	296.10
1.685	394.46	301.37	51.468	3.575	295.87
1.714	412.24	326.02	45.605	1.689	295.58
1.748	398.47	306.05	34.119	2.165	295.43
1.779	418.98	311.17	26.332	0.000	295.14
1.810	434.99	314.37	28.761	0.521	295.02
1.840	423.70	307.78	24.738	0.777	294.88
1.872	417.92	301.51	25.876	1.494	294.54
1.903	416.01	295.34	28.183	2.700	294.30
1.935	413.35	298.99	25.600	1.624	294.07
1.967	420.36	302.43	24.218	1.873	293.88
2.001	419.22	307.95	20.567	1.069	293.60
2.034	412.15	303.61	18.377	0.496	293.30
2.068	423.27	312.69	17.272	0.000	292.98
2.099	401.55	284.65	18.175	1.683	292.83
2.133	427.59	315.77	15.445	0.000	292.72
2.166	404.46	288.63	22.080	2.615	292.39
2.200	423.53	300.60	13.875	0.332	292.19
2.234	418.16	291.92	16.260	0.000	291.78

2.270	446.16	313.74	14.621	0.000	291.52
2.304	411.61	277.94	23.337	3.187	291.34
2.348	407.71	292.73	25.545	1.894	297.71
2.381	420.01	311.69	16.512	0.000	296.24
2.413	427.94	315.69	17.981	0.642	296.30
2.445	432.72	316.51	21.351	0.772	296.93
2.479	431.14	312.28	25.318	1.418	296.91
2.515	428.94	314.94	28.955	1.362	296.20
2.547	426.30	317.61	26.912	0.521	295.83
2.583	412.25	313.01	26.730	1.364	295.81
2.616	417.30	320.03	21.113	0.920	296.00
2.646	405.66	308.84	15.345	0.000	295.60
2.680	412.63	314.26	15.685	0.426	295.38
2.713	416.38	316.81	17.230	0.694	295.18
2.746	413.59	316.97	15.047	0.399	295.13
2.780	408.23	311.70	17.102	0.807	294.95
2.813	413.02	312.89	16.940	0.621	294.86
2.848	411.90	315.70	14.563	0.000	294.58
2.882	412.09	313.99	15.376	0.642	294.47
2.913	407.19	312.50	14.447	0.328	294.26
2.946	409.93	311.71	17.017	0.872	294.25
2.980	410.96	311.48	17.325	1.035	293.98
3.012	427.71	325.34	17.038	0.560	293.90
3.045	419.52	317.05	17.753	0.929	293.64
3.078	426.98	318.78	16.911	0.545	293.40
3.114	420.16	304.68	16.291	0.000	293.19
3.148	421.15	309.24	16.845	0.777	293.15
3.181	425.28	307.46	18.922	0.968	293.03
3.213	424.35	306.05	18.462	1.118	292.81
3.248	422.47	306.53	16.931	0.797	292.70
3.280	408.70	291.65	17.407	0.968	292.54
3.316	443.78	322.46	17.510	0.422	292.34
3.348	429.34	306.12	16.773	0.552	292.26
3.383	435.17	306.90	18.415	0.894	291.98
3.415	439.65	310.49	18.430	0.787	291.91

Table 5. Profile Data at Station 4 With Shock Interaction - Unheated

y/H	rho u	T(K)	(rho u)'	T'(K)	Tinf(K)
0.285	149.54	316.98	17.235	1.180	300.45
0.315	152.00	311.85	20.900	3.140	300.48
0.343	153.80	315.39	15.180	0.000	299.09
0.374	154.20	317.60	17.994	0.000	298.49
0.405	165.01	335.44	17.449	0.000	299.32
0.438	153.84	300.15	18.005	0.000	299.43
0.469	163.01	316.48	19.775	0.550	298.74
0.500	161.80	308.78	14.248	0.000	298.09
0.531	162.16	299.60	12.192	0.000	297.98
0.560	170.24	319.71	19.657	0.650	298.11
0.589	173.21	319.87	18.019	0.000	298.05
0.621	178.62	326.21	22.625	0.000	297.79
0.650	173.38	311.76	18.360	0.000	297.64
0.681	166.20	288.23	15.347	1.232	297.48
0.713	171.25	296.19	23.506	2.912	297.22
0.745	187.70	323.00	24.891	0.000	297.15
0.776	193.54	315.36	28.815	1.266	296.90
0.806	186.98	294.37	26.566	3.951	296.80
0.836	197.07	311.12	29.113	0.000	296.61
0.868	211.12	316.26	41.738	3.655	296.38
0.900	196.43	271.08	33.843	0.000	296.26
0.931	220.87	301.88	42.933	4.017	296.09
0.962	233.83	312.38	45.313	0.000	295.87
0.993	236.70	295.41	53.529	3.565	295.70
1.024	264.07	319.09	56.909	0.000	295.56
1.055	260.59	304.30	67.154	4.248	295.37
1.083	267.08	299.89	67.887	6.193	295.26
1.113	296.86	319.70	67.688	0.000	294.94
1.143	317.52	323.48	91.306	3.313	294.88
1.174	290.54	292.47	89.754	6.260	294.61
1.206	287.24	254.01	68.805	0.000	294.45
1.236	366.24	343.65	114.550	0.000	294.24
1.267	320.96	261.18	93.618	0.000	294.10
1.306	413.55	343.90	145.596	1.092	300.26
1.334	415.96	330.74	147.656	1.517	299.22
1.363	407.24	307.99	140.436	2.261	297.97
1.393	501.91	369.85	173.497	0.000	298.30
1.424	511.69	358.98	171.559	0.000	298.98
1.455	523.06	338.31	162.454	0.564	298.67
1.486	464.61	284.96	169.200	12.730	297.86
1.514	496.34	295.42	182.548	11.272	297.64
1.545	546.43	333.19	136.299	1.825	297.65
1.575	547.47	325.66	111.028	2.166	297.76
1.603	558.30	317.91	94.737	2.930	297.59
1.632	551.99	317.53	73.174	1.414	297.26
1.665	564.64	318.81	67.586	2.410	296.94
1.695	562.20	317.83	48.171	0.974	296.90
1.726	569.08	321.14	38.854	0.820	296.87
1.757	558.27	312.29	35.670	1.230	296.63
1.788	569.72	323.00	31.984	0.466	296.43
1.819	568.37	319.40	33.299	1.125	296.28
1.850	573.89	325.89	37.636	0.902	296.14
1.881	578.01	328.69	31.257	0.423	296.06
1.913	571.77	325.62	35.065	0.792	295.77
1.945	578.43	327.48	35.481	0.846	295.57
1.978	565.88	318.09	30.844	0.000	295.53
2.011	569.88	323.31	32.903	0.421	295.35
2.045	564.67	319.30	36.528	1.018	294.98
2.078	574.29	324.03	34.928	0.872	294.81
2.103	574.72	324.41	33.069	0.604	294.99
2.142	576.71	321.25	34.575	0.756	294.34
2.177	572.65	321.26	33.719	0.713	294.22
2.212	577.88	315.89	39.418	1.157	293.90
2.246	564.15	308.19	40.463	2.029	293.85

2.280	573.52	318.15	36.445	1.268	293.50
2.315	551.07	300.16	36.172	1.485	293.26
2.360	544.67	316.51	50.994	1.899	299.46
2.392	531.77	309.75	38.459	0.980	297.78
2.425	549.70	323.41	44.521	1.548	298.44
2.459	535.04	308.61	45.651	1.728	298.50
2.492	533.10	312.87	42.629	1.671	297.78
2.526	532.70	316.76	30.598	0.124	297.47
2.560	544.53	323.98	33.875	0.813	297.64
2.593	533.49	313.87	30.144	0.929	297.42
2.627	542.07	327.04	31.264	0.612	296.99
2.658	526.04	315.31	30.920	1.151	296.94
2.691	527.06	317.22	25.249	0.000	296.74
2.724	527.28	314.84	27.199	1.096	296.42
2.758	537.66	320.89	29.973	0.867	296.23
2.792	542.94	323.05	30.030	0.859	296.08
2.826	533.31	311.52	29.450	1.131	295.88
2.859	551.40	320.97	30.368	0.677	295.67
2.892	563.23	327.54	28.439	0.335	295.47
2.926	560.61	320.67	27.644	0.582	295.22
2.959	560.93	315.21	35.593	1.421	294.95
2.991	577.92	322.78	31.366	0.788	294.76
3.024	588.34	321.50	28.133	0.559	294.60
3.057	592.36	318.39	29.049	0.667	294.32
3.091	607.00	321.78	34.485	0.979	294.10
3.126	617.20	321.20	33.701	0.928	293.79
3.159	603.63	303.79	30.848	0.000	293.47
3.192	602.08	299.59	28.836	0.000	293.35
3.223	610.63	305.85	31.606	0.901	293.09
3.256	609.71	302.00	32.632	1.110	292.90
3.290	602.87	297.78	40.665	2.142	292.71
3.323	626.28	311.79	34.889	1.052	292.38
3.357	611.05	301.21	31.780	0.000	292.27
3.389	619.38	304.69	29.172	0.000	292.01
3.423	623.66	304.78	33.553	0.747	291.65

Table 6. Profile Data at Station 1 - Heated

y/H	rho u	T(K)	(rho u)'	T'(K)	Tinf(K)
0.182	86.63	417.89	2.973	0.000	295.20
0.215	87.83	414.37	1.130	0.000	296.13
0.249	85.27	416.60	1.768	0.000	294.90
0.282	84.11	427.90	2.818	0.096	294.11
0.313	86.75	410.30	0.000	0.000	294.60
0.347	85.81	417.30	1.789	0.000	295.05
0.378	86.09	420.94	1.880	0.000	294.45
0.410	86.62	411.02	0.000	0.000	294.02
0.444	89.02	425.23	2.706	0.000	293.68
0.477	88.78	405.07	0.000	0.000	293.82
0.510	90.81	426.17	2.483	0.000	293.85
0.545	92.38	414.75	0.000	0.000	293.59
0.578	91.56	419.90	1.432	0.000	293.23
0.611	89.67	415.82	1.346	0.000	293.20
0.643	89.68	419.67	1.392	0.000	293.12
0.676	88.08	428.03	2.987	0.114	292.97
0.708	86.37	413.06	2.032	0.000	292.52
0.742	82.22	416.08	1.652	0.000	292.37
0.775	77.71	417.78	0.000	0.000	292.26
0.809	74.22	413.55	0.000	0.000	292.39
0.842	79.91	420.17	0.000	0.000	292.03
0.873	87.00	410.15	0.292	0.000	291.82
0.905	83.98	410.33	2.844	0.000	291.68
0.940	75.47	397.04	1.689	0.000	291.69
0.971	75.09	337.87	0.000	0.000	291.42
1.006	102.65	285.48	9.838	3.417	291.36
1.037	112.73	312.38	21.011	15.297	291.07
1.070	112.20	296.33	4.789	0.000	290.95
1.103	118.49	290.46	32.169	27.252	290.72
1.136	128.12	288.21	0.000	0.000	290.56
1.166	152.88	285.73	0.000	0.000	290.39
1.199	167.92	298.93	30.650	10.314	290.33
1.231	174.99	297.55	21.085	0.000	290.09
1.287	228.56	289.38	55.348	18.083	291.05
1.320	231.21	285.80	32.827	10.410	291.38
1.354	244.34	292.68	12.163	0.000	290.27
1.387	267.46	291.71	58.380	17.132	289.48
1.420	286.18	295.89	58.421	16.543	289.93
1.453	300.67	283.93	9.786	0.000	290.19
1.486	316.97	269.15	79.238	25.812	290.05
1.520	354.56	269.09	0.000	0.000	289.53
1.552	341.03	300.63	0.000	0.000	289.27
1.585	387.65	279.41	0.000	0.000	289.23
1.620	422.16	245.58	67.213	17.515	289.12
1.653	400.97	265.64	39.132	9.201	288.92
1.686	416.34	294.18	0.000	0.000	287.94
1.719	403.71	268.91	14.446	3.173	287.94
1.751	432.04	270.37	41.348	12.205	287.94
1.783	419.69	280.74	36.570	10.669	287.94
1.817	418.27	274.85	33.735	9.963	287.94
1.850	408.70	281.35	12.913	4.721	287.89
1.884	408.84	301.03	31.819	8.138	287.76
1.917	420.59	274.18	25.392	7.196	287.53
1.951	409.99	304.54	0.000	0.000	287.41
1.982	432.49	282.03	21.041	6.656	287.21
2.015	417.63	282.15	27.720	8.599	287.04
2.049	423.68	275.80	32.924	9.644	286.88
2.081	424.43	286.88	30.212	8.414	286.78
2.113	429.16	278.12	30.659	8.686	286.38
2.149	427.33	278.76	28.472	8.088	286.23
2.183	439.85	275.18	17.612	6.242	286.15
2.216	433.71	273.60	40.913	11.754	285.98
2.248	430.92	286.60	23.813	6.870	285.56
2.280	431.67	263.61	0.000	2.432	285.31

2.311	441.19	282.83	27.632	7.723	285.24
2.344	442.70	279.27	40.804	10,689	284.80
2.396	417.90	296.92	19.201	5.118	293.83
2.430	416.56	281.71	37.736	10.293	293.98
2.462	431.28	292.27	26.412	7.130	293.02
2.495	424.27	296.93	11.798	2.879	292.29
2.527	427.88	285.39	39.446	10.293	292.68
2.557	425.34	297,66	27.907	7.806	292.95
2.590	416.94	298.89	18.164	4.711	292.76
2.624	417.94	300.61	32.263	8.086	292.09
2.656	417.23	287.74	33.952	8.957	291.86
2.690	416.92	298.58	20.447	5.589	291.85
2.724	402.40	299.88	28.043	7.475	291.90
2.756	389.63	294.48	27.882	5.938	291.70
2.789	382.78	291.62	38.858	11.476	291.38
2.821	380.65	290.83	25.620	6.785	291.25
2.852	382.41	296.20	24.218	6.887	291.22
2.887	389.09	293.09	18.371	6.223	290.89
2.921	390.63	294.87	38.103	10.169	290.75
2.956	386.01	292.41	21.963	6.175	290.64
2.988	396.28	282.97	30.372	9.195	290.63
3.022	397.19	294.81	21.685	6.486	290.34
3.054	397.43	288.40	28.258	8.560	290.16
3.086	398.11	293.76	21.073	6.084	289.99
3.117	405.16	291.35	16.912	5.113	289.97
3.151	398.87	290.51	35.811	9.702	289.74
3.183	400.68	300.68	23.630	6.315	289.49
3.216	401.25	292.38	30.155	8.475	289.33
3.248	399.18	290.67	15.966	4.847	289.27
3.282	398.89	277.90	25.627	8.147	289.00
3.313	406.66	289.07	15.581	5.757	288.81
3.343	412.24	286.27	19.009	6.186	288.01
3.373	408.29	295.94	22.488	6.117	287.94
3.403	413.74	281.20	23.577	6.780	287.94
3.435	419.40	285.96	30.339	8.811	287.94

Table 7. Profile Data at Station 2 - Heated

y/H	rho u	T(K)	(rho u)'	T'(K)	Tinf(K)
0.189	88.28	387.81	2.770	1.912	302.78
0.222	91.17	383.68	5.833	3.960	302.09
0.255	89.10	386.47	2.694	1.743	299.99
0.291	94.64	377.11	10.509	6.022	300.29
0.326	90.99	373.87	0.000	2.326	301.27
0.360	90.02	381.43	4.027	2.526	301.24
0.392	88.68	394.99	0.000	0.000	300.13
0.425	88.36	394.59	0.000	0.000	299.72
0.458	87.89	377.35	7.615	6.459	299.39
0.490	87.89	380.53	2.817	2.362	299.72
0.522	86.71	391.99	0.000	0.000	299.69
0.553	88.92	382.35	0.000	0.000	299.38
0.589	85.64	390.52	0.000	0.000	299.00
0.623	87.07	385.25	2.395	0.889	299.04
0.654	86.46	394.48	1.284	0.000	298.76
0.687	88.50	382.09	2.643	2.060	298.60
0.721	87.96	386.23	5.948	3.422	298.15
0.755	87.12	384.28	7.455	5.503	298.26
0.788	86.78	390.44	0.000	0.000	297.81
0.820	86.28	386.26	8.820	5.304	297.84
0.850	91.86	379.13	0.000	0.000	297.33
0.886	93.36	361.82	7.048	4.024	297.15
0.920	102.27	342.23	18.017	9.045	297.11
0.954	100.33	357.21	0.000	0.000	296.91
0.988	107.94	344.45	13.686	0.000	296.47
1.021	135.39	304.04	35.459	19.615	296.48
1.054	125.44	349.55	34.519	13.082	296.03
1.088	147.13	298.15	42.336	23.461	296.00
1.122	168.70	282.41	21.213	0.000	295.61
1.157	143.94	366.01	26.619	0.000	295.33
1.191	177.58	301.09	0.000	0.000	295.04
1.224	180.17	327.30	32.496	7.783	295.16
1.259	184.35	314.39	67.744	29.148	294.67
1.310	229.71	317.80	50.905	10.782	304.66
1.345	236.37	297.40	38.731	6.711	303.43
1.380	241.53	298.87	33.585	0.000	302.23
1.415	268.51	295.03	53.993	8.884	302.84
1.450	282.47	306.83	49.676	10.242	302.99
1.486	299.95	320.55	18.675	0.000	303.13
1.520	299.10	332.33	18.494	0.000	302.37
1.553	328.13	290.49	0.000	0.000	302.21
1.589	337.08	317.92	43.048	8.861	301.69
1.623	343.30	297.88	0.000	0.000	301.74
1.656	349.28	306.36	27.949	3.980	301.93
1.692	350.32	309.06	0.000	0.000	301.73
1.727	350.90	301.47	26.222	5.029	301.19
1.763	336.23	299.74	35.115	7.362	300.98
1.795	334.26	294.81	31.470	7.160	301.08
1.829	318.99	352.44	0.000	0.000	300.64
1.860	342.77	287.56	29.226	7.833	300.62
1.895	343.41	302.23	9.063	0.000	300.27
1.926	347.34	292.89	12.597	0.000	300.31
1.960	346.69	303.02	27.983	5.902	299.92
1.994	355.10	291.14	0.000	0.000	299.94
2.026	356.78	291.05	28.340	6.828	299.76
2.058	337.86	294.65	33.227	6.808	299.32
2.089	339.76	298.58	10.105	0.000	299.18
2.120	333.37	301.05	35.403	8.952	298.97
2.151	333.47	295.43	24.869	5.780	298.69
2.182	338.19	296.27	24.536	5.803	298.34
2.212	341.81	293.60	27.275	6.688	298.09
2.244	337.34	280.90	26.076	6.541	297.89
2.277	328.85	298.86	18.506	0.000	297.46
2.308	316.37	288.45	14.610	0.000	297.44

2.340	308.81	305.81	10.434	0.000	297.24
2.370	308.87	306.43	17.180	2.625	296.78
2.419	307.89	295.83	27.925	7.248	300.80
2.449	321.28	289.07	18.328	4.741	301.26
2.481	318.17	295.48	22.929	6.236	300.82
2.513	320.42	301.51	17.011	2.138	300.11
2.546	333.95	277.48	26.103	5.112	299.60
2.577	331.03	297.54	24.298	5.674	299.33
2.610	333.44	295.96	17.198	3.272	299.57
2.640	343.26	294.71	17.842	3.879	299.41
2.672	344.59	308.45	0.000	0.000	299.31
2.703	350.82	299.83	0.000	0.000	299.08
2.736	352.57	310.15	22.186	5.098	298.65
2.768	357.96	302.68	13.004	2.841	298.57
2.801	363.27	295.63	21.700	1.623	298.60
2.835	363.87	305.31	37.005	7.603	298.33
2.866	364.89	300.49	35.753	6.740	297.94
2.897	372.69	291.76	38.917	8.435	297.92
2.929	373.52	293.11	36.845	7.274	297.60
2.963	380.96	289.31	16.519	0.000	297.41
2.996	371.02	301.97	43.453	8.280	297.29
3.028	384.85	280.86	0.000	0.000	296.99
3.060	385.20	289.53	40.549	7.853	296.97
3.093	384.42	296.59	41.740	8.403	296.76
3.128	389.00	303.76	9.447	0.971	296.35
3.161	401.48	297.43	33.808	6.887	296.13
3.191	380.61	301.61	37.736	7.425	296.16
3.224	395.01	302.83	12.562	0.000	295.91
3.256	382.94	305.16	34.996	6.860	295.61
3.289	386.89	311.56	25.692	3.821	295.47
3.322	390.85	282.18	7.878	2.875	295.14
3.355	382.19	279.33	24.952	4.243	295.09
3.389	383.62	311.52	25.788	3.027	294.84
3.421	382.63	283.52	23.770	6.011	294.49
3.451	375.30	290.89	0.000	0.000	294.35

Table 8. Profile Data at Station 3 - Heated

y/H	rho u	T(K)	(rho u)'	T'(K)	Tinf(K)
0.180	84.39	383.43	9.293	5.178	293.50
0.213	89.40	385.96	8.408	4.692	293.33
0.245	91.95	389.88	5.806	3.086	292.44
0.277	91.90	390.47	4.274	2.600	292.04
0.311	93.21	390.96	4.134	2.698	292.38
0.343	94.48	394.01	3.921	2.457	292.45
0.376	92.54	392.17	2.390	1.284	292.07
0.407	93.46	392.41	3.339	2.427	291.53
0.440	91.86	388.47	0.000	0.000	291.42
0.473	92.54	388.48	3.524	2.501	291.49
0.506	92.80	392.76	1.892	1.347	291.25
0.540	92.65	394.27	3.934	1.805	290.97
0.576	93.18	390.44	6.953	3.874	290.80
0.611	93.62	391.25	2.354	0.000	290.70
0.645	93.69	389.48	8.006	2.483	290.52
0.677	96.37	392.02	7.452	0.000	290.32
0.711	97.07	388.48	0.000	0.000	290.23
0.745	96.40	376.18	0.000	0.000	289.96
0.778	97.30	369.18	0.000	0.000	289.93
0.811	104.51	377.27	24.607	13.121	289.52
0.845	104.29	361.07	0.000	0.000	289.42
0.878	109.25	351.33	25.162	18.835	289.29
0.912	113.90	316.28	31.904	21.648	289.06
0.945	112.47	317.68	36.894	31.688	288.36
0.977	128.33	322.88	17.602	0.000	288.42
1.010	135.04	331.11	0.000	0.000	287.94
1.041	129.05	295.43	0.000	0.000	287.94
1.074	145.18	290.45	45.206	33.518	287.94
1.108	167.02	300.25	0.000	0.000	287.80
1.141	177.61	296.98	0.000	0.000	287.56
1.174	186.59	308.14	0.000	0.000	287.40
1.206	202.83	311.44	31.662	0.000	287.25
1.237	208.88	289.53	0.000	0.000	287.07
1.287	237.49	286.73	36.121	7.759	290.64
1.319	270.00	315.66	0.000	0.000	290.70
1.352	257.60	294.66	0.000	0.000	289.88
1.383	287.15	300.43	63.505	18.501	289.53
1.416	286.59	291.86	17.536	0.000	289.57
1.447	291.82	276.85	17.958	0.000	289.68
1.479	332.51	282.80	67.048	21.213	289.36
1.509	348.30	289.53	22.070	7.839	289.16
1.540	341.14	282.83	42.187	2.776	288.97
1.574	357.42	280.12	0.000	0.000	288.90
1.604	362.93	284.34	25.737	6.671	288.00
1.636	366.50	280.25	45.569	14.221	287.94
1.669	378.82	280.63	54.843	18.216	287.94
1.701	372.49	277.83	34.166	11.675	287.94
1.731	379.08	280.34	13.986	4.932	287.94
1.761	386.38	286.67	34.239	11.455	287.66
1.791	376.16	277.29	44.372	15.282	287.61
1.824	381.53	286.36	27.877	8.546	287.46
1.854	374.42	281.91	21.441	8.725	287.29
1.886	368.36	280.05	36.568	12.855	287.01
1.919	371.41	280.67	11.130	4.950	286.91
1.951	366.00	278.17	24.209	9.778	286.76
1.982	377.66	281.60	22.304	8.833	286.54
2.014	375.78	280.48	32.183	11.187	286.30
2.045	384.64	277.39	30.786	10.375	286.10
2.075	388.23	281.60	30.407	10.817	285.82
2.106	401.73	288.52	31.112	10.831	285.46
2.138	389.99	277.52	21.829	8.306	285.28
2.170	391.78	281.44	29.348	9.368	285.01
2.203	388.00	286.30	28.714	10.473	284.79
2.237	402.86	290.13	0.000	0.236	284.53

2.267	396.50	286.06	13.428	5.900	284.47
2.296	389.89	290.04	23.313	7.631	283.93
2.347	387.10	282.02	31.228	10.822	291.72
2.378	387.80	287.47	40.124	12.615	290.76
2.411	393.62	291.22	26.108	8.554	291.02
2.442	396.60	288.41	35.530	10.985	291.11
2.477	400.19	292.41	33.529	10.708	290.58
2.508	399.32	290.21	23.839	7.743	290.39
2.541	394.84	292.50	25.472	8.471	290.32
2.573	392.56	291.84	11.413	5.103	290.08
2.605	395.57	292.76	37.835	11.730	289.77
2.638	384.15	284.02	33.676	11.906	289.58
2.671	382.05	298.16	34.403	10.415	289.34
2.707	387.61	291.11	34.941	11.248	289.18
2.735	382.90	284.99	35.568	11.917	288.70
2.775	398.09	288.12	28.758	9.495	288.46
2.809	395.91	287.94	43.833	13.631	287.94
2.842	385.56	286.53	10.263	4.868	287.94
2.874	381.97	289.63	34.396	11.123	287.94
2.901	384.16	289.52	27.163	9.170	287.80
2.942	389.62	290.57	26.177	9.537	287.68
2.975	383.52	285.84	31.505	11.816	287.40
3.010	389.67	288.99	22.696	8.079	287.14
3.046	388.31	285.69	32.976	11.253	287.07
3.081	381.52	281.51	31.284	10.950	286.74
3.113	390.60	293.41	33.109	10.180	286.67
3.147	387.53	288.56	27.011	9.305	286.41
3.182	382.19	289.20	29.048	9.822	286.10
3.208	379.83	284.02	26.491	8.838	285.80
3.251	380.40	287.49	37.214	12.253	285.62
3.286	377.51	286.71	30.055	10.856	285.32
3.320	377.37	286.91	31.114	10.305	285.16
3.354	373.18	278.55	28.048	10.541	284.85
3.385	380.21	289.48	31.164	10.375	284.66
3.418	376.80	286.03	14.978	6.573	284.33

Table 9. Profile Data at Station 4 - Heated

y/H	rho u	T(K)	(rho u)'	T'(K)	Tinf(K)
0.215	82.41	384.44	3.762	0.000	294.20
0.245	87.96	380.14	8.304	2.508	294.58
0.275	87.64	384.95	6.952	4.798	293.45
0.305	91.79	378.87	7.598	0.000	293.03
0.335	99.48	396.05	0.000	0.000	293.77
0.368	97.66	352.26	23.975	19.895	293.42
0.399	102.87	386.77	14.160	6.102	292.35
0.431	105.58	380.21	0.000	0.000	292.68
0.464	102.16	352.79	0.000	0.000	292.97
0.498	112.90	377.78	0.000	0.000	292.25
0.529	111.33	370.60	0.000	0.000	291.73
0.562	104.47	301.74	22.020	25.228	292.17
0.593	116.09	356.38	23.152	11.061	292.21
0.625	121.03	333.79	0.000	0.000	291.55
0.658	120.71	327.67	31.248	12.398	291.22
0.692	127.85	331.52	28.340	13.551	291.10
0.724	127.35	300.72	18.979	0.000	291.25
0.758	152.10	335.32	0.000	0.000	290.84
0.790	158.29	345.61	37.714	16.141	290.69
0.822	157.31	303.10	35.566	20.333	290.52
0.855	155.14	293.19	40.863	15.980	290.39
0.888	177.68	326.01	16.259	0.000	290.15
0.922	179.71	301.85	30.953	12.693	289.92
0.956	203.00	290.86	37.059	18.807	289.77
0.992	202.77	284.80	0.000	0.000	289.71
1.027	205.33	323.00	37.592	0.000	289.58
1.063	219.53	294.80	0.000	0.000	289.27
1.095	223.53	266.78	46.631	20.481	289.06
1.128	252.59	324.14	21.498	0.000	288.86
1.161	261.20	313.00	43.923	2.962	288.25
1.194	253.38	290.97	37.241	7.828	287.94
1.228	278.21	298.38	39.229	0.000	287.94
1.262	282.68	295.92	0.000	0.000	287.94
1.291	257.79	270.32	25.892	0.000	291.51
1.325	318.17	300.55	42.449	8.080	291.02
1.358	315.45	304.46	81.708	23.563	292.07
1.391	321.10	289.49	54.022	12.976	291.94
1.422	338.09	291.39	65.835	20.255	290.83
1.454	320.71	290.06	38.250	7.726	290.65
1.487	349.49	288.40	0.000	0.000	290.98
1.521	343.59	293.21	57.016	17.275	291.03
1.554	357.56	298.54	25.020	5.586	290.29
1.587	362.84	292.98	60.513	18.962	290.11
1.619	372.07	295.98	30.388	8.312	290.15
1.651	367.20	288.01	38.065	12.875	290.22
1.681	352.36	277.97	13.994	5.731	289.89
1.715	365.82	286.46	31.661	9.503	289.62
1.747	358.32	291.09	32.829	9.655	289.57
1.780	362.70	281.44	39.579	13.089	289.36
1.812	354.55	284.84	23.219	8.344	289.30
1.843	355.80	289.22	0.000	0.000	288.98
1.875	354.65	285.43	30.136	11.025	288.83
1.906	360.11	292.91	30.694	10.500	287.94
1.938	364.75	292.68	28.836	9.758	287.94
1.968	359.69	281.72	34.036	12.000	287.94
2.000	363.26	282.08	33.082	12.366	287.94
2.033	365.46	279.83	21.750	7.697	287.83
2.066	376.03	290.10	19.988	7.130	287.64
2.098	378.41	285.36	26.970	9.392	287.42
2.130	391.46	289.86	28.355	9.221	287.12
2.155	383.00	283.28	15.881	4.217	286.90
2.193	393.56	286.03	35.941	11.822	286.75
2.224	404.88	291.17	30.634	9.434	286.43
2.255	400.62	280.11	24.879	8.959	286.27

2.287	403.45	279.38	40.255	12.123	286.01
2.320	409.49	290.78	24.728	6.634	285.67
2.359	392.05	287.98	30.878	6.949	294.02
2.391	366.50	280.35	31.488	10.218	293.21
2.423	374.85	291.82	39.375	11.862	294.01
2.454	374.66	282.13	33.686	10.731	294.05
2.484	375.66	290.46	35.696	11.616	293.45
2.516	360.72	285.09	29.324	10.085	292.89
2.548	371.43	287.85	25.288	9.393	292.99
2.580	387.10	287.51	30.655	8.801	293.02
2.614	382.57	293.58	23.564	7.646	292.78
2.646	367.68	278.89	29.938	10.794	292.42
2.678	386.68	296.83	41.974	12.394	292.35
2.709	373.94	290.36	0.000	3.472	292.22
2.740	372.56	286.70	28.939	9.771	292.08
2.774	370.11	283.54	23.381	9.107	291.82
2.803	372.96	290.94	18.762	8.146	291.77
2.837	369.80	284.55	31.843	10.700	291.40
2.870	366.42	285.84	17.309	6.175	291.31
2.904	366.71	287.56	25.480	8.808	291.03
2.934	373.93	289.48	19.756	6.499	290.98
2.967	365.98	282.41	26.381	8.914	290.82
3.000	369.27	289.93	23.884	7.948	290.68
3.032	369.18	281.68	16.456	6.338	290.48
3.064	372.65	286.14	32.028	9.845	290.22
3.100	375.00	298.01	21.713	7.202	290.00
3.133	375.56	293.26	14.104	4.985	289.88
3.169	365.80	283.18	25.815	10.355	289.63
3.202	374.94	290.53	32.784	10.405	289.62
3.235	366.82	286.15	27.221	10.591	289.27
3.268	374.18	290.52	34.581	10.564	289.23
3.302	367.76	288.16	29.207	10.192	288.99
3.337	365.14	285.25	24.092	9.331	288.88
3.372	371.50	288.15	25.465	9.058	287.94
3.406	370.23	286.56	22.271	8.195	287.94

Table 10. Profile Data at Station 4 With Shock Interaction - Heated

y/H	rho u	T(K)	(rho u)'	T'(K)	Tinf(K)
0.197	90.05	389.32	19.502	6.181	292.73
0.229	97.76	397.90	11.008	0.000	291.59
0.256	93.51	397.72	18.448	7.505	291.78
0.288	99.31	386.73	15.937	3.761	292.23
0.316	104.87	402.25	15.837	0.000	292.04
0.348	102.22	391.24	11.709	0.000	291.46
0.379	106.34	393.44	17.738	3.700	291.08
0.412	112.66	399.18	12.994	0.000	290.99
0.445	111.33	397.46	19.826	6.357	291.10
0.477	111.52	389.56	0.000	0.000	290.87
0.509	119.08	394.66	10.498	0.000	290.57
0.541	117.29	392.77	0.000	0.000	290.43
0.572	117.44	375.89	0.000	0.000	290.23
0.606	121.88	385.83	0.000	0.000	290.01
0.637	124.27	367.92	11.793	5.339	289.63
0.670	142.04	406.41	37.218	1.487	289.72
0.704	133.60	334.86	61.256	42.563	289.41
0.735	159.60	379.14	0.000	0.000	289.36
0.769	152.93	349.08	67.759	35.859	289.10
0.801	178.93	338.98	21.157	0.000	288.94
0.832	170.23	341.18	0.000	0.000	287.94
0.867	229.32	364.70	99.378	25.572	287.94
0.899	215.63	292.10	116.014	55.625	287.94
0.933	220.22	305.75	0.000	0.000	287.94
0.969	257.49	330.38	104.071	30.647	287.80
1.003	270.84	302.60	42.676	0.000	287.48
1.038	302.59	334.83	112.738	30.380	287.30
1.072	307.96	268.99	0.000	0.000	287.00
1.105	319.99	272.36	0.000	0.000	286.71
1.138	326.52	276.19	0.000	0.000	286.48
1.172	374.94	307.61	96.293	9.804	286.15
1.205	391.15	288.43	80.227	0.000	285.78
1.237	432.26	282.35	0.000	0.000	285.58
1.292	406.31	303.09	149.996	33.901	295.81
1.326	454.72	300.05	211.090	49.000	294.59
1.358	489.99	286.84	35.400	0.000	294.34
1.390	504.69	287.97	180.532	38.297	295.03
1.422	557.77	307.44	72.166	0.000	294.82
1.454	541.12	273.45	63.376	0.000	294.42
1.487	591.21	287.29	88.322	15.033	293.84
1.520	611.71	275.99	26.440	4.553	293.94
1.554	628.02	289.40	105.354	20.883	293.89
1.586	612.18	291.81	84.913	15.209	293.70
1.619	613.70	293.05	50.537	8.868	293.44
1.649	628.73	295.94	61.335	11.456	293.29
1.681	629.22	290.38	70.051	13.168	293.08
1.713	620.02	292.81	44.855	6.875	292.94
1.746	618.70	287.99	43.255	7.110	292.67
1.779	627.67	290.11	43.111	8.053	292.47
1.812	626.93	278.18	0.000	0.000	292.33
1.847	641.09	291.34	31.948	5.208	292.24
1.875	624.95	289.49	54.839	10.536	291.91
1.905	615.97	277.81	35.413	7.135	291.85
1.936	623.65	292.20	30.992	5.654	291.52
1.969	625.78	285.31	76.512	13.989	291.34
2.000	619.51	288.78	75.692	13.803	291.18
2.032	600.49	283.12	46.334	9.375	290.99
2.066	596.45	288.97	39.465	8.393	290.76
2.098	580.11	272.88	70.085	16.077	290.64
2.129	577.09	293.52	46.693	9.451	290.28
2.160	563.05	275.11	72.746	16.028	290.25
2.191	564.01	291.71	55.368	10.290	289.97
2.224	564.15	288.08	55.354	11.747	289.74
2.255	561.50	283.33	63.265	13.708	289.61

2.287	543.85	281.45	46.707	10.462	289.45
2.319	535.62	281.34	38.328	9.921	289.16
2.375	612.41	276.42	81.047	15.534	293.14
2.407	607.72	292.32	30.516	4.856	292.29
2.438	599.56	296.42	61.571	10.149	291.74
2.469	613.62	286.31	41.839	7.768	292.03
2.499	615.04	269.18	61.592	12.740	291.77
2.531	610.00	289.58	52.083	9.868	291.31
2.563	608.27	290.47	47.648	9.158	291.05
2.594	619.12	275.43	63.614	13.004	290.99
2.628	616.05	290.17	37.574	6.942	290.74
2.662	629.34	287.26	34.701	4.413	290.56
2.692	626.46	278.33	29.527	6.350	290.32
2.723	624.31	287.03	52.090	9.641	290.21
2.755	626.97	286.12	60.734	11.002	289.92
2.786	630.42	283.35	48.442	9.294	289.75
2.819	629.66	281.04	53.819	9.633	289.53
2.852	645.74	281.02	40.187	7.221	289.22
2.886	643.19	280.67	52.477	9.897	288.97
2.918	664.61	286.70	46.200	7.165	287.94
2.951	675.65	286.51	32.795	6.307	287.94
2.983	676.47	273.03	27.113	6.287	287.94
3.016	677.60	283.22	38.239	7.008	287.94
3.048	684.96	288.45	28.592	4.682	287.81
3.081	681.05	286.84	36.681	6.256	287.56
3.115	696.06	280.93	73.490	11.813	287.46
3.151	684.14	281.14	17.183	3.036	287.25
3.185	690.71	277.55	64.990	11.801	286.97
3.216	697.01	255.18	229.914	42.074	286.00
3.249	573.82	361.09	94.968	6.847	286.00
3.285	527.01	240.38	48.146	4.724	286.11
3.319	503.96	282.84	74.785	16.945	285.89
3.354	495.81	278.81	58.972	15.282	285.65
3.388	492.01	279.98	52.513	13.143	285.43
3.423	485.62	282.18	34.267	9.147	285.23

APPENDIX F

Wire Calibration Curves

Wires D.2 and E.1, used in the heated injection case, were calibrated with a reduced number of data points because oil contamination of the flow affected some of the data (see Chap. 4).

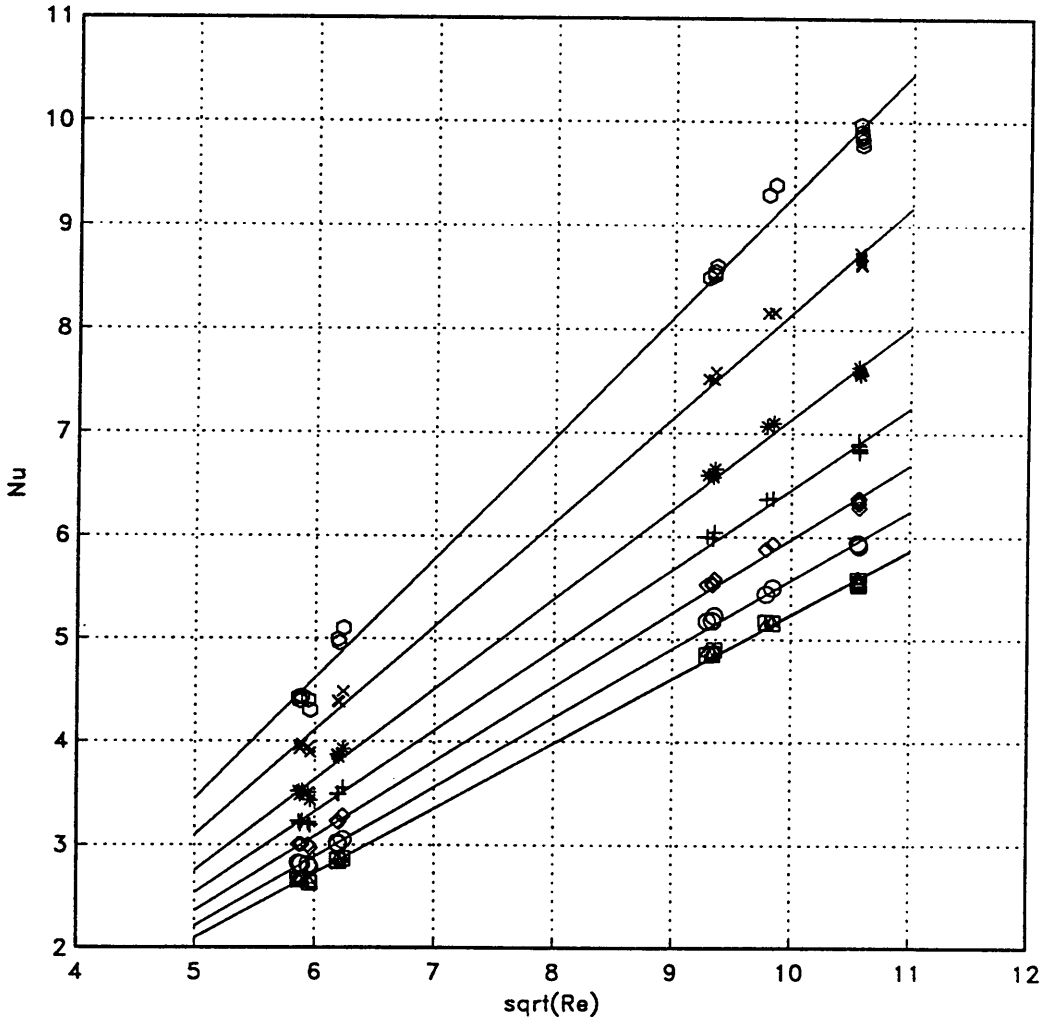

Calibration of Hot Wire 4 (Used in Unheated Injection Cases)

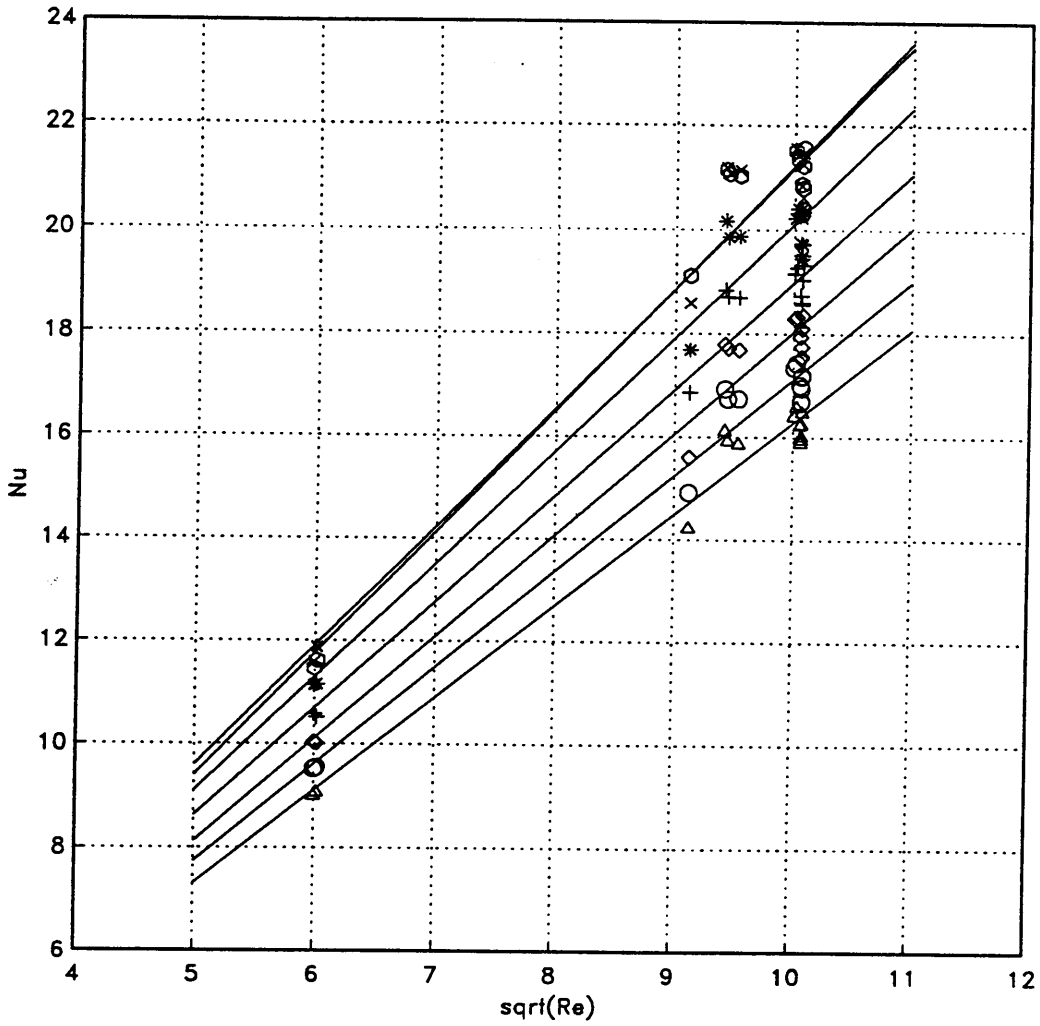

Calibration of Hot Wire D.2 (Used in Heated Injection Cases)

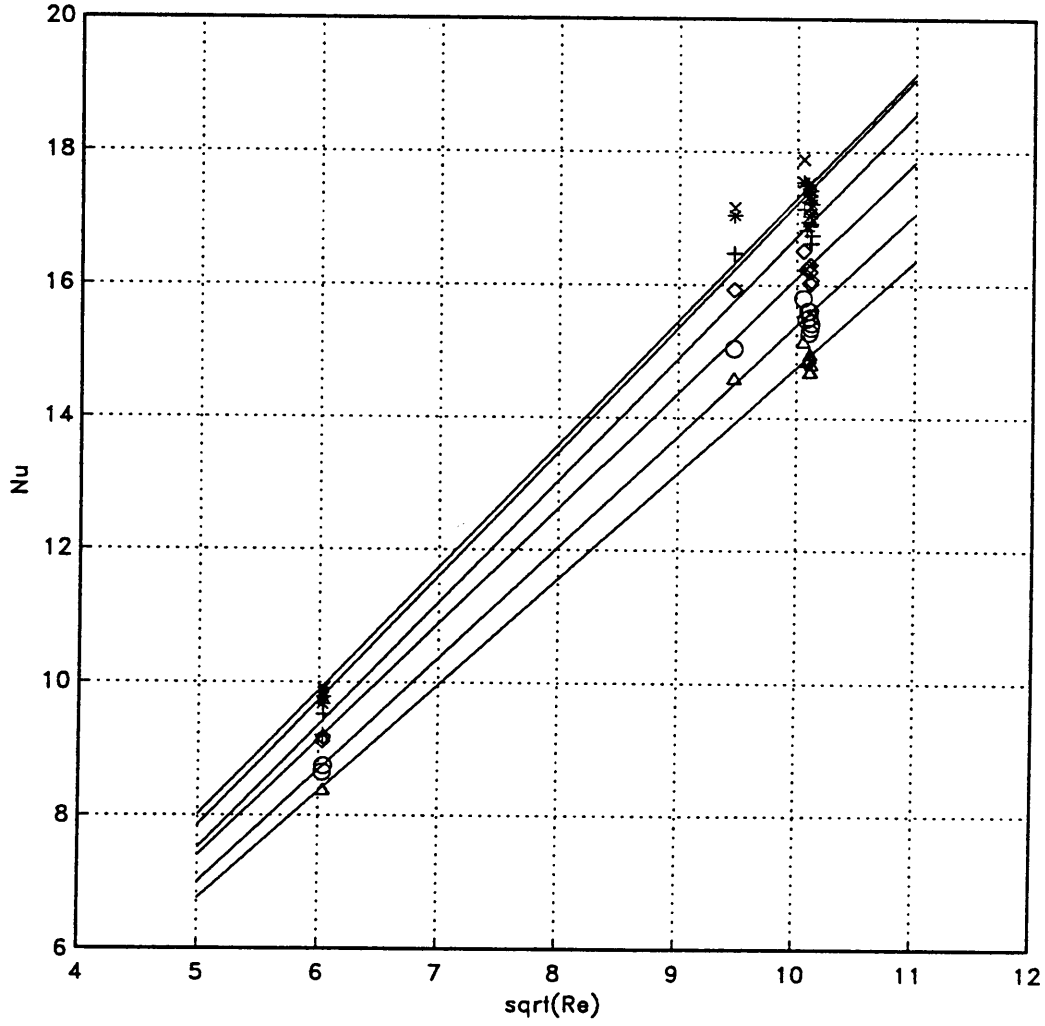

Calibration of Hot Wire E.1 (Used in Heated Injection Cases)

TABLE

Table 1: Nondimensionalization Parameters			
Station #	Traverse	T_{tj} (°K)	$\overline{(\rho u)}_\infty$ ($\frac{kg}{m^2\ sec}$)
1; Heated	Low	417	2.700
	Middle	428	
	High	431	
1; Unheated	Low	Ambient	2.530
	Middle	Ambient	
	High	Ambient	
2; Heated	Low	408	2.295
	Middle	417	
	High	417	
2; Unheated	Low	Ambient	2.302
	Middle	Ambient	
	High	Ambient	
3; Heated	Low	419	2.349
	Middle	423	
	High	429	
3; Unheated	Low	Ambient	2.479
	Middle	Ambient	
	High	Ambient	
4; Heated	Low	411	2.214
	Middle	433	
	High	433	
4; Unheated	Low	Ambient	2.631
	Middle	Ambient	
	High	Ambient	
4; Shock Heated	Low	431	2.214
	Middle	431	
	High	417	
4; Shock Unheated	Low	Ambient	2.631
	Middle	Ambient	
	High	Ambient	

Table 1. Nondimensionalization Parameters for Flow Variables

REFERENCES

1. Walker, D.A., R.L. Campbell, ad J.A. Schetz,"Turbulence Measurements for Slot Injection in Supersonic Flow," AIAA Paper No. 88-0123, Jan. 1988, also submitted to *AIAA Journal.*

2. Horstman, C.C. and W.C. Rose,"Hot-Wire Anemometry in Transonic Flow," *AIAA Journal* Vol. 15, 3, 1972, pp. 395-401.

3. Schetz J.A., and Gilreath, H.E.,"Tangential Slot Injection in Supersonic Flow," *AIAA Journal,*Vol. 5, No. 12, 1967, pp. 2149-2154.

4. Samimy, M. and A.L. Addy,"Interaction Between Two Compressible, Turbulent Free Shear Layers," *AIAA Journal,* Vol. 24, 1986, pp. 1918-1923.

5. Clark, R.L., W.F. Ng, A.L. Rettew, D.A. Walker, and J.A. Schetz, "Turbulence Measurements in High-Speed Shear Flow Using a Dual-Wire Probe," AIAA Paper No. 88-3055A, July 1988, also submitted to *AIAA Journal.*

6. Visich, Jr., M., and Libby, P.A.,"Experimental Investigation of Mixing of Mach Number 3.95 Stream in Presence of Wall," NASA TN D-247, Feb. 1960.

7. Samimy, M. and G.S. Elliot,"Effects of Compressibility on the Structure of Free Shear Layers," AIAA Paper No. 88-3054A, July 1988.

8. Bogdanoff, D.W.,"Compressibility Effects in Turbulent Shear Layers," *AIAA Journal,* Vol. 25, No.6, 1983, pp. 926-927.

9. Papomoschou, D. and A. Roshko,"Observations on Supersonic Free Shear Layers," AIAA Paper No. 86-0162, Jan. 1986.

10. Tillman, T.G., W.P. Patrick, and R.W. Paterson,"Enhanced Mixing of Supersonic Jets," AIAA Paper No. 88-3002, July 1988.

11. Owen, F.K. and W. Calarese,"Turbulence Measurement in Hypersonic Flow" from *Aerodynamics of Hypersonic Lifting Vehicles*, AGARD-CP-428.

12. Yanta, W.J.,"Use of the LDV in Subsonic and Supersonic Flow," from the proceedings of a Project SQUID Workshop, *The Use of the Laser Doppler Velocimeter for Flow Measurements*, Purdue University, March, 1972.

13. Pike, E.R.,"The Applications of Photon-Correlation Spectroscopy to Laser Doppler Velocimetry," from the proceedings of a Project SQUID Workshop, *The Use of the Laser Doppler Velocimeter for Flow Measurements*, Purdue University, March, 1972.

14. Kovásznay, L.S.G.,"The Hot-Wire Anemometer in Supersonic Flow," *Journal of Aeronautical Sciences,* Vol. 17, 1950, pp. 565-584.

15. Morkovin, M.,"Fluctuations and Hot-Wire Anemometry in Compressible Flow," AGARDOGRAPH 24, 1956.

16. Kovásznay, L.S.G.,"Turbulence in Supersonic Flow," *Journal of Aeronautical Sciences,* Vol.20, 1953, pp. 657-682.

17. Kistler, A.L.,"Fluctuation Measurements in a Supersonic Turbulent Boundary Layer," *The Physics of Fluids,* Vol. 2, 1959, pp. 290-296.

18. Walker, D.A., W.F. Ng, and M.D. Walker,"Experimental Comparison of Two Hot-Wire Techniques for Resolution of Turbulent Mass Flux and Local Stagnation Temperature in Supersonic Flow," *AIAA Journal,* Vol. 26, March 1989.

19. *Probe Catalog* , Dantec Elektronik, Denmark, 1982.

20. Freymuth, P. and L.M. Fingerson,"Electronic Testing of Frequency Response for Thermal Anemometers," Thermo-Systems Inc. *Quarterly,* 3, No. 4, pp. 5-12, 1977.

21. Walker, D.A., and M.D. Walker,"Method for Fast Sine Wave Calibration of Hot Wire Frequency Response," submitted to *Review of Scientific Instruments,* Dec. 1988.

22. Campbell, R.L.,*Experimental Study of Supersonic Slot Injection into a Supersonic Stream,*Thesis, Virginia Tech, 1987.

23. Smith, B.R.,*Mean Flow Measurements of Heated Supersonic Slot Injection into a High Reynolds Number Supersonic Stream,* Thesis, Virginia Polytechnic Institute and State University, February 1989.

24. *Complete Temperature Measurement Handbook and Encyclopedia* , 1986, Omega Engineering Inc., USA, copyright 1985.

25. Holman, J.P.,*Experimental Methods for Engineers, 4th Ed.*, McGraw-Hill Book Company, 1984.

26. Walker, D.A. and W.F. Ng, and M.D. Walker, "Hot-Wire Anemometry in Supersonic Shear Layers,"AIAA Paper No. 87-1372, June 1987.

27. Smits, A.J., K. Hayakawa, and K.C. Muck,"Constant Temperature Hot-Wire Practice in Supersonic Flows," *Experiments in Fluids,* Vol.1, 1983, pp. 83-92.

28. Logan, P., R.L. McKenzie, and Daniel Bershader,"Hot-Wire Accuracy in Supersonic Turbulence from Comparisons with Laser-Induced Fluorescence," *AIAA Journal,* Vol 26, No. 6, aug. 1987, pp. 316-322.

29. Bradshaw, P.,*An Introduction to Turbulence and Its Meaasurement,* First Ed., Pergamon, 1975.

30. Stainback, P.C.,"Some Influences of Approximate Values for Velocity, Density, and Total Temperature Sensitivities on Hot-Wire Anemometer Results," AIAA Paper No. 86-506, Jan. 1986.

31. Ames Research Staff,"Equations, Tables, and Charts for Compressible Flow," NACA Report 1135, 1953.

32. Horowitz, P., and Hill, W.,*The Art of Electronics,* Cambridge University Press, 1980.

33. Holman, J.P., *Heat Transfer,*, 6th Ed., McGraw-Hill Book Co., 1986.

FIGURES

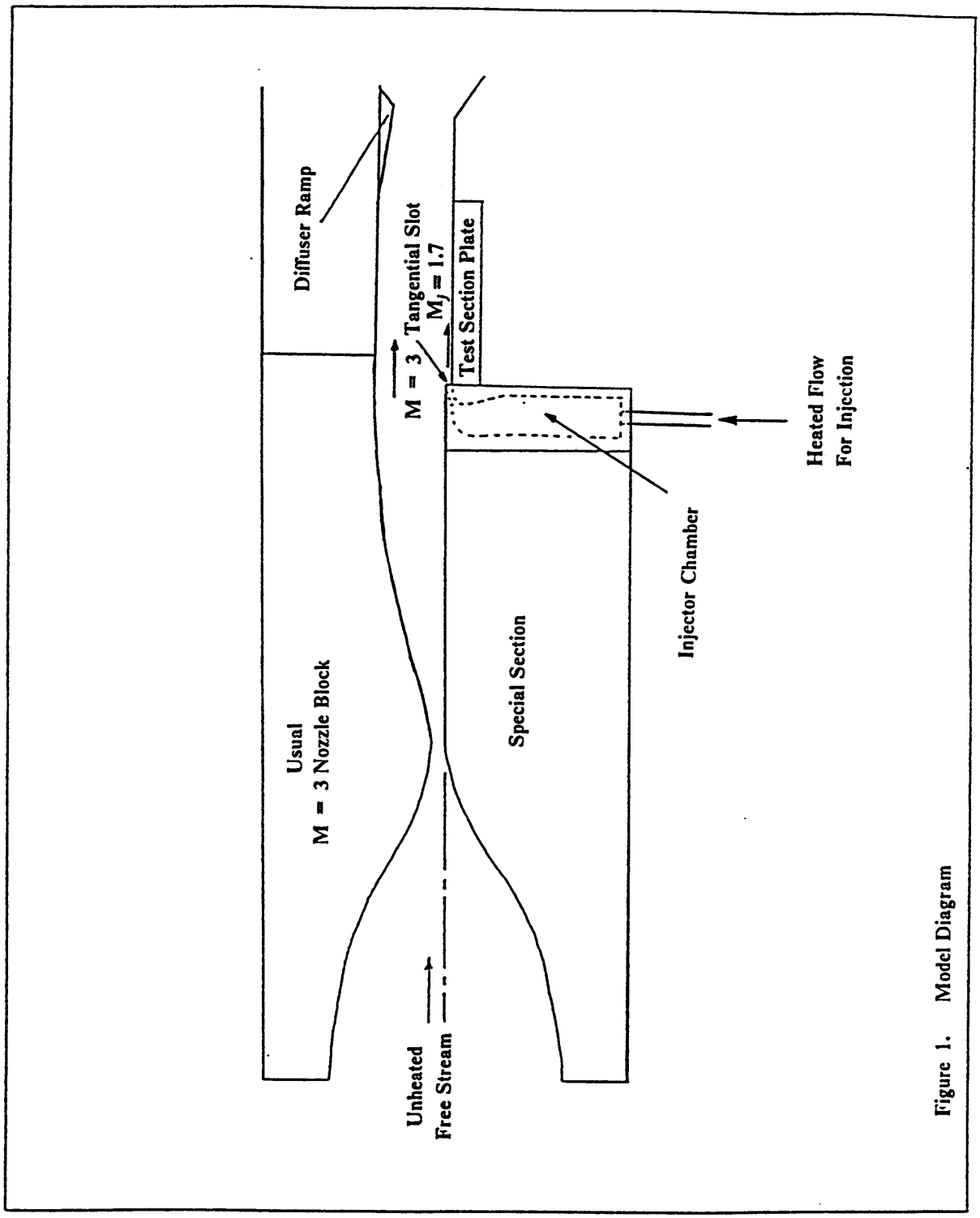

Figure 1. Model Diagram

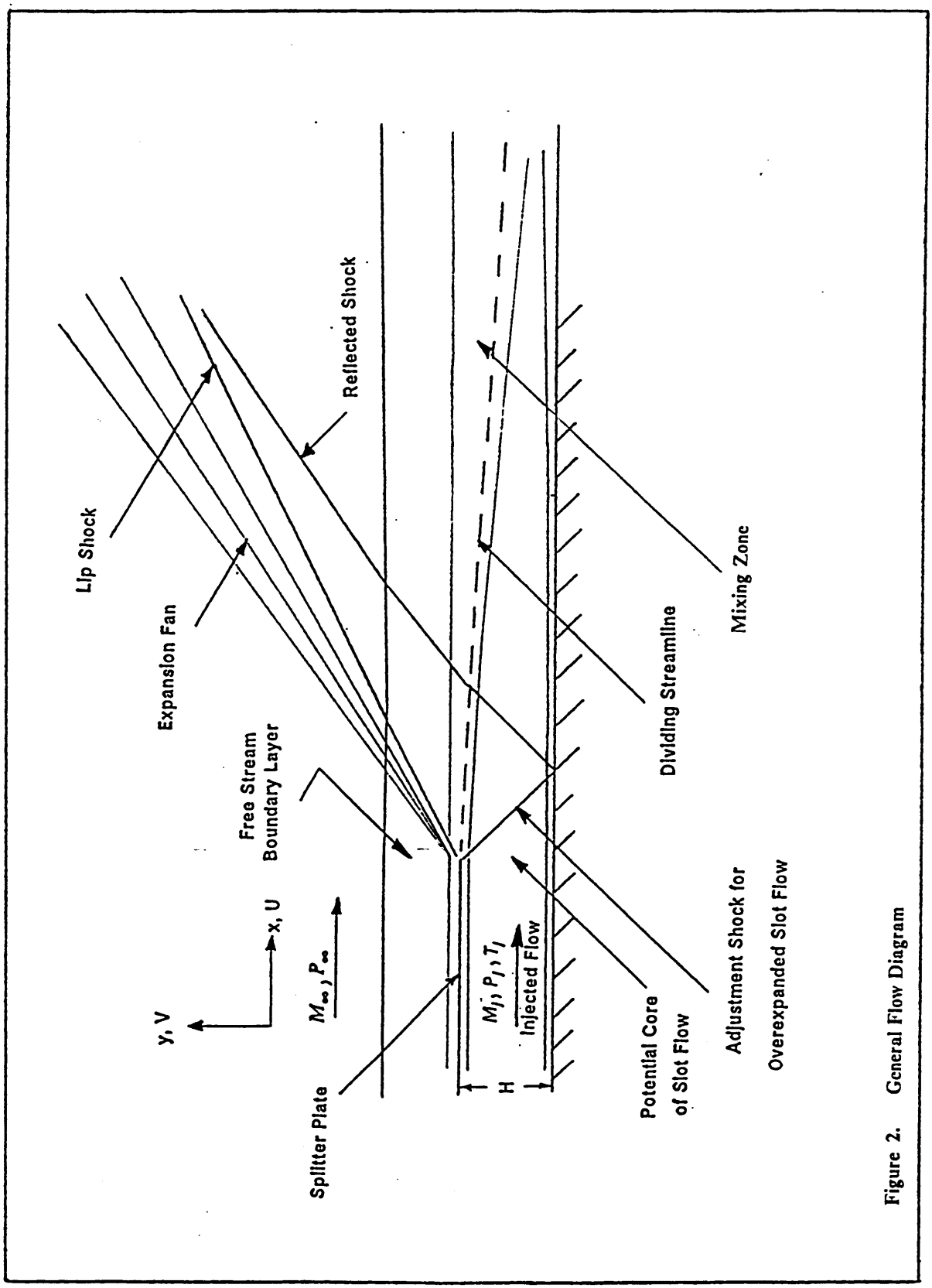

Figure 2. General Flow Diagram

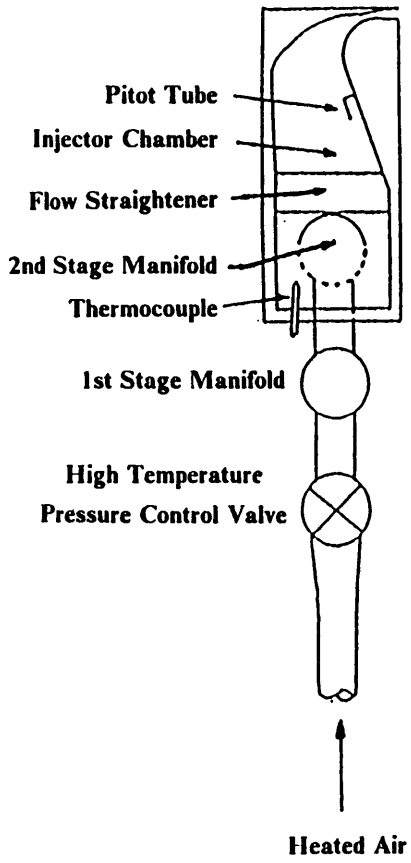

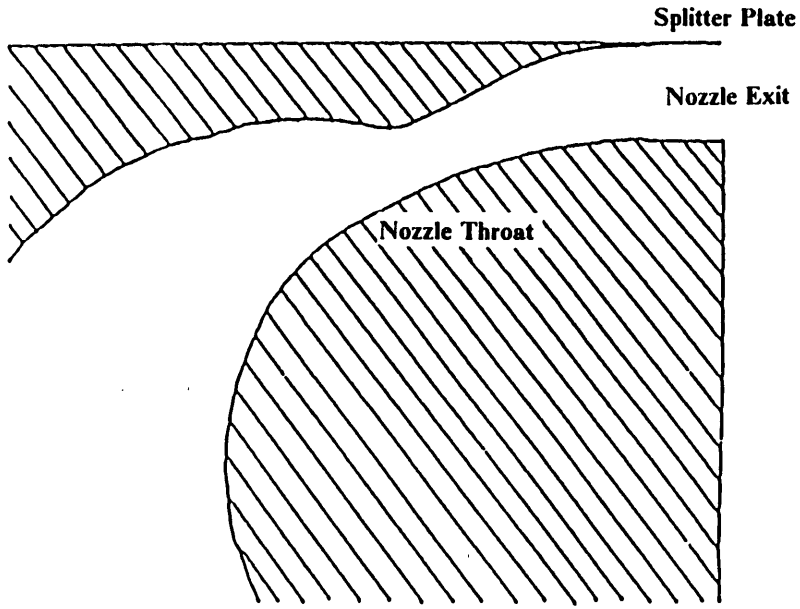

Detail of Injector Nozzle

Figure 3. Injector Diagram

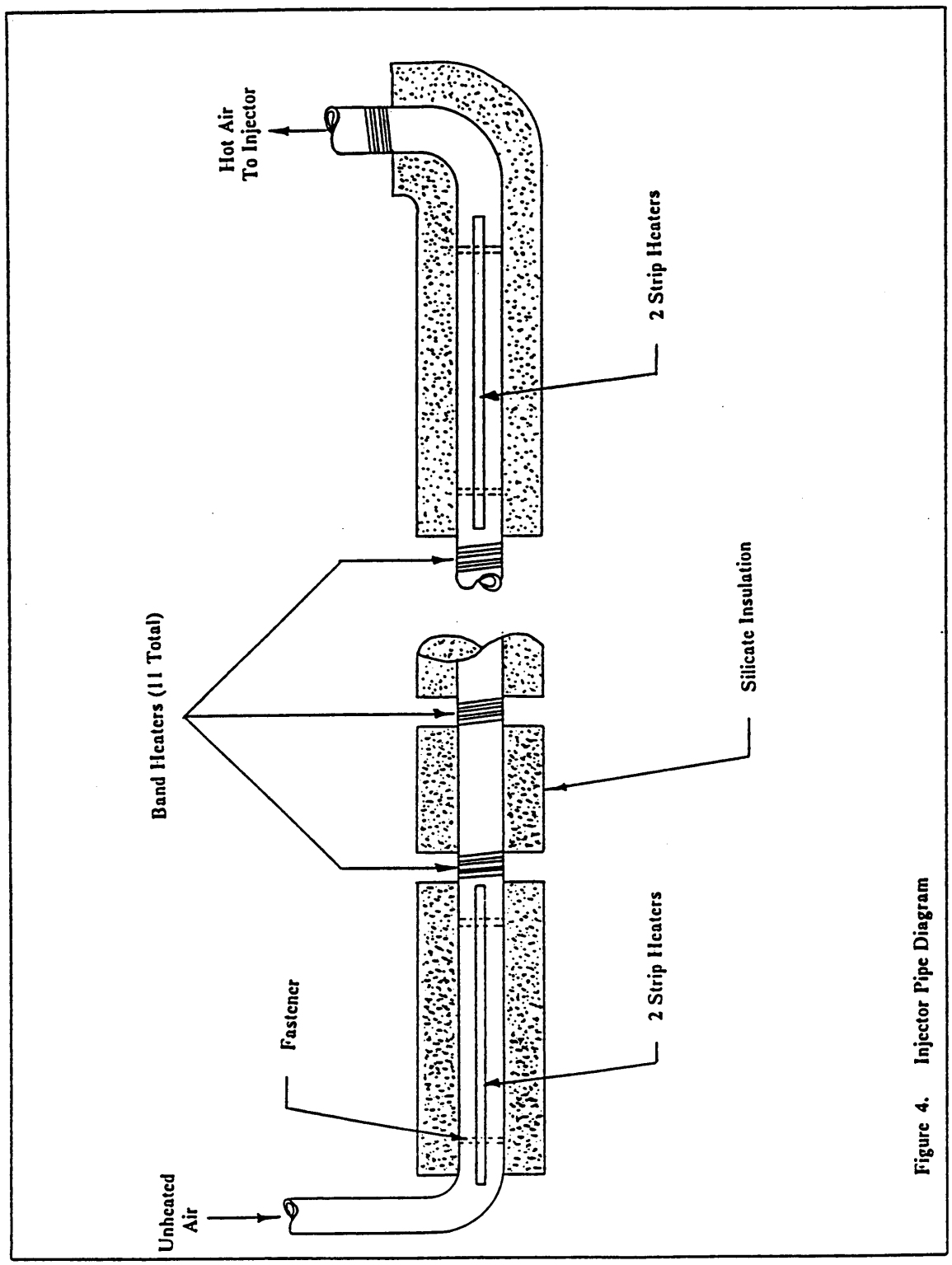

Figure 4. Injector Pipe Diagram

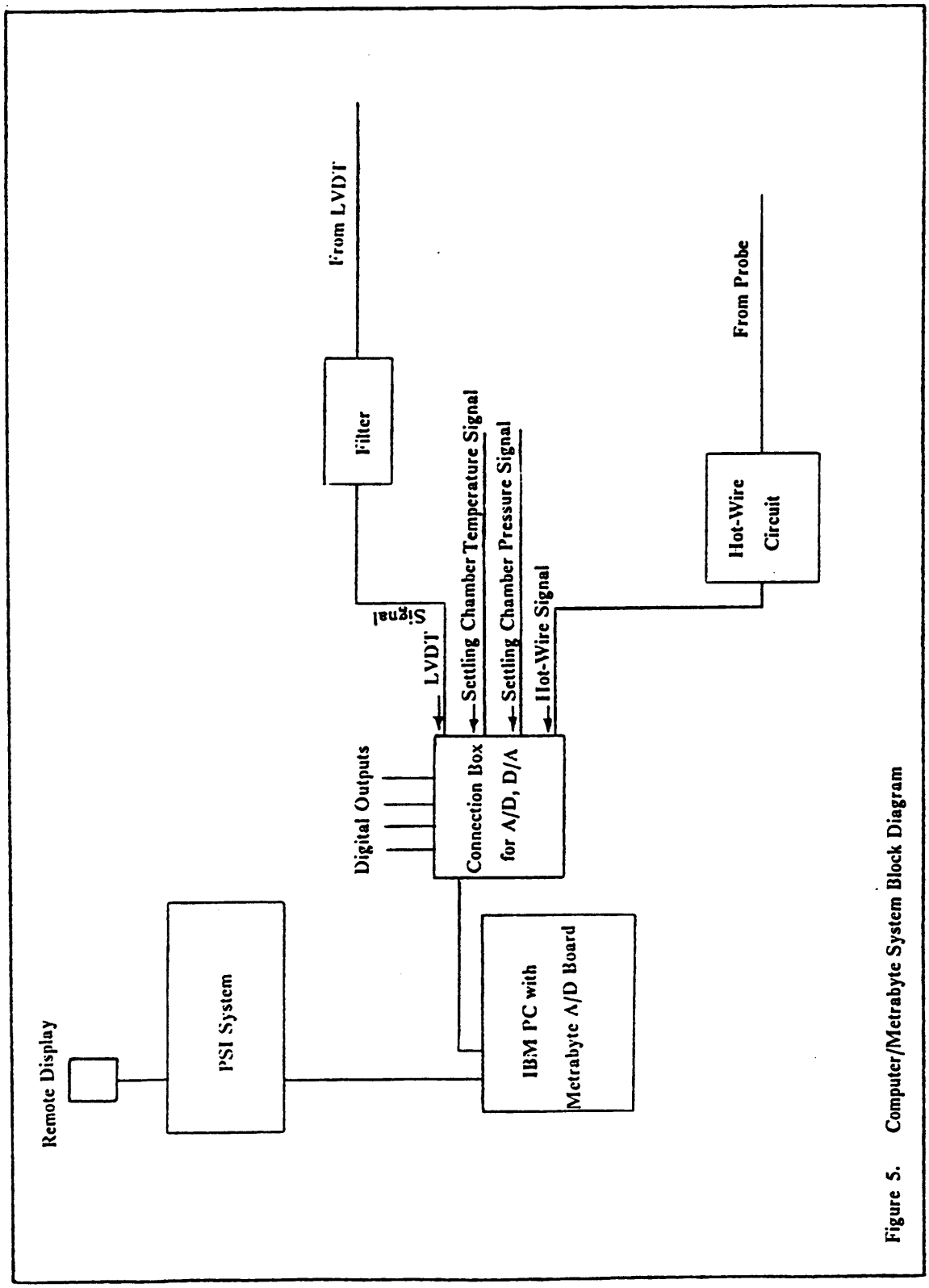

Figure 5. Computer/Metrabyte System Block Diagram

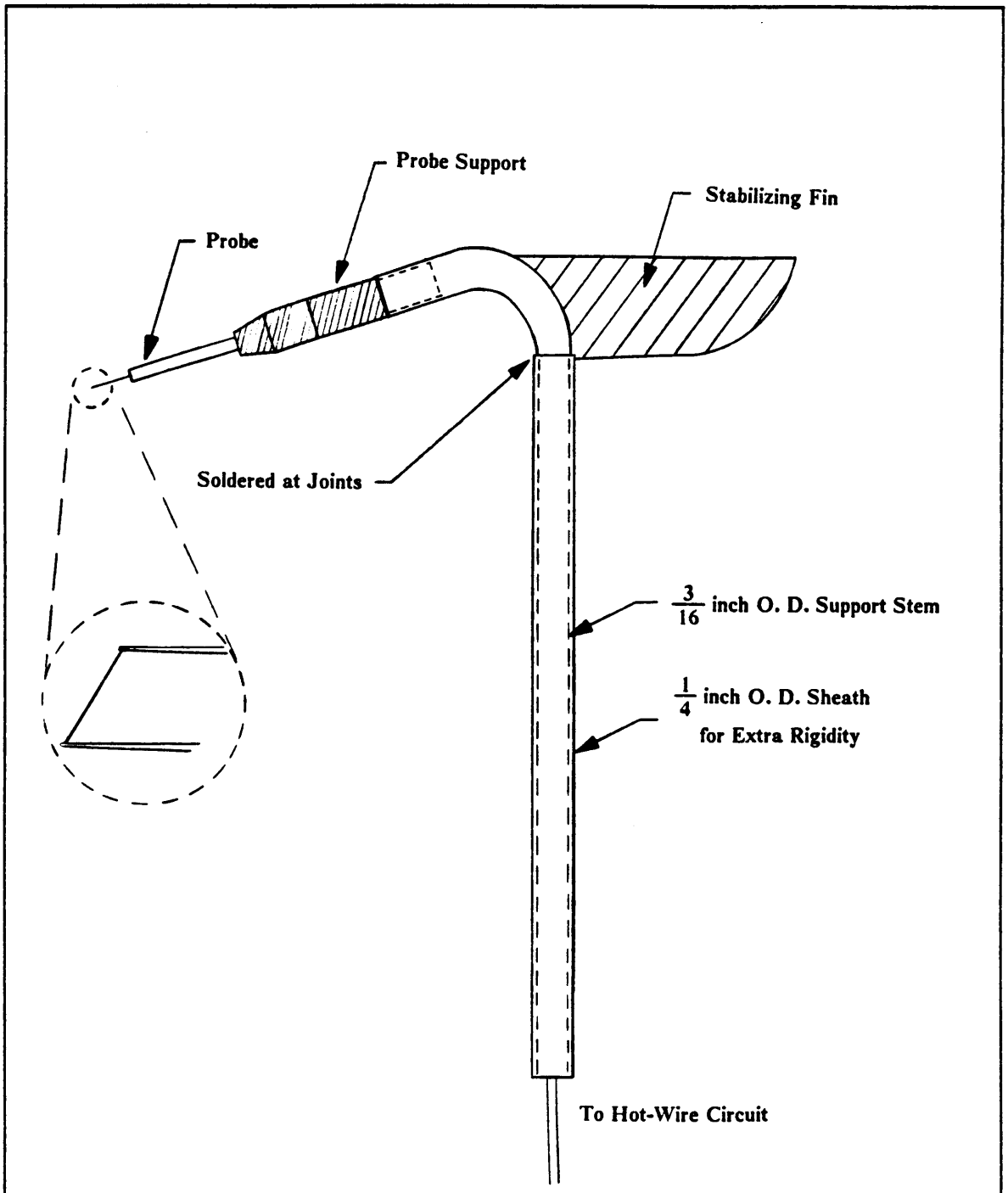

Figure 6. Probe and Support Schematic

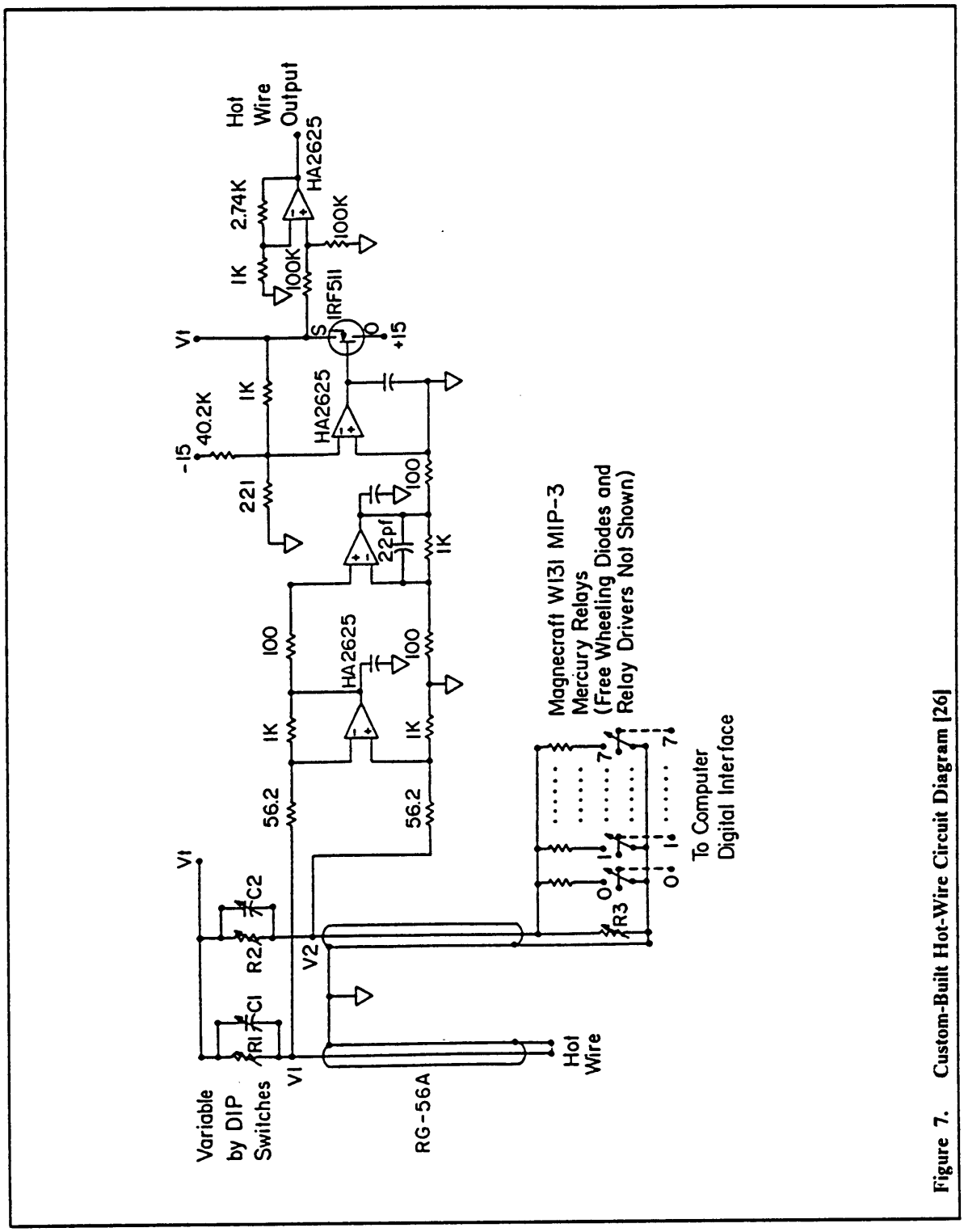

Figure 7. Custom-Built Hot-Wire Circuit Diagram [26]

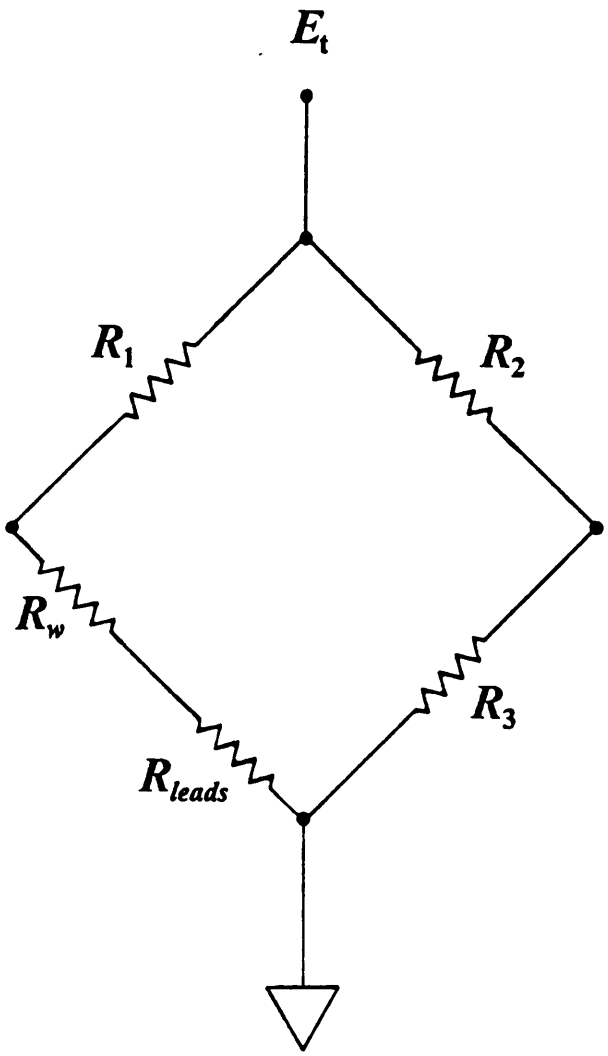

Figure 8. Simplified Hot-Wire Bridge Circuit Diagram

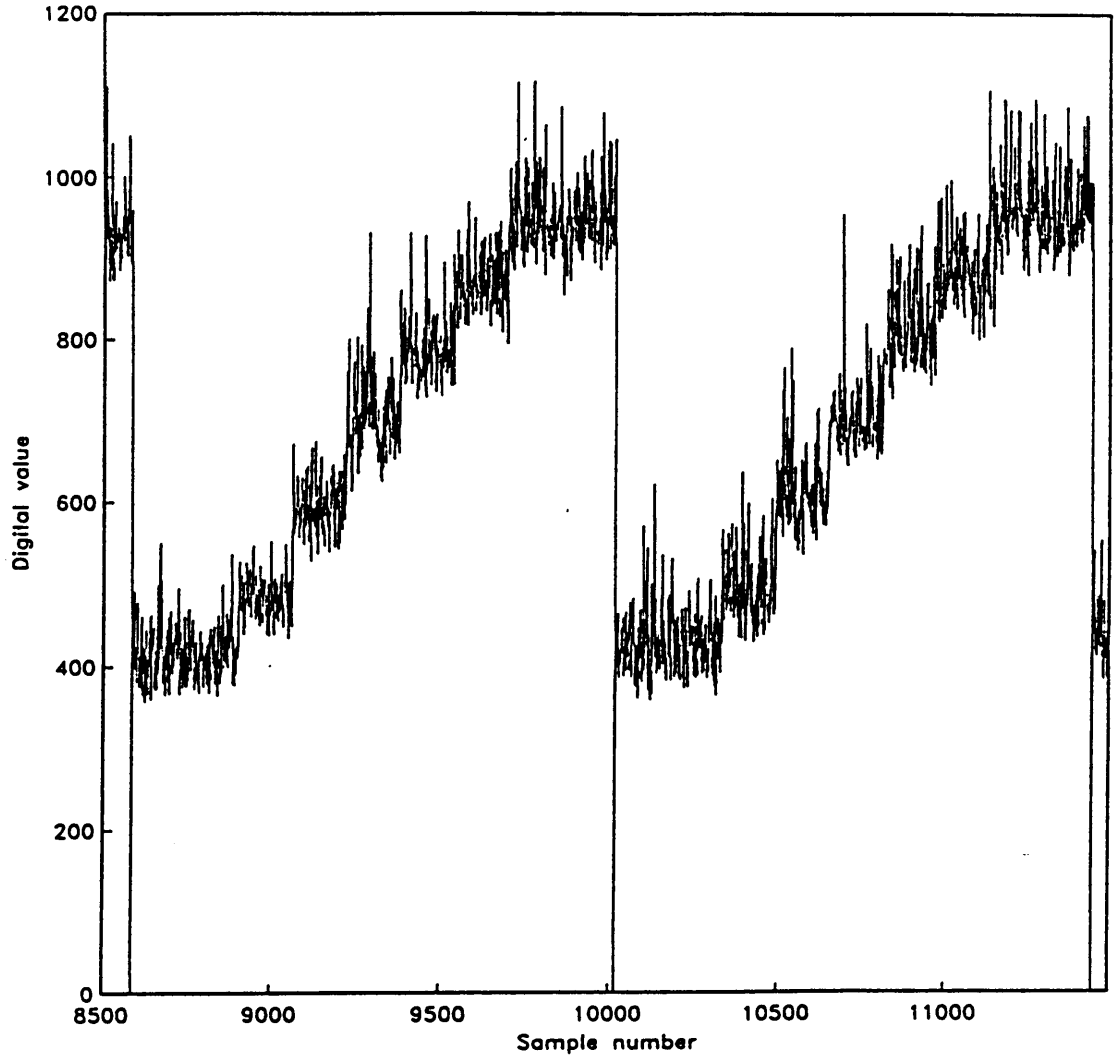

Figure 9. Raw Hot-Wire Voltages

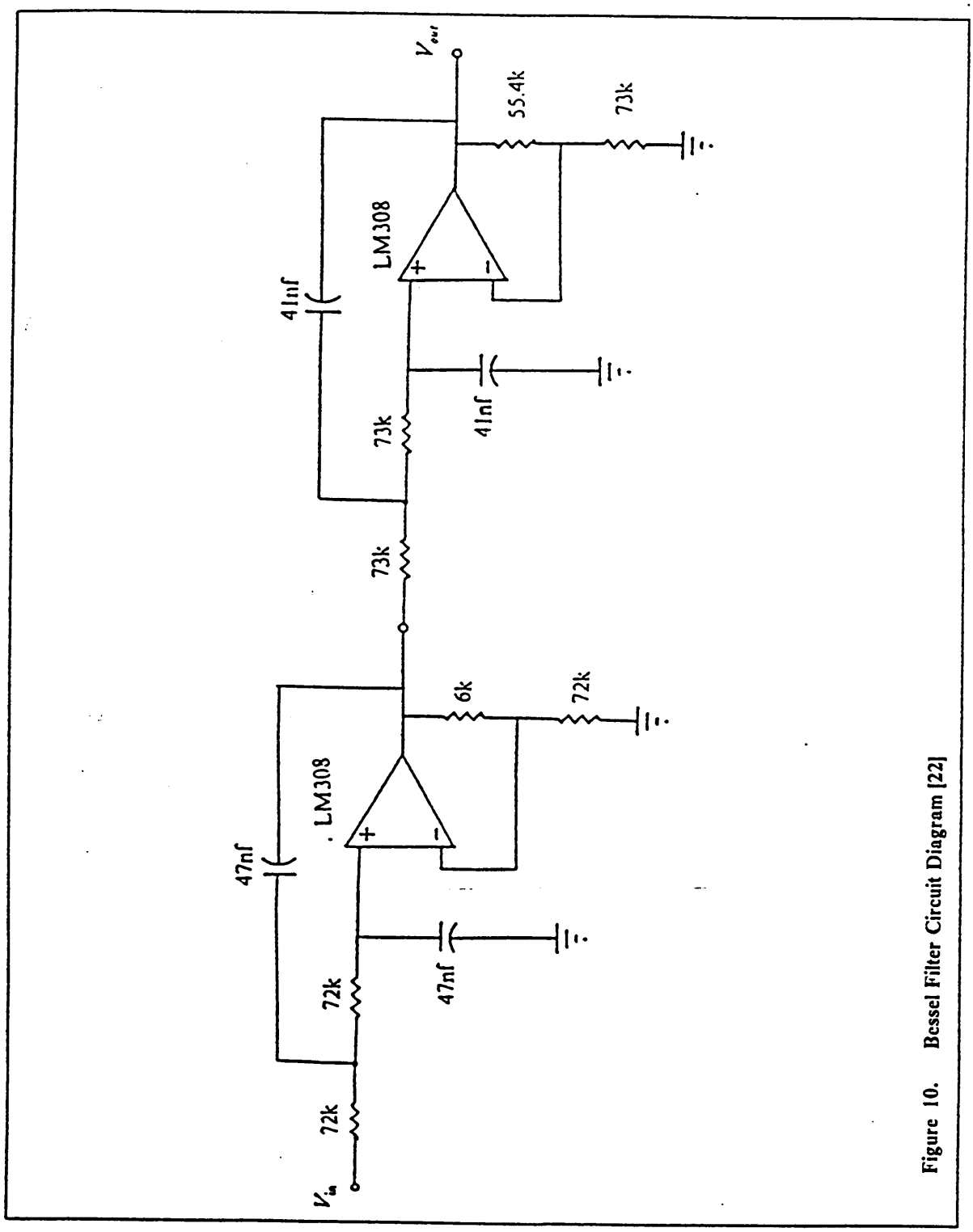

Figure 10. Bessel Filter Circuit Diagram [22]

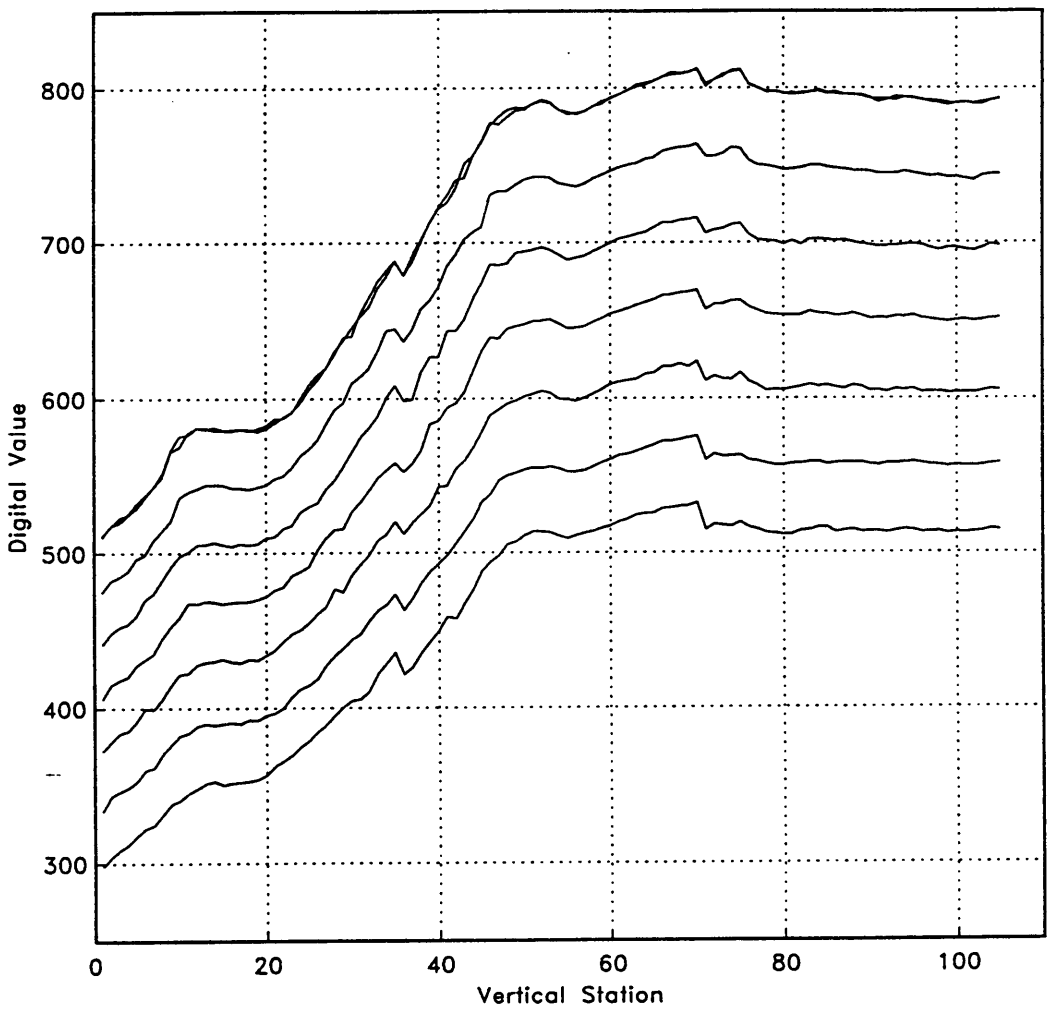

Figure 11. Averaged Hot-Wire Data (Stn. 3, Unheated)

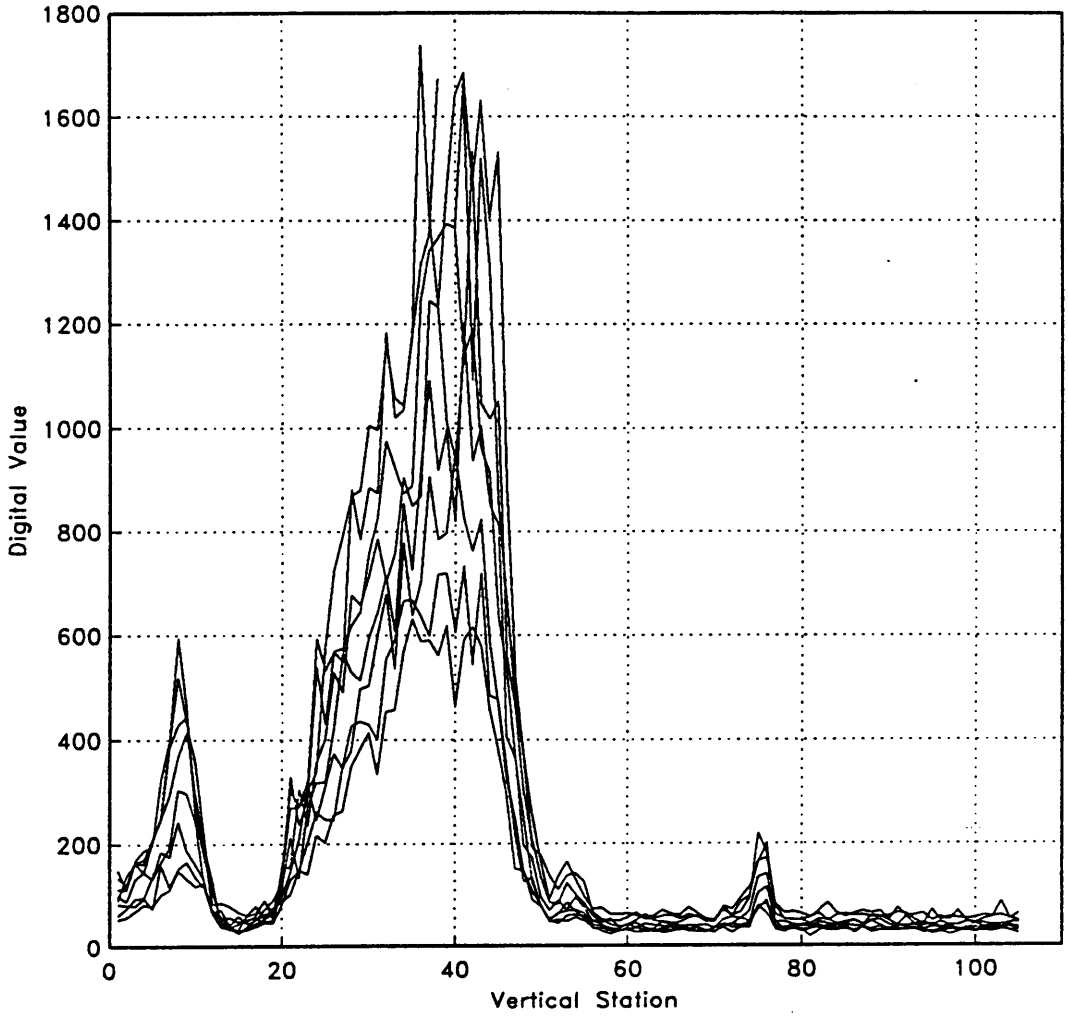

Figure 12. Rms Hot-Wire Data (Stn. 3, Unheated)

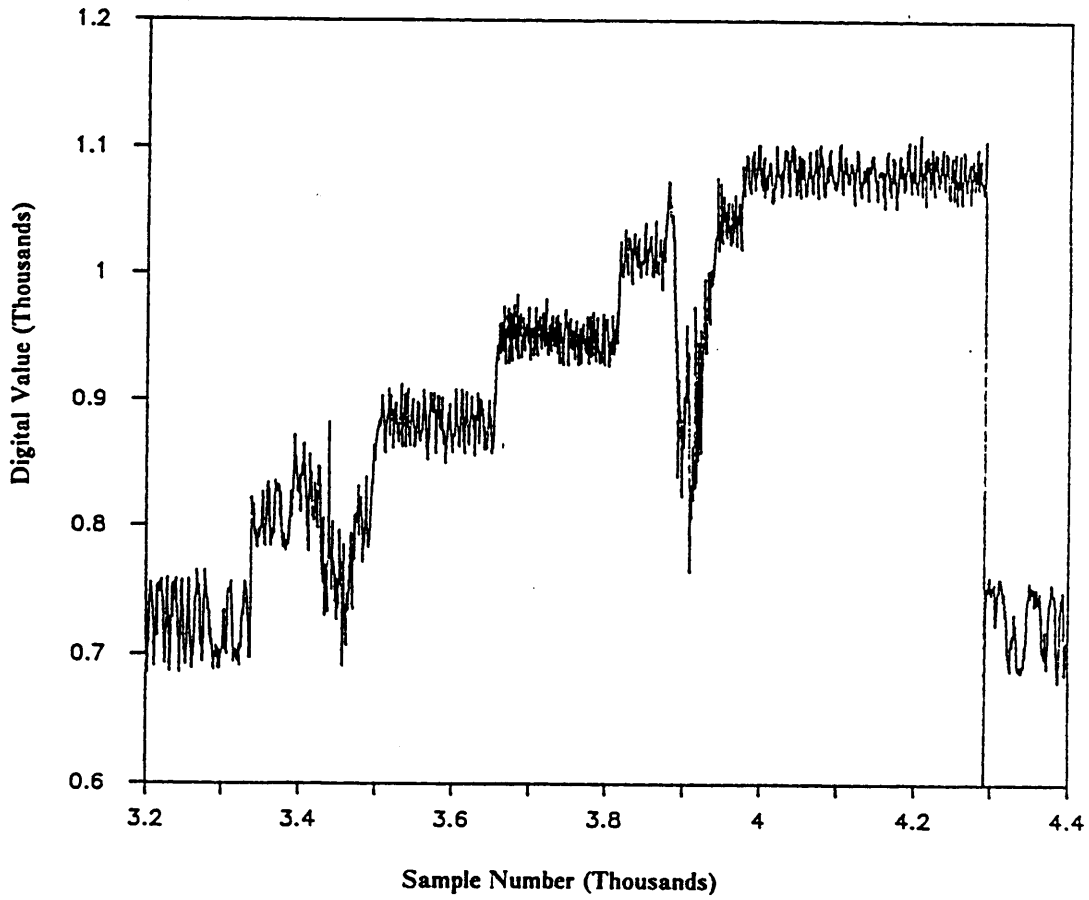

Figure 13. Hot-Wire Voltage with Oil Strikes

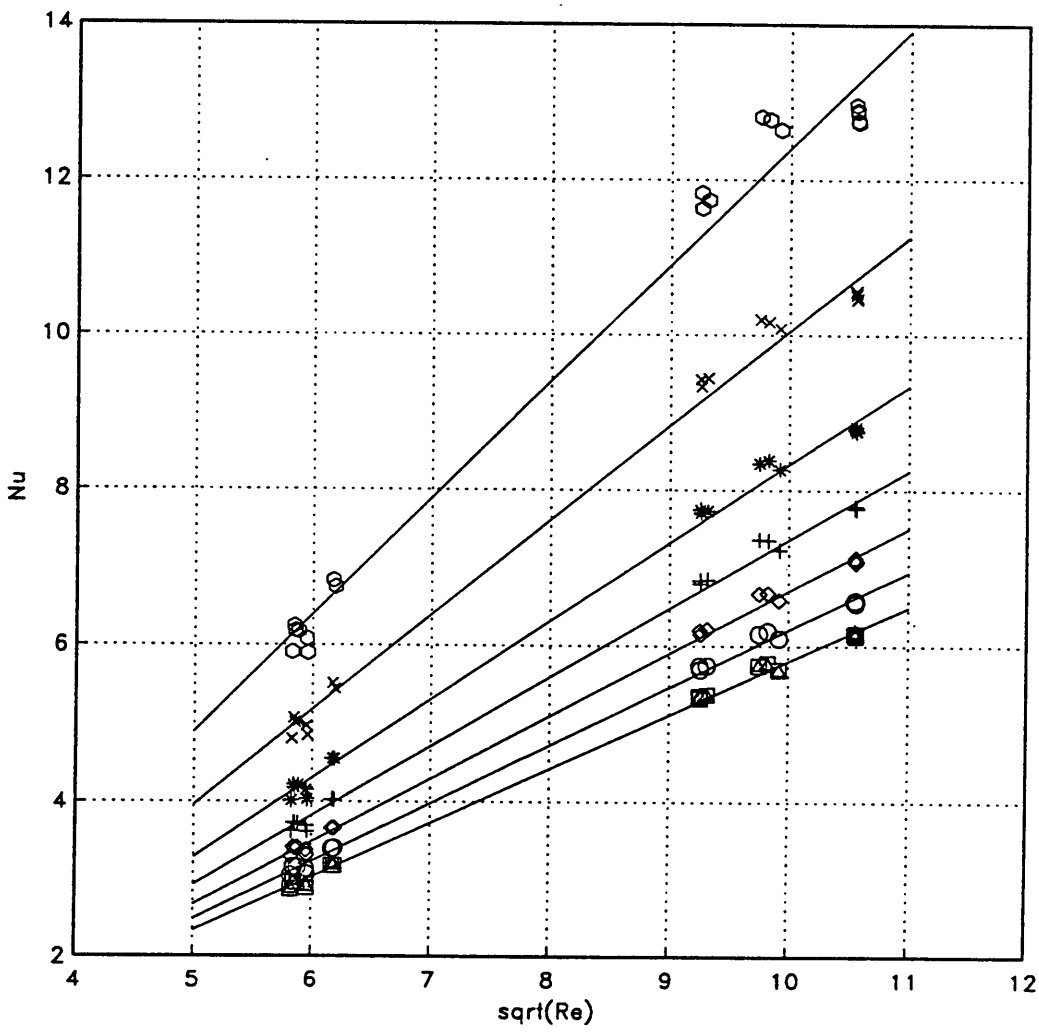

Figure 14. Sample Calibration Curves of Hot Wire B (Used in Unheated Injection Cases)

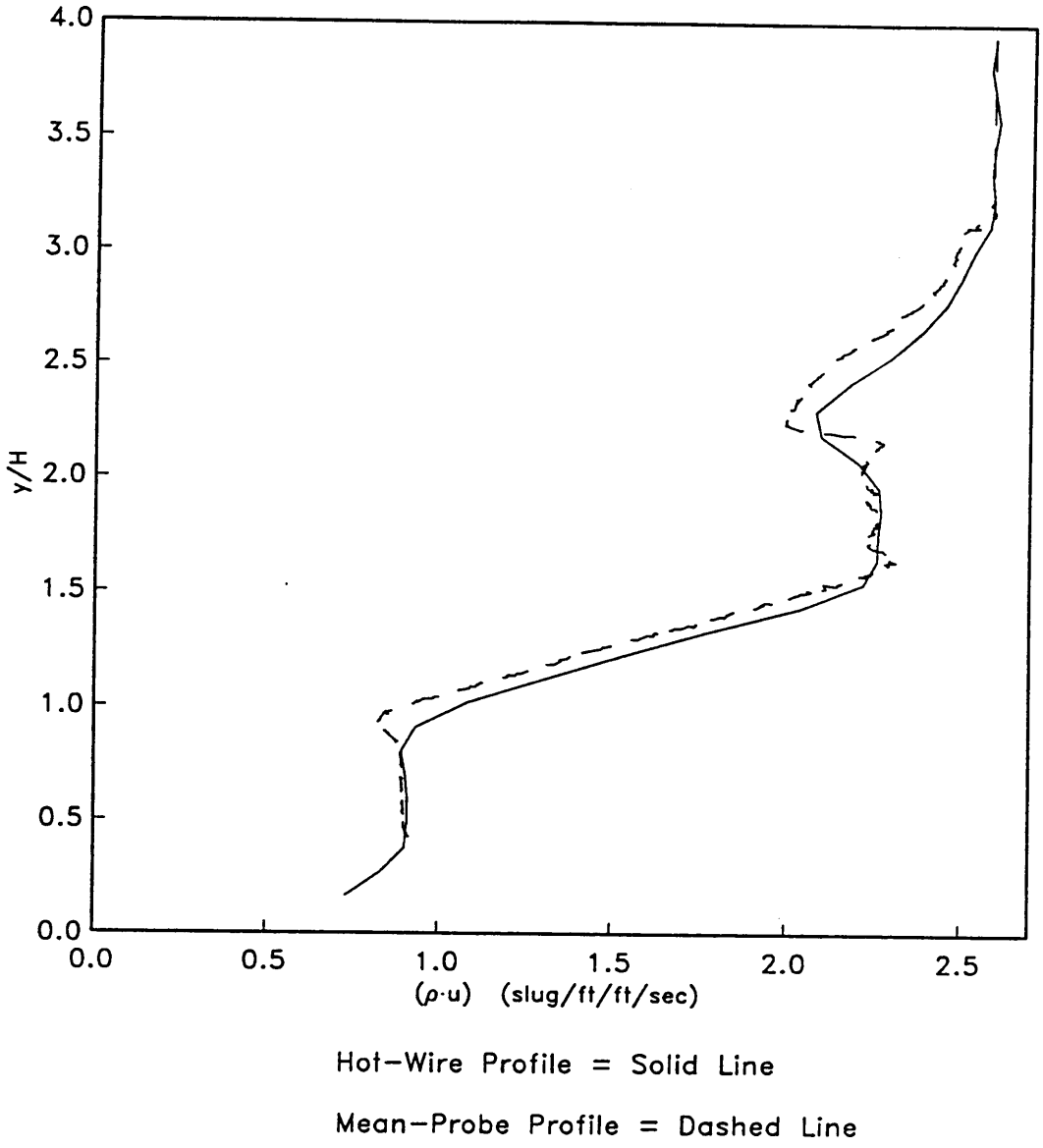

Figure 15. Comparison of Hot Wire and Mean Probe [23] Mass Flux Profiles Used in Calibration of Hot Wire B

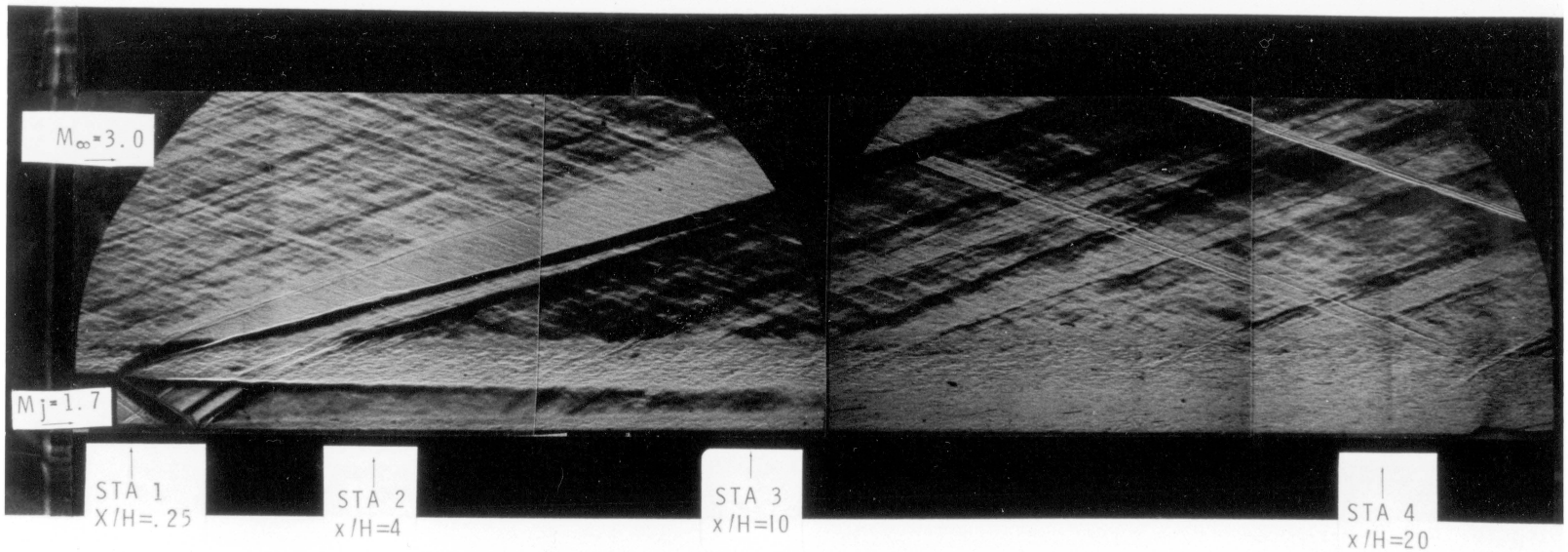

Spark Schlieren Photograph of Unheated Freestream ($T_{tinf} = 540R$) with Unheated Tangential Injection ($T_{tj} = 540R$, $P_{tj} = 10.7$ psia), H = 0.5 inches.

Figure 16. Spark Schlieren of Unheated Injection Case

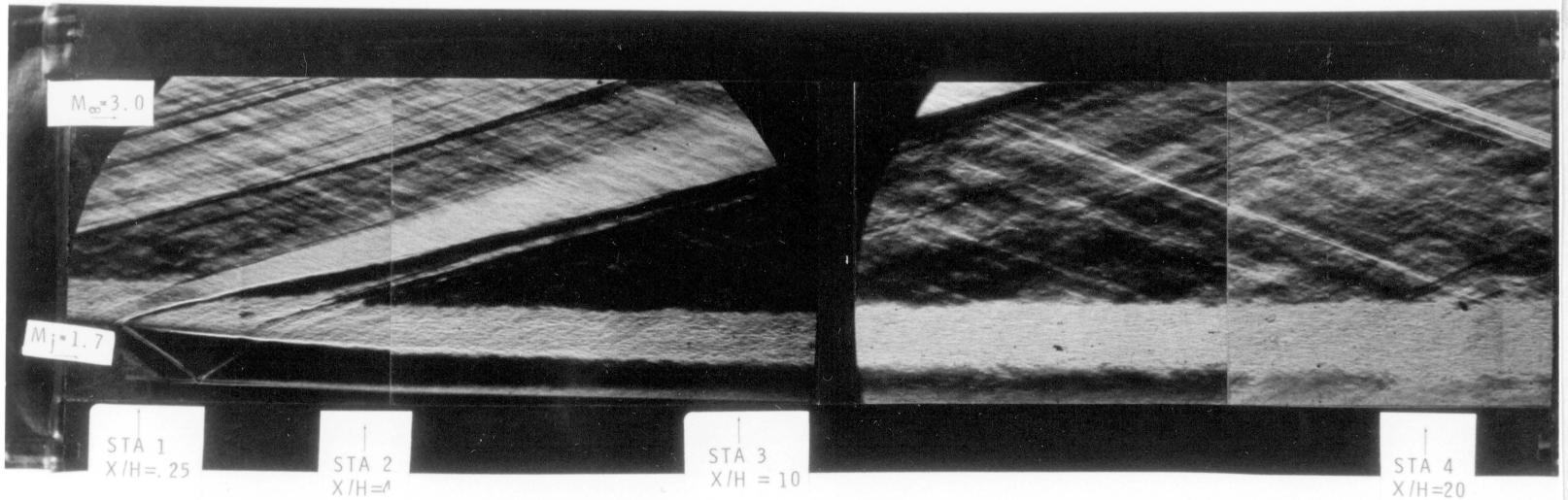

Spark Schlieren Photograph of Unheated Freestream ($T_{tinf} = 540R$) with Heated Tangential Injection ($T_{tj} = 760R$, $P_{tj} = 10.7$ psia), H = 0.5 inches.

Figure 17. Spark Schlieren of Heated Injection Case

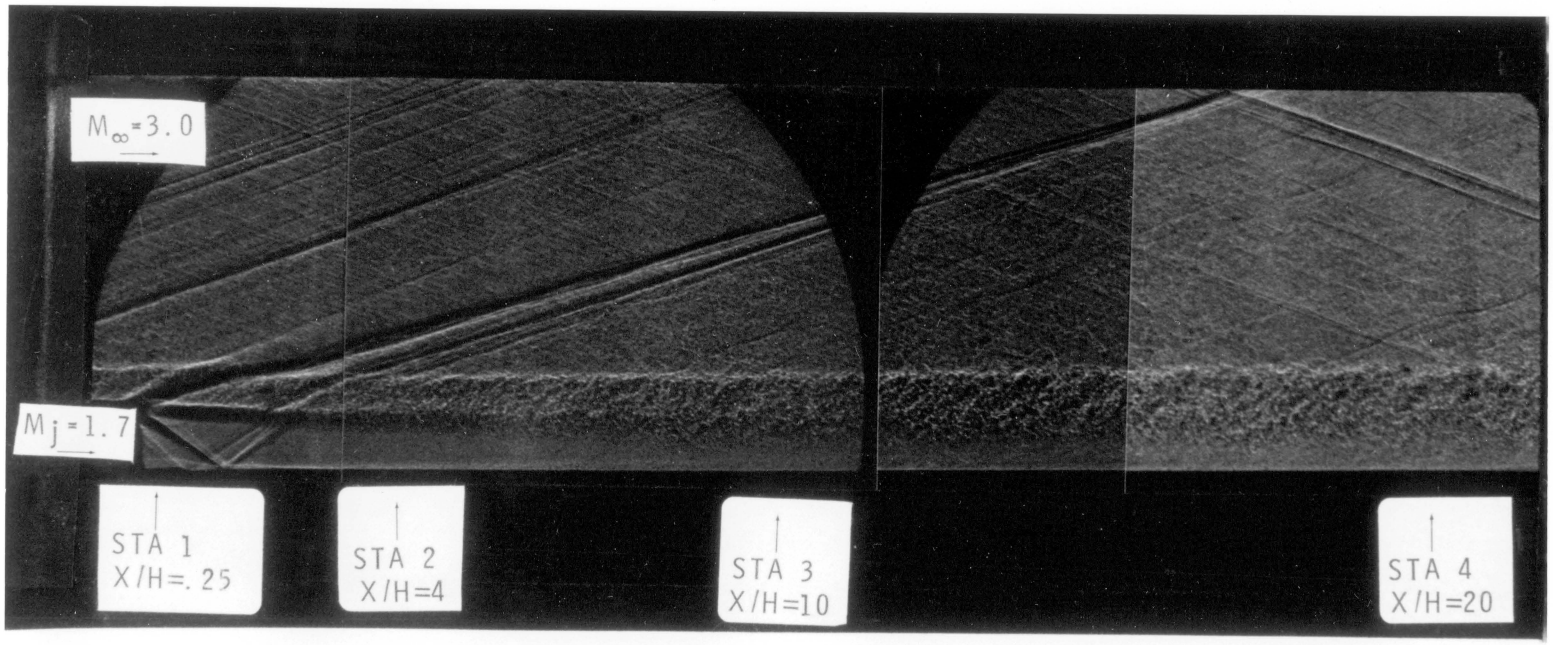

Nanosecond Shadowgraph of Unheated Freestream ($T_{tinf} = 540R$) with Heated Tangential Injection ($T_{tj} = 760R$, $P_{tj} = 10.7$ psia), H = 0.5 inches.

Figure 18. Nanosecond Shadowgraph of Heated Injection Case

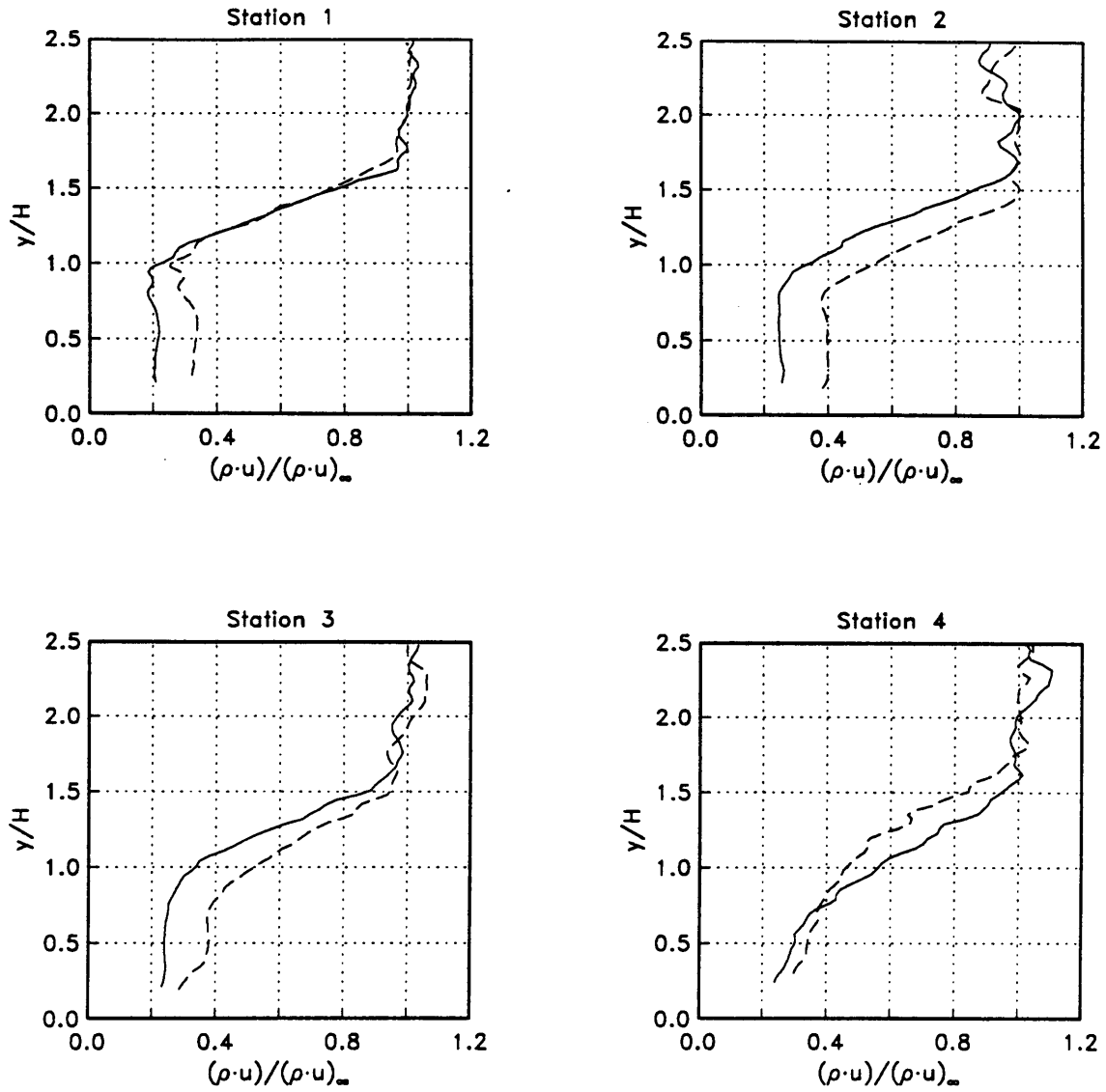

Figure 19. Mean Mass Flux Profiles

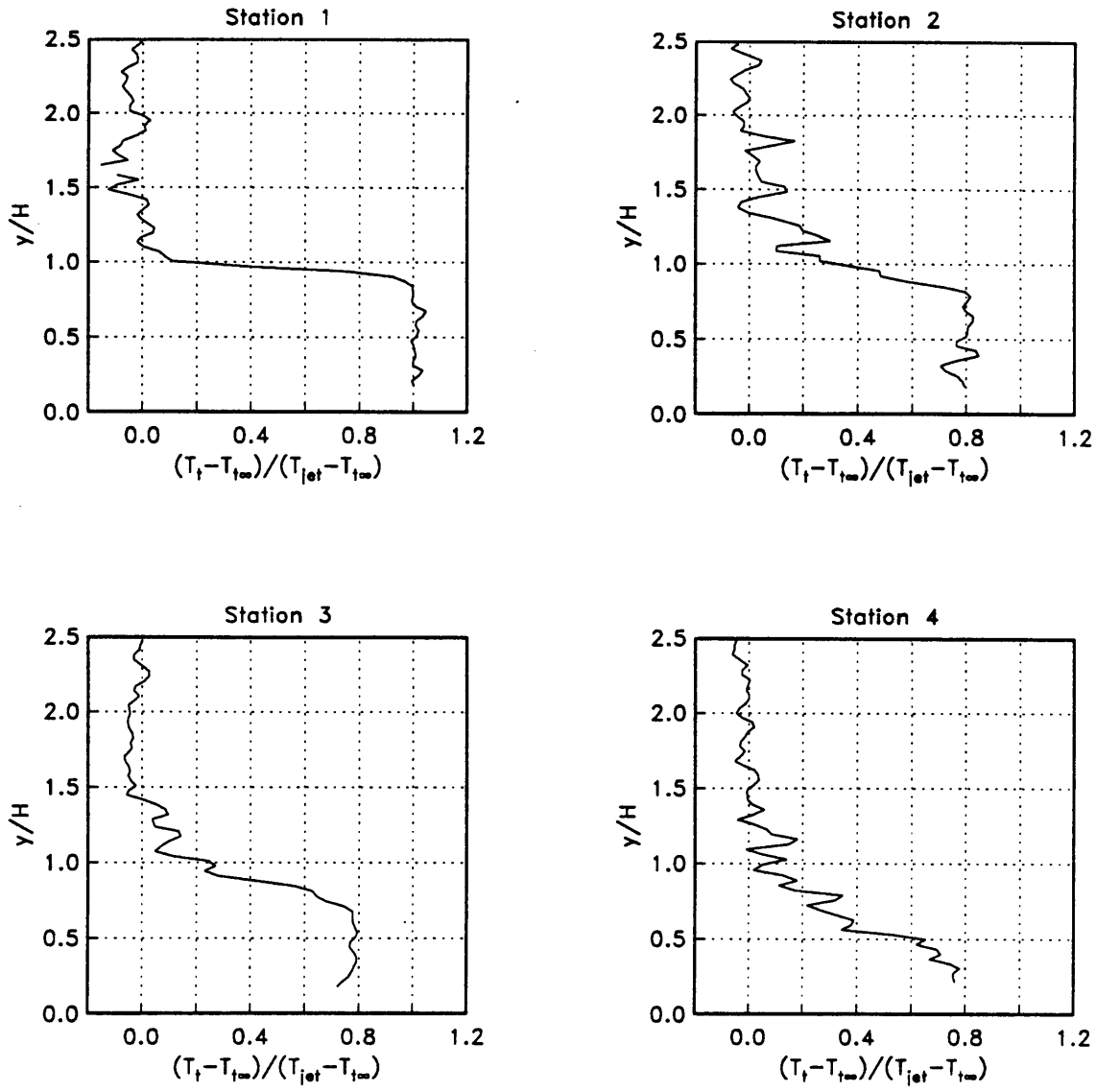

Figure 20. Profiles of Mean Total Temperature Coefficient - Heated Injection

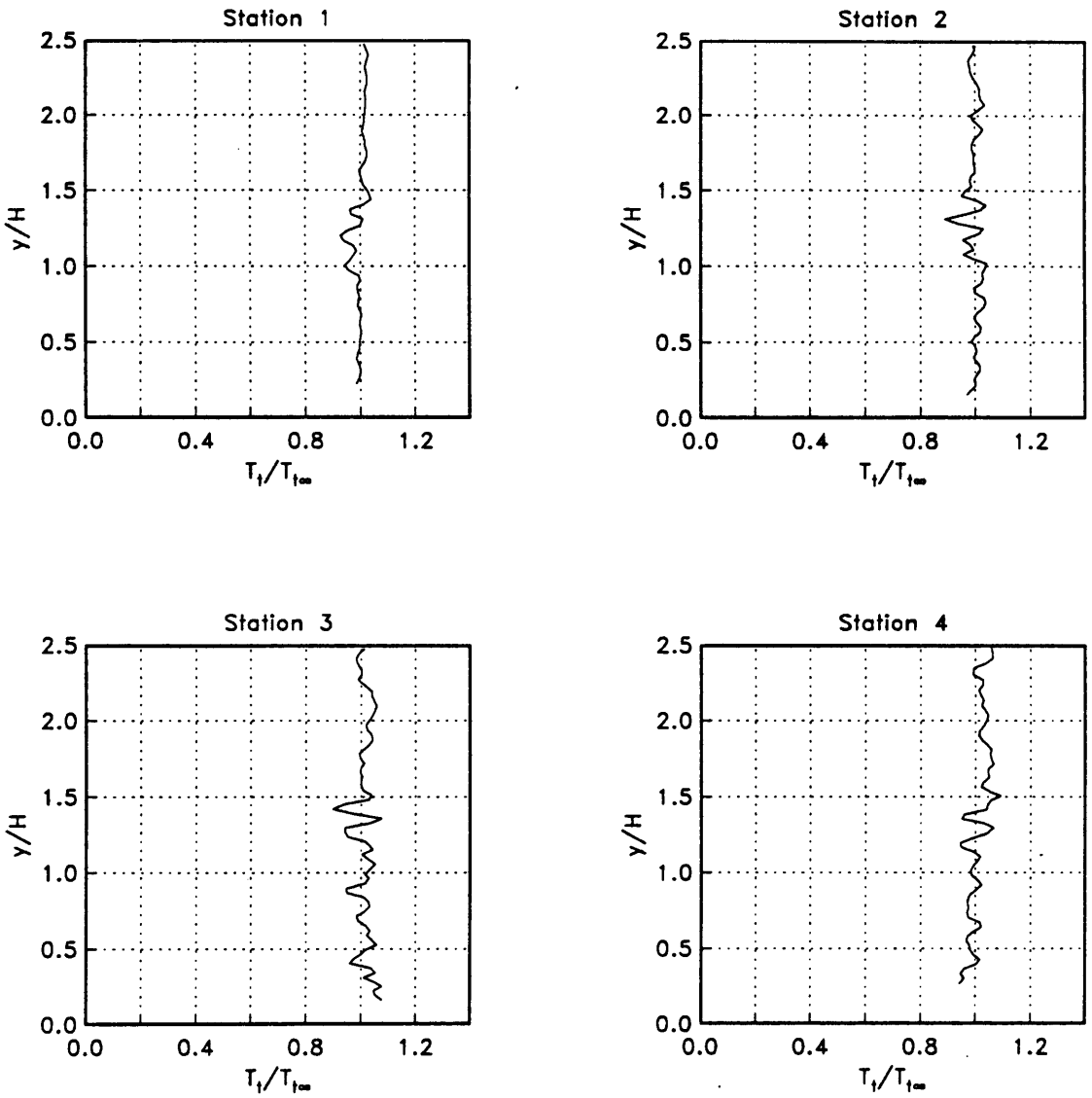

Figure 21. Profiles of Mean Total Temperature - Unheated Injection

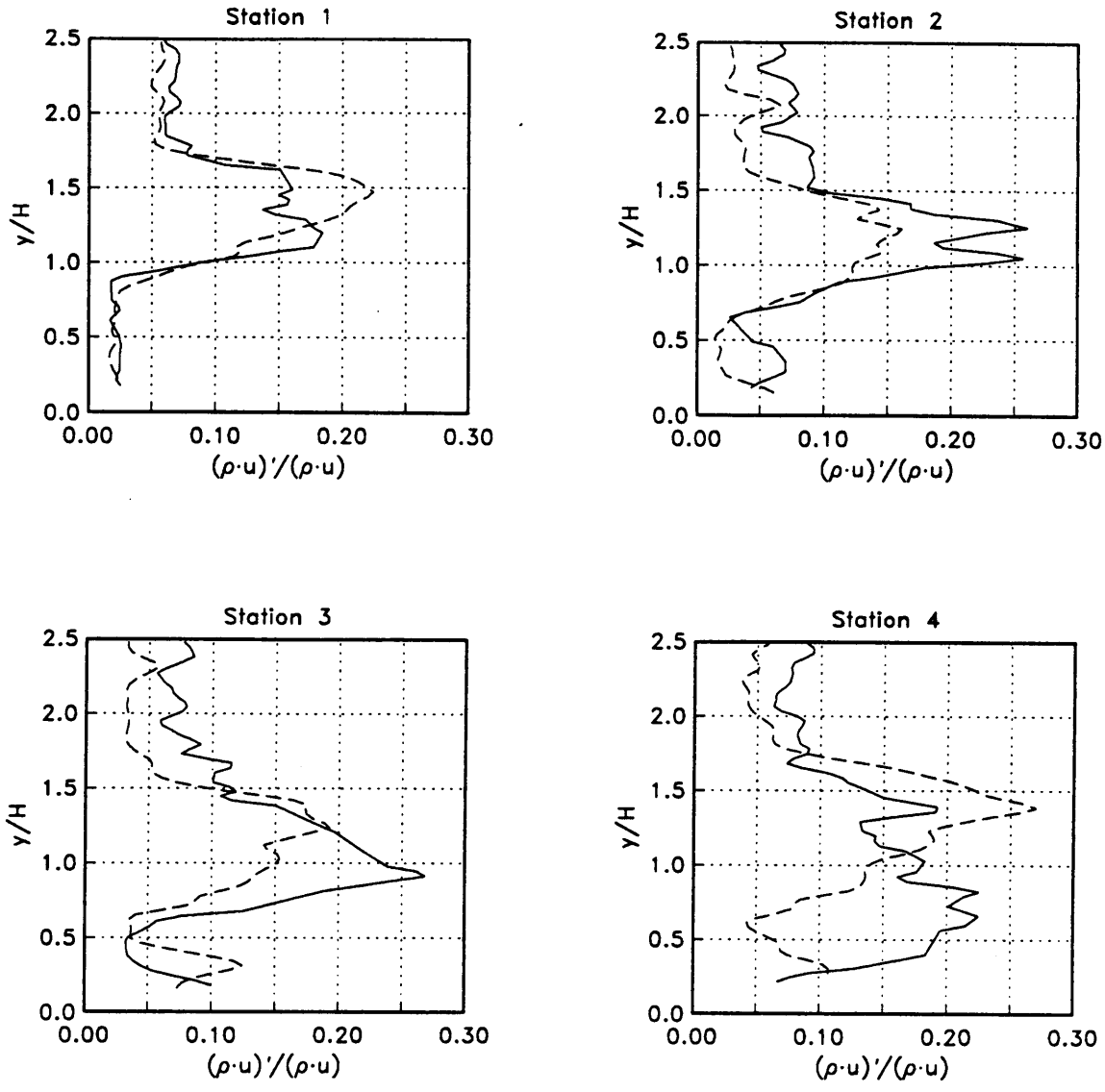

Figure 22. Turbulent Mass Flux Intensity Profiles

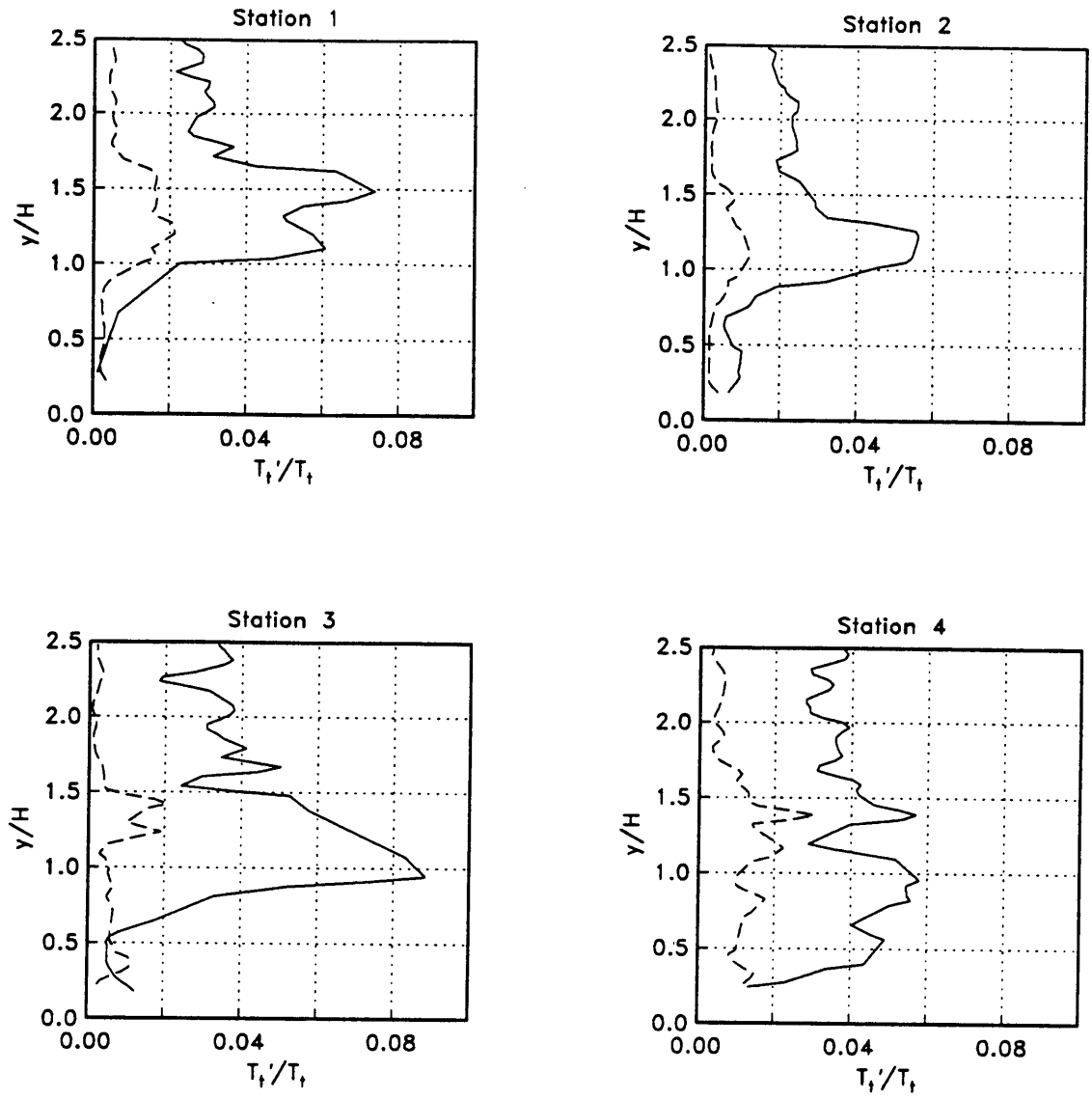

Figure 23. Turbulent Temperature Intensity Profiles

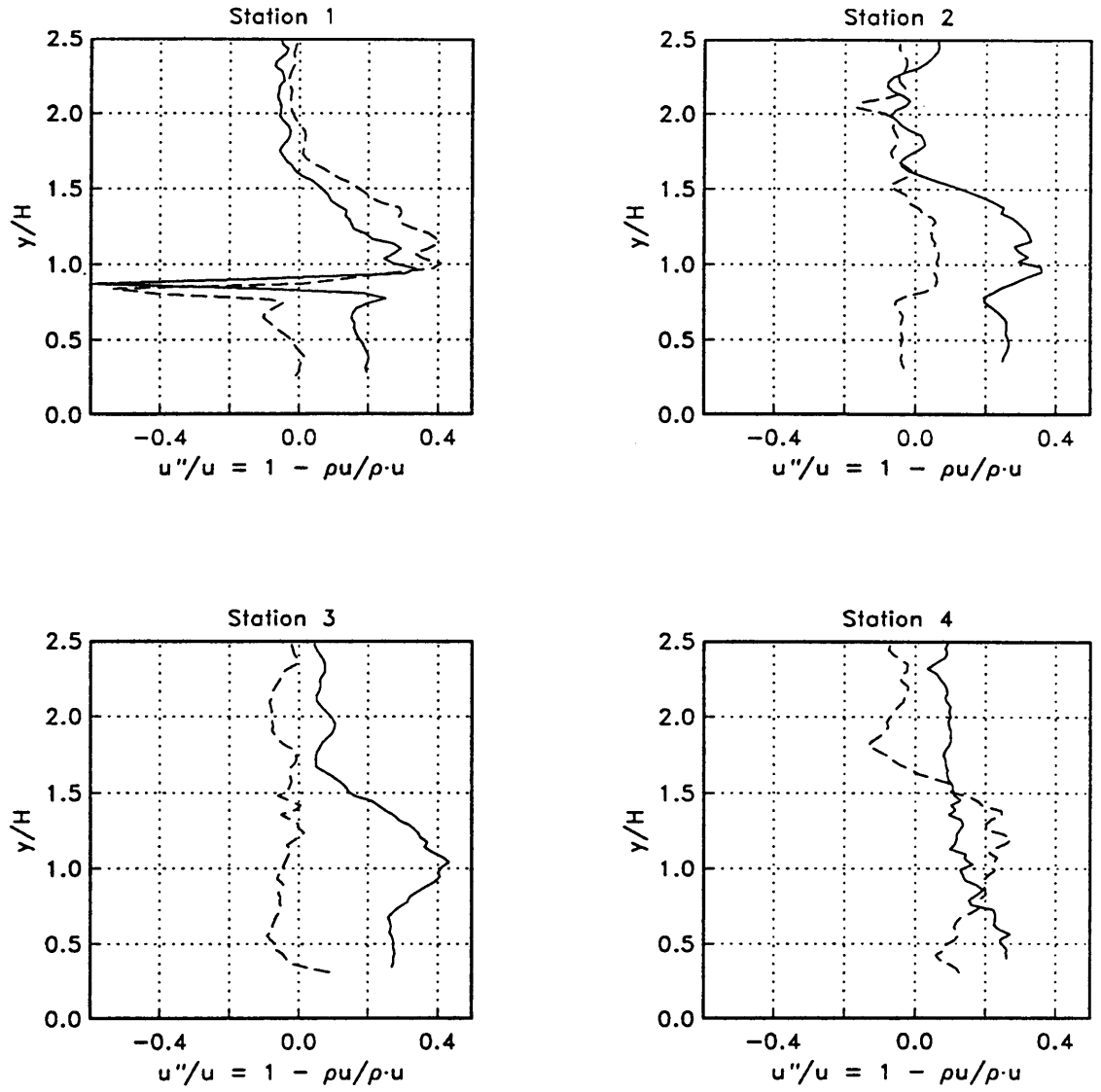

Figure 24. Favre-Averaged Turbulence Intensity Profiles

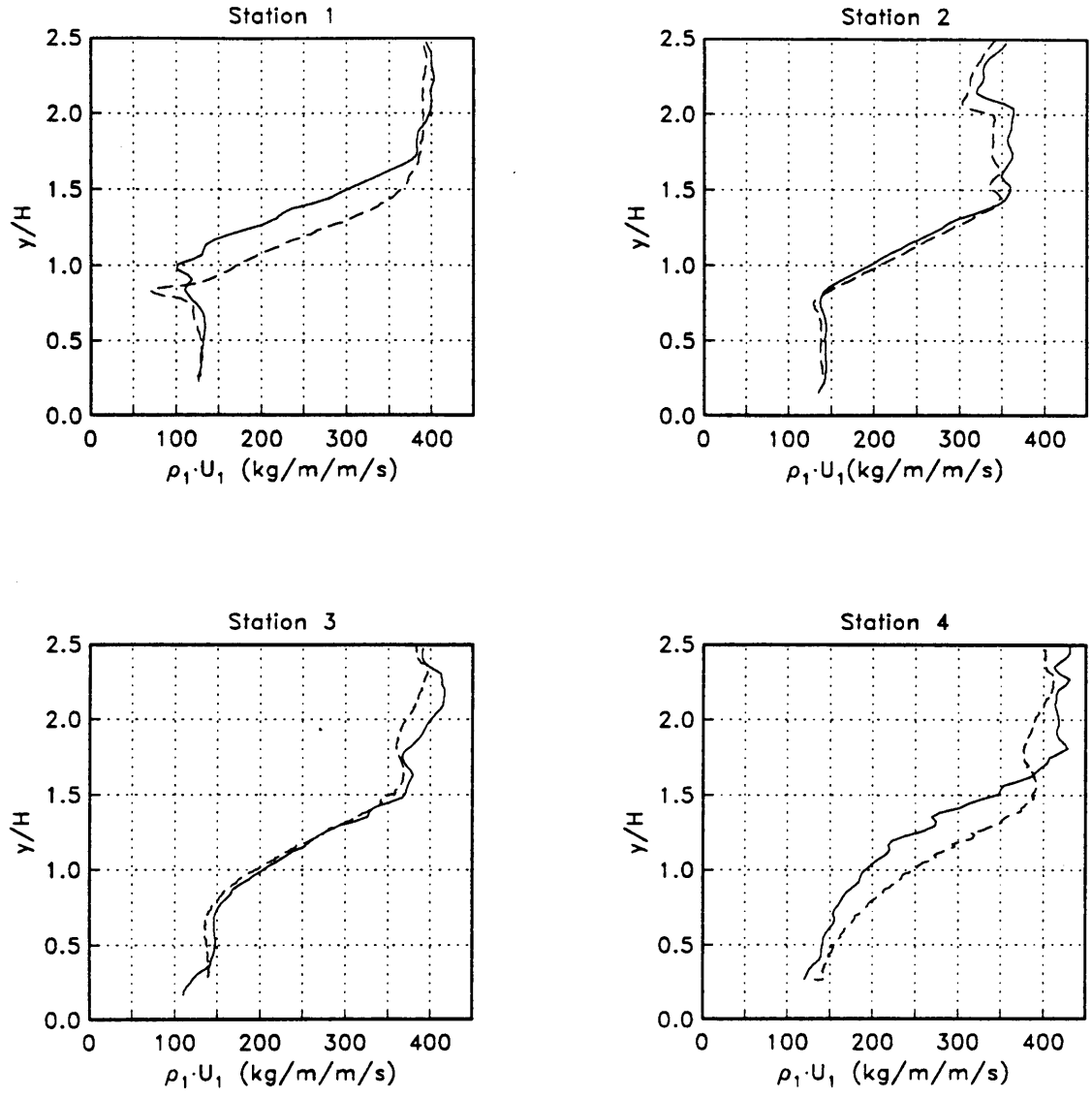

Figure 25. Comparison of Ambient Injection Profiles Found Using Mean [23] and Hot Wire Probes

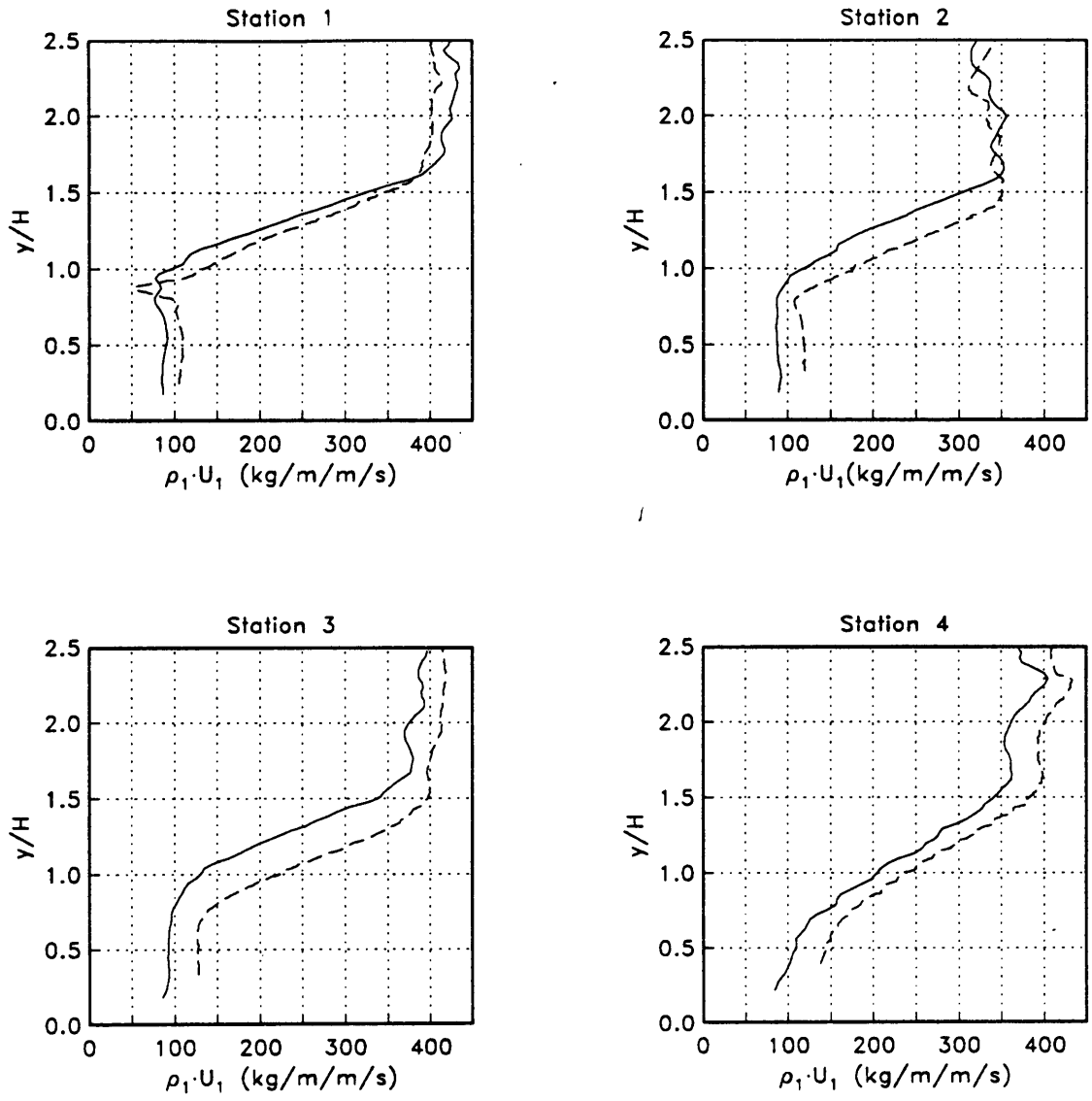

Figure 26. Comparison of Heated Injection Profiles Found Using Mean [23] and Hot Wire Probes

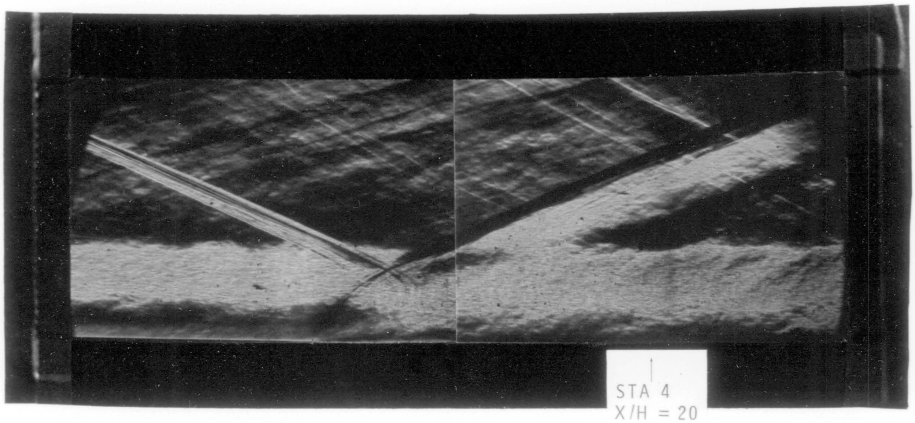

Spark Schlieren Photograph of Shock Impingement Region. Unheated Freestream ($T_{inf} = 540R$) with Heated Tangential Injection ($T_{tj} = 760R$, $P_{tj} = 10.7$ psia), H = 0.5 inches.

Figure 27. Spark Schlieren of Shock Impingement

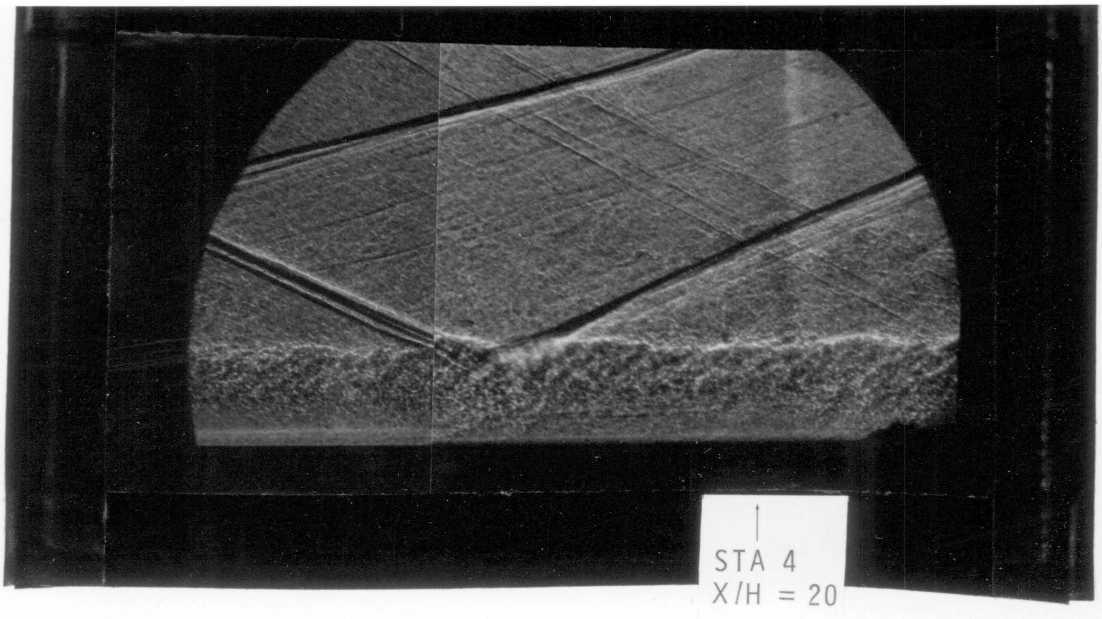

Nanosecond Shadowgraph of Shock Impingement Region. Unheated Freestream ($T_{tinf} = 540R$) with Heated Tangential Injection ($T_{tj} = 760R$, $P_{tj} = 10.7$ psia), H = 0.5 inches.

Figure 28. Nanoshadowgraph of Shock Impingement

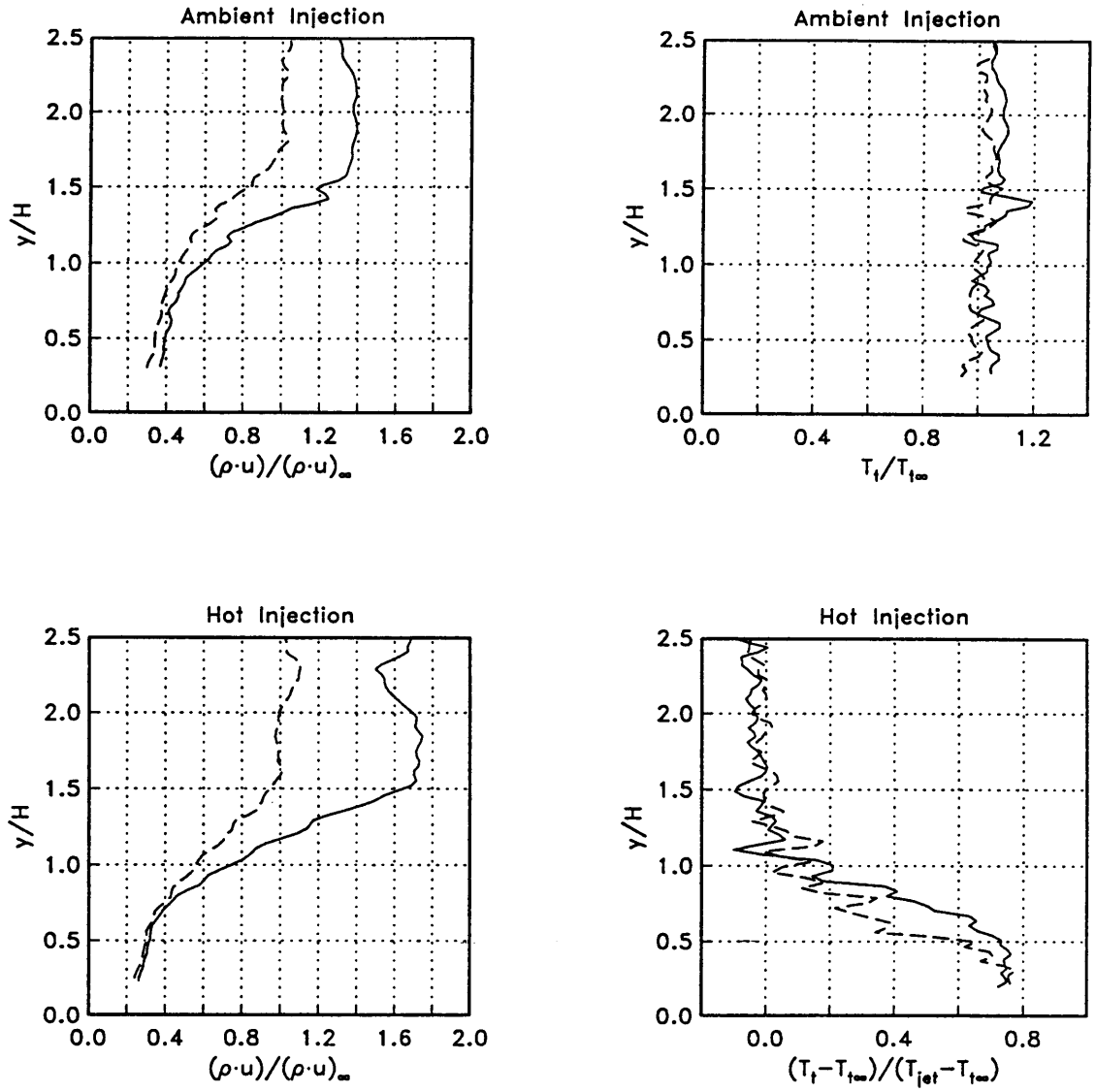

Figure 29. Mean Profile Changes Induced by Shock Impingement (Stn. 4)

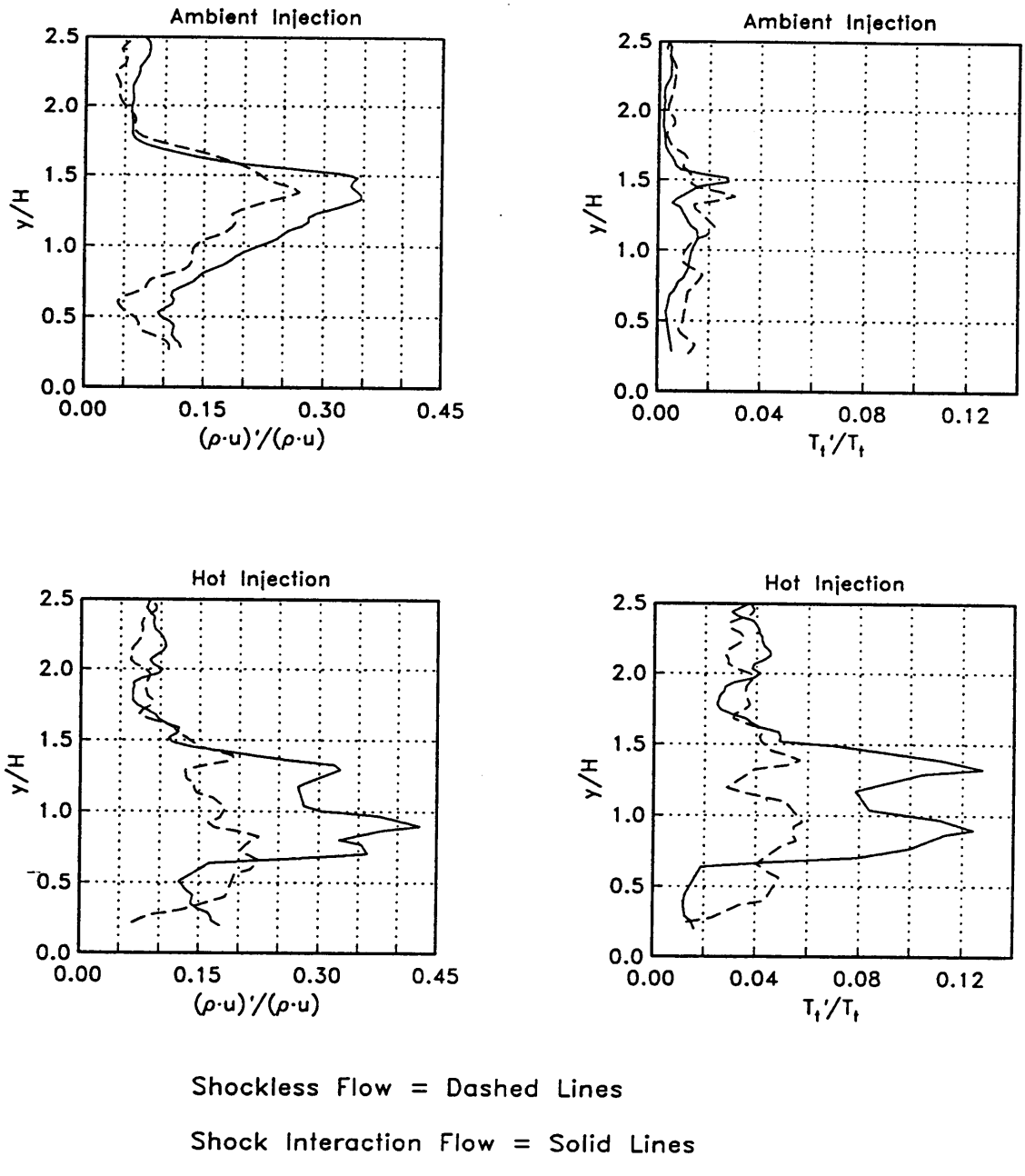

Figure 30. Turbulence Profile Changes Induced by Shock Impingement (Stn. 4)

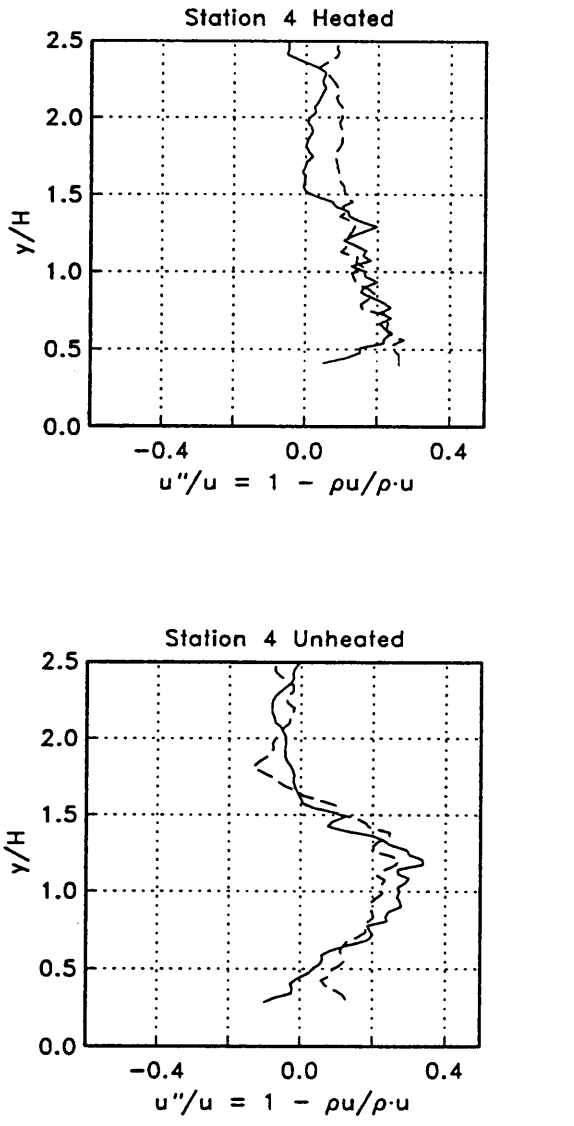

Figure 31. Favre-Averaged Turbulence Intensity Profiles Induced by Shock Impingement (Stn. 4)

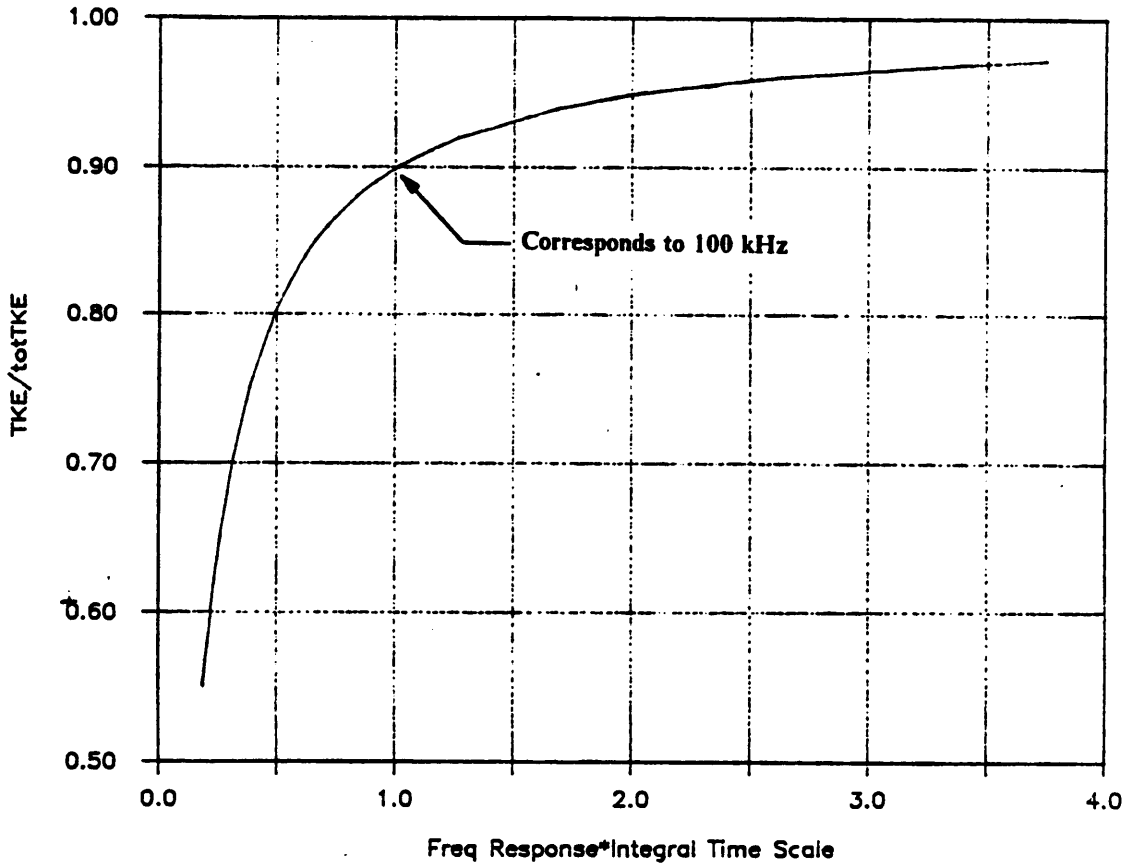

Figure 32. Fraction of Total Turbulent Energy Based on Hot-Wire Frequency Response [21]

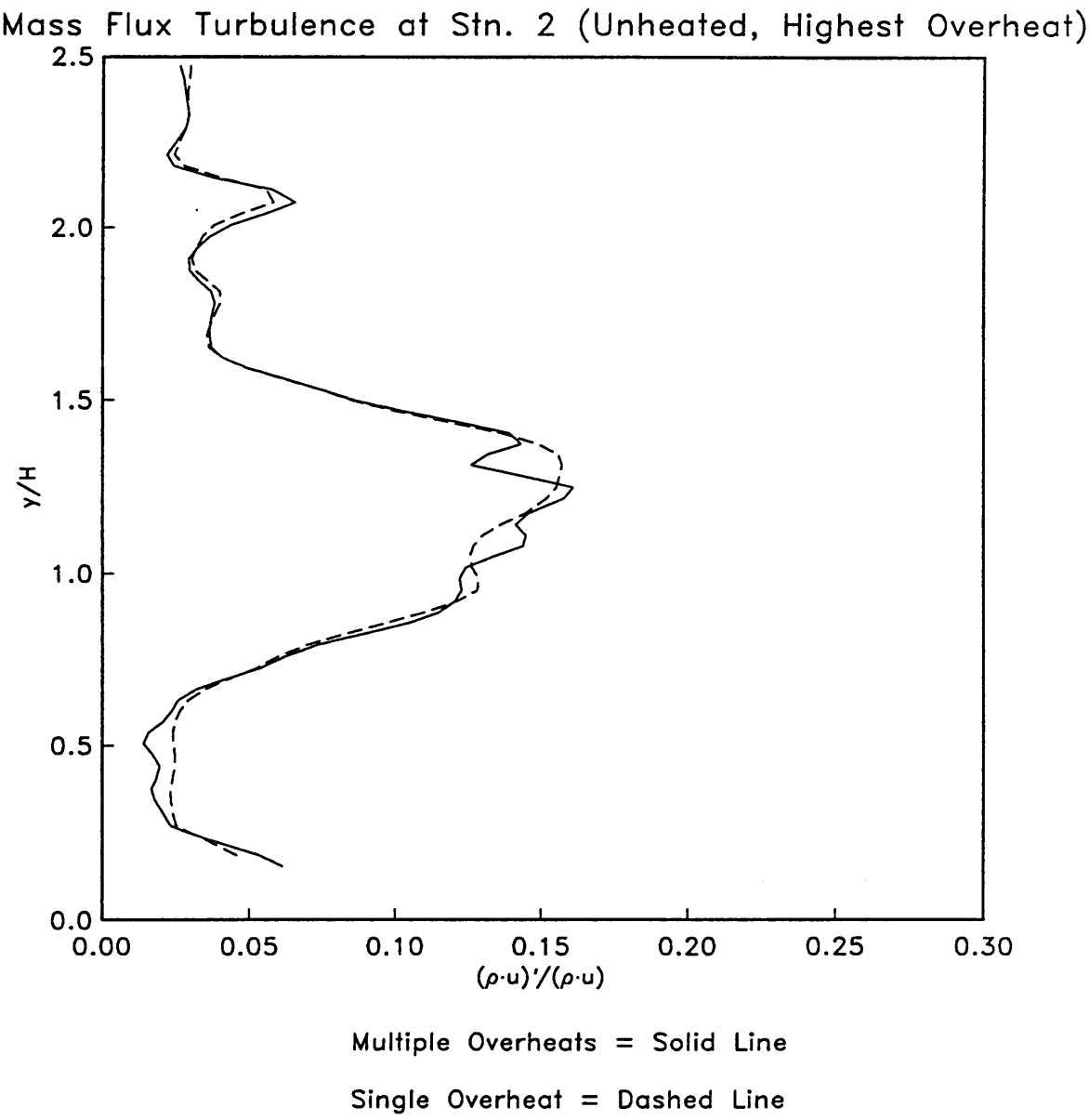

Figure 33. Comparison of Two Hot-Wire Methods (Stn. 2, Unheated)

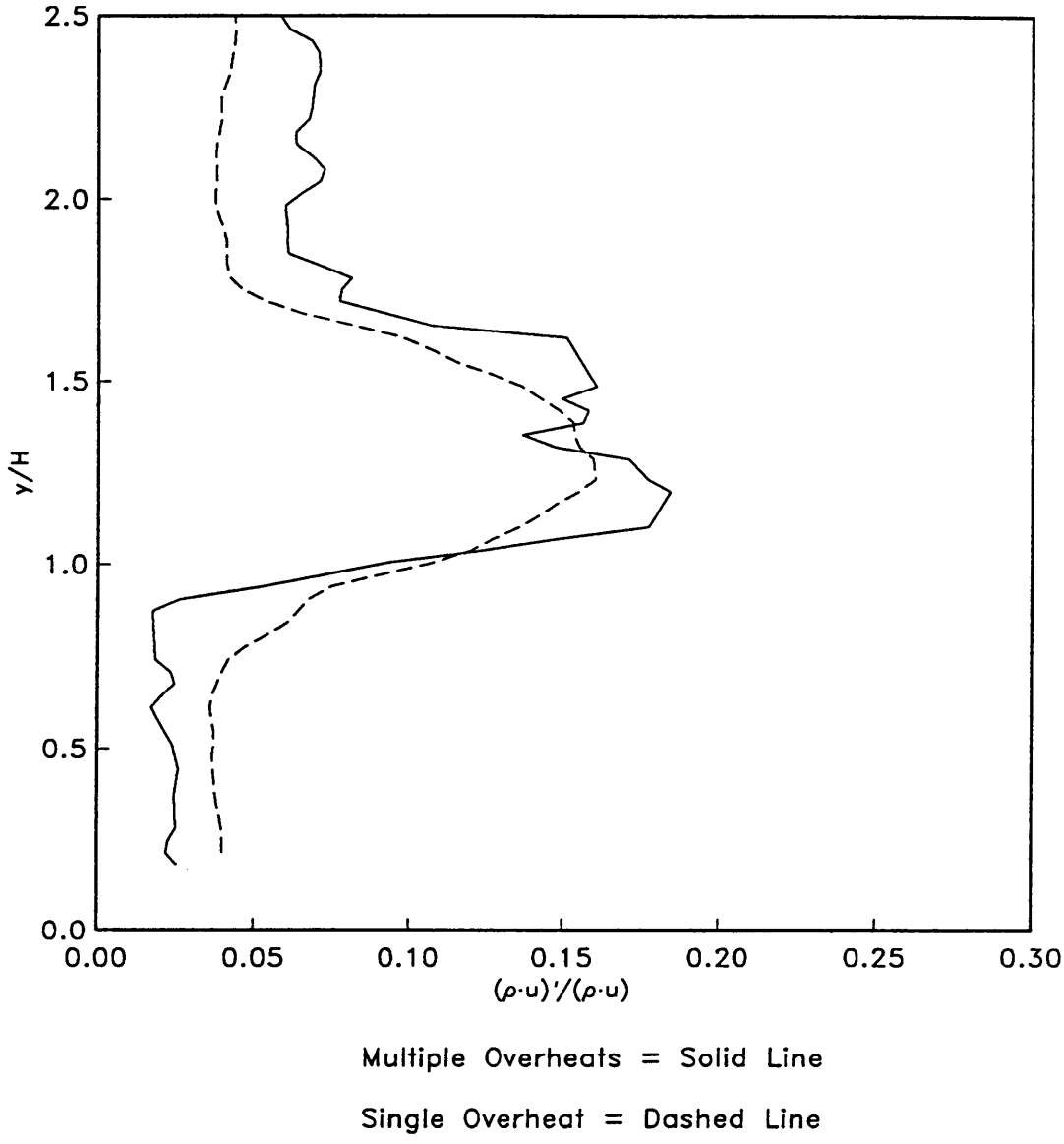

Figure 34. Comparison of Two Hot-Wire Methods (Stn. 1, Heated)

The vita has been removed from the scanned document